

Production of lipids by the oleaginous yeast *Cutaneotrichosporon oleaginosus* using the organic fraction of municipal solid waste as the feedstock

Master Thesis
by Line Nielsen

contact information: liniel19@student.aau.dk
Project Group Number: BIO10-2-F22



**AALBORG
UNIVERSITY**

This master thesis was submitted to Aalborg University in Esbjerg in fulfillment with the requirements for the M.Sc. in Bioengineering

Department of Chemistry and Bioscience – Section of Chemical Engineering

Aalborg University, Esbjerg

June 2022

Abstract

Biodiesel derived from lipids has proven to be a promising alternative when it comes to transportation fuels. However, its development and use have been hindered by low lipid yields and high production costs when compared to e.g., fossil fuels. Therefore, an increasing interest has emerged in investigating new and economically favorable methods for producing lipids that can be used for biodiesel production.

In this thesis, two time-studies were conducted to enlighten the optimal fermentation setup (Separate Hydrolysis and Fermentation (SHF) vs. Simultaneous Saccharification and Fermentation (SSF)) when using the organic fraction of municipal solid waste (OFMSW) as the feedstock while having an economic and sustainable point of view. The biomass hydrolysates were produced by enzymatic hydrolysis for 24 hours of the untreated waste to obtain the optimal sugar accessibility after which the non-detoxified hydrolysate was adopted as media for shake-flask fermentations. The maximum total lipid production that was extracted per liter waste media after fermentation with *Cutaneotrichosporon oleaginosus* was 34.53 g/L for SHF after 4 days and 35.30 g/L for SSF after 7 days. This is an increase in the lipid content of 10.20 g/L and 9.67 g/L using SHF and SSF, respectively, compared to the OFMSW media (50 % w/v), which corresponds to 61.41 g of lipids being produced from each kg of dry OFMSW for SHF and 57.80 g of lipids produced per kg dry OFMSW for SSF.

Furthermore, a new vector system, pFLEXI-hyg-yfp, was developed with the aim of enhancing the future possibilities of genetic engineering of *C. oleaginosus*. The plasmid was successfully used for transformation of *C. oleaginosus* with *Agrobacterium tumefaciens* mediated transformation (ATMT), the obtained mutants were validated for successful integration by colony PCR and an optimized protocol for the ATMT procedure of *C. oleaginosus* was established. Lastly, the effect of random integration on the level of expression was investigated by measuring the yfp fluorescence over time of several different *C. oleaginosus* mutants.

Preface

This master thesis was submitted to Aalborg University in Esbjerg in fulfillment with the requirements for the M.Sc. in Bioengineering. The laboratory experiments were conducted at the laboratory facilities at Aalborg University, Esbjerg and I would like to thank Linda Birkebæk Madsen (*Laboratory technician*) and Jonas Bjerring Christensen (*Laboratory trainee*) for their help with HPLC as well as their guidance during the period of this master thesis.

Furthermore, a special thank you to my supervisor Jens Laurids Sørensen (*Associate Professor, Section of Chemical Engineering*) for his trust, support, help, and encouragement in all aspects of this master thesis. It has been a pleasure to discuss ideas, results, and perspectives for this project as well as for the entire Flexi Green Fuels Project in collaboration with colleagues from the Section of Energy Technology at Aalborg University in Esbjerg. In this context, I would also like to thank Mette Hedegaard Thomsen (*Associate Professor, Section of Energy Technology*), Tanmay Chaturvedi (*Assistant Professor, Section of Energy Technology*) and Eva Mie Lang Spedtsberg (*Ph.D. fellow, Section of Energy Technology*) for our valuable discussions and their inputs in general during conferences and meetings concerning the Flexi Green Fuels project.

Esbjerg, 10th of June 2022

Line Nielsen



Table of contents

1	Introduction.....	1
2	Literature review	3
2.1	Biofuels	3
2.1.1	<i>Microbial oils as a feedstock for production of biofuels</i>	4
2.1.2	<i>Cutaneotrichosporon oleaginosus: a yeast candidate for optimal lipid production</i>	4
2.2	The biochemistry of lipid production in <i>C. oleaginosus</i>	6
2.3	Using a low-cost feedstock for the lipid production by <i>C. oleaginosus</i>	8
2.3.1	<i>Chemical composition of OFMSW.....</i>	9
2.3.2	<i>Pretreatment methods</i>	10
2.3.3	<i>Enzymatic hydrolysis.....</i>	12
2.4	Improving the fermentation strategy	15
2.4.1	<i>Mode of enzymatic hydrolysis and fermentation</i>	15
2.4.2	<i>Genetic engineering for enhanced lipid production.....</i>	16
2.5	Methods for genetic engineering of <i>C. oleaginosus</i>	17
2.5.1	<i>Interesting possibilities for genetic engineering of C. oleaginosus</i>	18
2.5.2	<i>Choosing a cellulase-encoding gene for expression in C. oleaginosus.....</i>	18
2.5.3	<i>Improving the transformation system for C. oleaginosus.....</i>	20
3	Problem formulation.....	23
4	Materials and methods	24
4.1	Time studies on yeast fermentations using OFMSW as the feedstock.....	24
4.1.1	<i>Preparation of OFMSW.....</i>	24
4.1.2	<i>Enzymatic hydrolysis of OFMSW.....</i>	25
4.1.3	<i>Yeast strain and media</i>	26
4.1.4	<i>Separate hydrolysis and fermentation (SHF)</i>	26
4.1.5	<i>Simultaneous saccharification and fermentation (SSF)</i>	27
4.1.6	<i>Analytical methods</i>	27
4.2	Genetic engineering of <i>Cutaneotrichosporon oleaginosus</i>	28
4.2.1	<i>Yeast and bacterial strains</i>	29
4.2.2	<i>Growth and selection media</i>	30
4.2.3	<i>Cloning methods.....</i>	30
4.2.4	<i>Plasmid validation</i>	33
4.2.5	<i>Transformation of Cutaneotrichosporon oleaginosus</i>	33
4.2.6	<i>Validation of the C. oleaginosus mutants.....</i>	34
4.2.7	<i>Level of yellow fluorescent protein expression in C. oleaginosus mutants</i>	34
5	Results and discussion	35
5.1	Time studies on the yeast fermentations using OFMSW as the feedstock	35
5.1.1	<i>Enzymatic hydrolysis.....</i>	35
5.1.2	<i>Separate hydrolysis and fermentation (SHF)</i>	36

5.1.3	<i>Simultaneous saccharification and fermentation (SSF)</i>	37
5.1.4	<i>SHF vs. SSF</i>	39
5.1.5	<i>Discussion on the sustainable industrial implementation of the process</i>	41
5.2	Genetic engineering of <i>Cutaneotrichosporon oleaginosus</i>	43
5.2.1	<i>PCR products</i>	43
5.2.2	<i>Plasmid validation</i>	45
5.2.3	<i>Transformation of <i>A. tumefaciens</i></i>	50
5.2.4	<i>Transformation of <i>C. oleaginosus</i></i>	50
5.2.5	<i>Validation of the successful transformation of <i>C. oleaginosus</i></i>	52
5.2.6	<i>Level of yellow fluorescence protein expression in <i>C. oleaginosus</i> mutants</i>	53
6	Conclusions	55
7	Perspectives	56
8	Bibliography	57
9	Appendices	66
9.1	Appendix A – Protein sequence of the Tr-Te chimeric CBH1 (Tr-TeCBH1)	66
9.2	Appendix B – Codon optimized gene sequence of <i>Tr-Te cbhl</i>	66
9.3	Appendix C – Cassette sequence of the TEF1- α + <i>Tr-Te cbhl</i>	67
9.4	Appendix D – Primer sequences and PCR settings	68
9.5	Appendix E – Protocol for ATMT of <i>C. oleaginosus</i>	70

1 Introduction

One of the largest issues for the world population in the near future is the production of fuels that are renewable, biodegradable, non-toxic and have low negative environmental impacts [1,2]. The expected increase in world population to higher than 9.8 billion by 2050, combined with significant economic growth in emerging economies will result in substantially increasing energy consumption [2–4]. The decreasing amount of fossil fuels available, the consequences for the environment associated with the use of these fossil fuels as well as humanity's increased dependence on fuels in everyday life means that new alternative ways of producing fuels must be developed to reduce the impact of this sector on the environment [5]. To be able to respond to this growing demand, it is necessary to use natural resources more efficiently and to increase the use of renewable energy, such as biofuels [6].

The replacement of fossil fuels with biofuels has been suggested as a promising solution for the transportation sector by several researchers within the field of bioenergy [6–8]. However, a major concern with the production of biofuels for the transportation sector is the actual sustainability of these biofuels with respect to the reduction of green house gasses, issues with the use of large areas of land, and the availability of biomass [5,9]. Furthermore, the cost competitiveness with fossil fuels is a barrier for large-scale production with the currently developed technologies for production of biofuels [4,9].

The environmental and economic sustainability of producing biofuels is largely dependent on the feedstock as well as the technology used for the process [9,10]. The most common raw materials used to produce biodiesel are vegetable oils derived from edible plants, but the ethical conflicts that arise from the use of food as fuel and the high costs that are associated with its use have encouraged researchers to search for cheaper non-food alternative feedstocks to produce biodiesel [3,5,6]. This has led to an increased interest in the production of microbial oils, from microalgae, yeasts, fungi or bacteria, and the potential development of a large-scale production process for commercialization.

Oleaginous yeasts produce lipids consisting of long-chain fatty acids comparable to those of conventional vegetable oils [7,11]. Thus, microbial lipids produced by oleaginous yeasts have been suggested as a potential feedstock for environmental and economic sustainable biodiesel production due to several advantages, such as accumulation of large amounts of lipids, shorter incubation time compared to plant and animal resources, less need for labor, independent of season, climate, and geography, easier to scale up and no need for agricultural land [7,12]. Furthermore, oleaginous yeast can be used to convert cheap agro-industrial waste and even municipal waste into high quality lipids [7,12]. However, the conversion of these lignocellulosic feedstocks to high-quality lipids is dependent on the addition of commercially available enzymes to hydrolyze the carbohydrates to free fermentable sugar molecules [13,14]. This need for large amounts of commercial enzymes at a large-scale production facility makes the economic aspect of the production process of lipids from oleaginous yeast unfavorable [14]. Thus, the entire production

process must be optimized, and new techniques must be developed to make it environmentally as well as economically sustainable. One possibility to enhance the economic viability of the lipid production process is to genetically engineer the oleaginous yeasts [15,16]. There are several ways in which genetic engineering of oleaginous yeasts could conceivably contribute to a more economically favorable lipid production process. Genes involved in metabolic pathways towards the production of lipids within the yeasts could be altered, overexpressed, or deleted depending on the function of the genes [17–19]. Furthermore, the need for pretreatment of the lignocellulosic materials with commercial enzymes could potentially be reduced by inserting genes responsible for the production of specific enzymes from other microorganisms to the genome of the oleaginous yeasts [20,21].

In the light of the above, this master thesis aims to study the production of lipids in the oleaginous yeast *Cutaneotrichosporon oleaginosus* using the organic fraction of solid municipal waste (OFMSW) as the feedstock, to reduce the need for addition of commercial enzymes in the pretreatment of the OFMSW by genetic engineering of *Cutaneotrichosporon oleaginosus* and to test the genetically engineered yeast strains as well as the wild-type yeast strain in small laboratory scale batch fermentations.

2 Literature review

2.1 Biofuels

Global energy demand is expected to increase by 48 % in the next 20 years due to the increasing global population [22]. Currently, 80 % of the energy demand is met by fossil fuels. However, the depleting fossil fuel reserves together with the negative environmental impacts from its combustion has increased the interest in the development of sustainable biofuels significantly because of its unique characteristics, regarding toxicity, biodegradability, and greenhouse gas emissions [1,4,5,7]. Biofuels can be differentiated according to some key characteristics, including type of feedstock, conversion process, and its use. Generally, generation-terms are used to distinguish the different types based on the type of feedstock used for their production [9].

- First-generation biofuels
- Second generation biofuels
- Third generation biofuels

First generation biofuels utilize food or animal feed crops which has sparked controversy because it competes with global food needs [23]. However, a key feature of first-generation biofuels is that they are produced through well-established technologies and processes, such as fermentation, distillation, and transesterification. On the other hand, second-generation biofuels are derived from non-food feedstocks, such as dedicated energy crops, agricultural residues, forest residues and other waste materials. Biodiesel produced from microalgae through conventional transesterification or hydro-treatment of algal oil is commonly known as third-generation biofuel. The production techniques or pathways for second- and third-generation biofuels are still in the research and development, pilot, or demonstration phase [6,9].

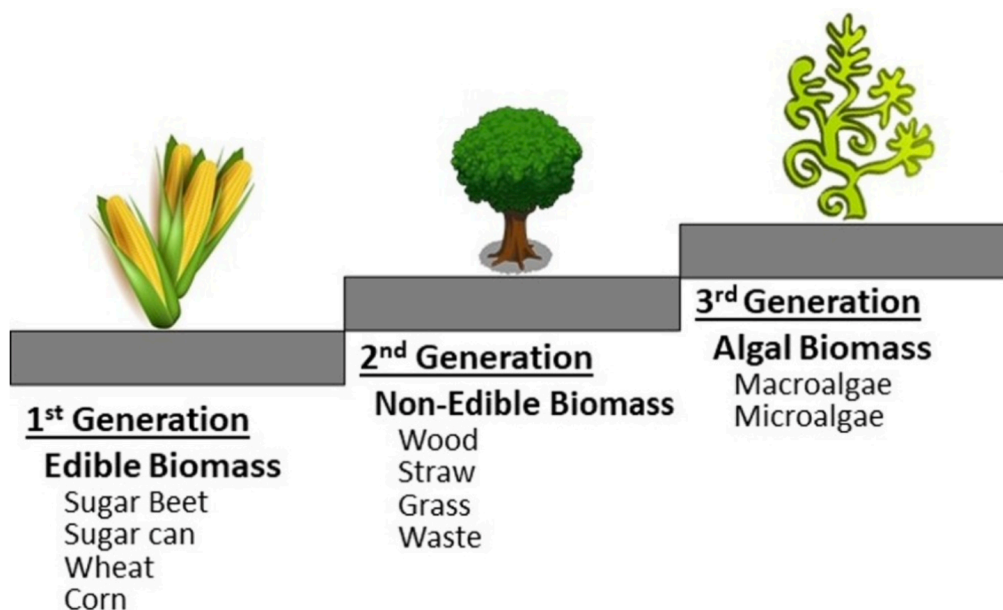


Figure 2.1: Biomass used as the feedstock for production of first, second and third generation biofuels. First generation utilize edible biomass, second generation use non-edible biomass, and third generation use algal biomass as the feedstock. Figure from [23].

The main portion of the biodiesel produced using transesterification nowadays are using vegetable and non-edible oils [7,24]. However, biodiesel derived from these feedstocks can deliver only a small fraction of the rising demand for transport fuels [25]. Furthermore, the high cost of using vegetable and non-edible oils, the great need for land and the lower yield of oil have resulted in less interest in using these raw materials for biodiesel production [24]. Therefore, it is necessary to explore new raw materials that can deliver environmental benefits over fossil fuels, are economically competitive, can be produced in large quantities, and do not compete with food production [25]. Oils produced by microorganisms can potentially meet these requirements if they can be produced in an economically feasible way.

2.1.1 Microbial oils as a feedstock for production of biofuels

Microbial oils are considered as a promising candidate for biodiesel production because the fatty acid composition is very similar to that of vegetable oils [3,25]. The oil composition is crucial for the utility of the biodiesel as it determines the physical and chemical properties of the oil mixture such as energetic density, melting point, and viscosity. However, it should be noted that oils produced from microbial sources have been studied to less extent than vegetable oils and it is important to establish the quality of biodiesel produced from microbial oils [26]. Nevertheless, the future use of these microbial oils for biodiesel production is considered to be very promising [6].

In most microorganisms, the lipid content does not exceed 20 % of their dry biomass. However, there are some examples of species that are known to greatly exceed this limit and they are therefore referred to as oleaginous species [27]. Several studies have been conducted with oleaginous yeasts, molds, microalgae, and bacteria to assess their potential in the attempt to develop a lipid-producing platform. Oleaginous yeasts are considered as the most promising microorganism for the production of lipids by several researchers, since they can accumulate up to more than 70 % of their dry weight as lipids [26]. Furthermore, they exhibit several advantages for lipid production, related to their relatively fast growth, the less area of land needed for their cultivation, and the fact that they are less affected by season and climatic conditions compared to other oleaginous microorganisms [3,12,15]. In addition, oleaginous yeasts can generate lipids from various carbon sources and are more flexible utilizing substrates compared to fungi, bacteria, and microalgae [27].

Several oleaginous yeasts have been extensively studied and are considered potential candidates for the development of an industrial lipid-producing process. The most studied yeast species are within the *Yarrowia*, *Rhodotorula*, *Cryptococcus*, *Trichosporon*, *Lipomyces*, *Cutaneotrichosporon*, *Candida*, and *Rhodospiridium* genera. However, screening studies are still performed, leading to the constant identification of new oleaginous yeast species and new potential candidates [28].

2.1.2 *Cutaneotrichosporon oleaginosus*: a yeast candidate for optimal lipid production

Among the extensively studied yeast species, *Cutaneotrichosporon oleaginosus* ATCC 20509 has gained a lot of interest lately due to its ability to grow on a wide range of industrially interesting

substrates such as food waste, municipal wastewater, whey permeate, office paper production waste, complex biomass hydrolysates, and crude glycerol – even in the presence of fermentation inhibitors [29–31].

Taxonomically, *C. oleaginosus* is a basidiomycete yeast of the Tremellomycetes class and recently added to the *Cutaneotrichosporon* genus [29]. However, over the last few decades, the yeast has been published under various names including *Candida curvata*, *Apiotrichum curvatum*, *Cryptococcus curvatus*, *Trichosporon cutaneum*, *Cutaneotrichosporon oleaginosus*, and *Trichosporon oleaginosus* [31]. Although the two names *Trichosporon oleaginosus* and *Cutaneotrichosporon oleaginosus* has been most extensively used in more recent literature, the diverse designation over the years makes the collection of relevant information and data more difficult [32]. Nevertheless, the yeast is a GRAS (Generally Recognized As Safe) microorganism, it grows fast, it grows on a variety of substrates, and it can accumulate up to 70 % of its dry cell weight as lipids which positions *C. oleaginosus* as a prime candidate to realize ecologically and economically sustainable microbial lipid production targeted at production of biodiesel [19,32,33].

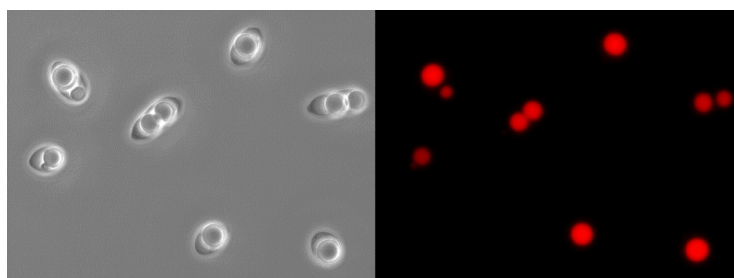


Figure 2.2: Fluorescence microscopic picture of wild type *C. oleaginosus* cells with 48 % lipids of their cell dry weight. Transmitted microscopy is shown on the left side, while the fluorescence (stained with Nile Red) is illustrated on the right side [17].

To improve the sustainability of microbial lipids from an economic aspect, other oleaginous yeast species such as *Y. lipolytica* has undergone extensive genetic engineering aimed at simultaneous sugar uptake (both hexoses and pentoses) from complex hydrolysate feedstocks, but that is in fact an inherent ability of *C. oleaginosus* [34]. Furthermore, *C. oleaginosus* has been shown to be able to utilize various lignin-derived aromatic compounds as sole carbon source, while maintaining the high accumulation of lipids [32,35,36]. Even though the exact pathway of aromatic metabolism remains to be determined for *C. oleaginosus*, it shows great promise for conversion of lignin-derived monoaromatics to lipids [35].

The ability of *C. oleaginosus* to utilize highly diverse carbon sources for the lipid production is a main feature that distinguish it from other oleaginous yeast species [17]. Additionally, it has been shown that the lipid and biomass production are mostly unaffected by fermentation inhibitors such as HMF or furfural, which is often present in waste hydrolysates [27,37]. Consequently, *C. oleaginosus* can potentially be the ideal oleaginous yeast candidate for the development of a sustainable process that converts waste biomass hydrolysates into high-value lipids which in turn can be used to produce biodiesel.

Though *C. oleaginosus* has been shown to grow a wide range of carbon and nitrogen sources, very little is known about the biochemistry of its metabolic potential [38].

2.2 The biochemistry of lipid production in *C. oleaginosus*

As previously mentioned, *C. oleaginosus* can metabolize a wide range of oligo- and monomeric sugars as well as both pentoses and hexoses, and the type of carbon source metabolized influences the lipogenesis within the cell. Both xylose and glucose can be converted to pyruvate via the pentose phosphate pathway, which can then be used as intermediate for further metabolic processes that converts pyruvate to cytosolic acetyl-CoA [29,38].

In oleaginous yeasts, the lipid precursor, cytosolic acetyl-CoA, is mainly produced via the mitochondrial pyruvate dehydrogenase (PDH) pathway and the mitochondrial tricarboxylic acid (TCA) cycle as indicated with the black arrows in Figure 2.3. However, in non-oleaginous yeasts, cytosolic acetyl-CoA is mainly produced via the PDH bypass pathway (red arrows in Figure 2.3) [19].

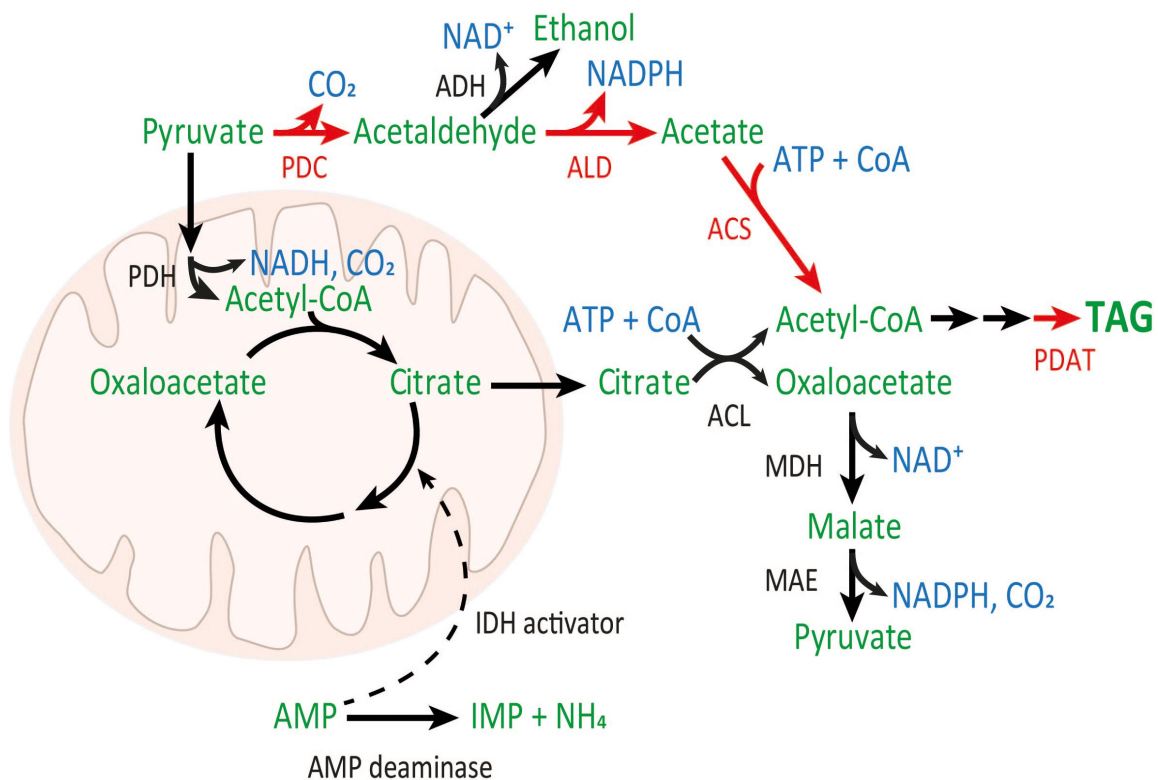


Figure 2.3: PDH (black arrows) and PDH bypass (red arrows) pathways from pyruvate to cytosolic acetyl-CoA. Metabolites are shown in green, cofactors and CO₂ are shown in blue, and enzymes involved in PDH bypass pathway are shown in red. Enzymes: pyruvate dehydrogenase (PHD), pyruvate decarboxylase (PDC), alcohol dehydrogenase (ADH), acetaldehyde dehydrogenase (ALD), acetyl-CoA synthetase (ACS), ATP:citrate lyase (ACL), phospholipid:diacylglycerol acyltransferase (PDAT), malate dehydrogenase (MDH) and malic enzyme (MAE) [19].

The regulation and lipid yield of the PDH pathway and the PDH bypass pathway differ, particularly in the response to nitrogen limitation. Nitrogen limitation causes activation of an adenosine monophosphate (AMP) deaminase, which utilizes AMP to produce NH₄ [39]. The decrease in AMP concentration inhibits the activity of mitochondrial isocitrate dehydrogenase (IDH), which is part of the TCA cycle as presented in Figure 2.3. Decrease in IDH activity results in citrate accumulation. Excess citrate is transferred to the cytosol where it is cleaved and combined with coenzyme A (CoA) by ATP:citrate lyase (ACL) to form acetyl-CoA and oxaloacetate with ATP consumption [19,39].

The cytosolic acetyl-CoA produced by the various pathways described above is subsequently used as the precursor for the biosynthesis of fatty acids by the acetyl-CoA carboxylase 1 (ACC1) enzyme and the fatty acid synthase (FAS) complex as illustrated in Figure 2.4.

The FAS in yeast consists of two subunits: Fas1 (β subunit) and Fas2 (α subunit).

- The α -subunit contains the catalytic centers: phosphopantetheine transferase (PT), ACP, ketoacyl synthase (KS), ketoacyl reductase (KR) and part of the malonyl-palmitoyl transferase (MPT) domain.
- The β -subunit contains acetyl-transferase (AT), enoyl reductase (ER), dehydratase (DH) and the major part of the MPT domain [40].

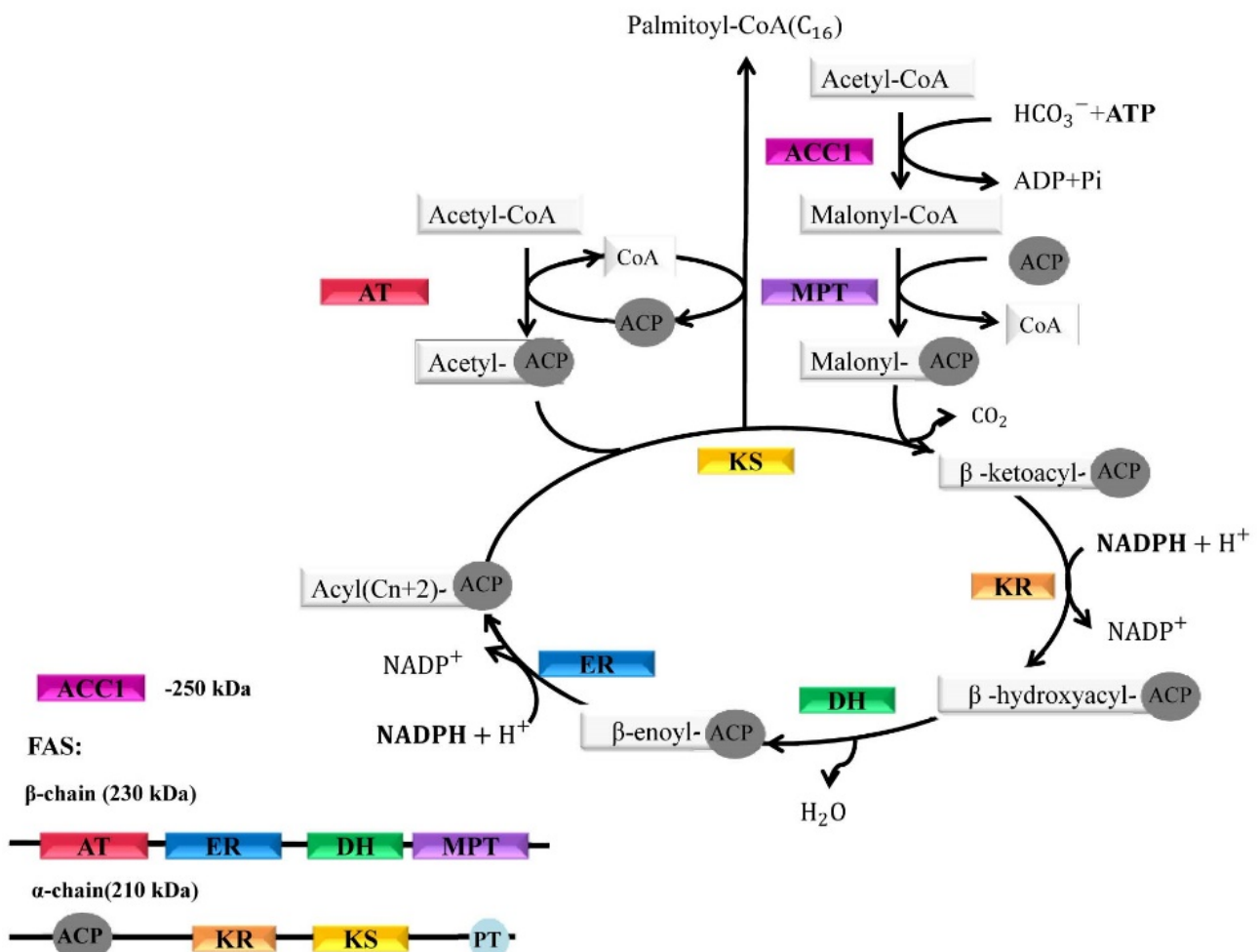


Figure 2.4: Fatty acid synthesis and elongation in yeast by the fatty acid synthase (FAS) complex [40]. AT: acetyltransferase, ER: enoyl reductase, DH: dehydratase, MPT: malonyl-palmitoyl transferase, KS: ketoacyl synthase, KR: ketoacyl reductase, ACP: acyl carrier protein, PT: phosphopantetheine transferase.

Starting with two molecules of acetyl-CoA, one is carboxylated into malonyl-CoA by the ACC1 enzyme. Next, both molecules have their CoA portions replaced by an acyl-carrier protein (ACP) to form acetyl-ACP and malonyl-ACP, respectively [41]. These two reactions are catalyzed by AT and MPT, respectively, as illustrated in Figure 2.4 [40]. Joining of acetyl-ACP with malonyl-ACP by KS splits out the carboxyl that was added and creates β -ketoacyl-ACP.

The ketone is thereby the first intermediate of the following cycle of reactions. First, it is reduced to a hydroxyl by KR using NADPH. Next, water is removed from carbons 2 and 3 of the hydroxyl intermediate by DH to produce a trans doubled bonded molecule. And lastly, the double bond is hydrogenated by ER to yield a saturated intermediate [40,41]. The process cycles with the addition of another malonyl-ACP to the growing chain until ultimately the 16-carbon palmitic acid is produced. Once a 16:0 carbon fatty acid has been formed, the cytoplasmic synthesis ceases. However, the fatty acid can undergo small modifications by enzymes found in the endoplasmic reticulum, resulting in desaturation and/or elongation which leads to the small diversity observed in the lipid profile when extracting lipids from oleaginous yeasts [41]. In general, the most abundant lipids produced by oleaginous yeasts are C16:0 (palmitic acid), C16:1 (palmitoleic acid), C18:0 (stearic acid), C18:1(oleic acid), and C18:2 (linoleic acid), whereas the lipids like C14:0 (myristic acid) and C18:3 (linolenic acid) are less abundant [39].

However, there are several external factors that can affect the biochemistry within the oleaginous yeast cell and thereby also the production of lipids, which (among others) include the type and composition of the substrate, the presence of inhibition compounds, the settings of the fermentation process, etc. Obviously, the optimization of the process is necessary to improve the economic feasibility, that is influenced by several factors such as the substrate cost, the production rate, and the lipid yields [39].

2.3 Using a low-cost feedstock for the lipid production by *C. oleaginosus*

At present, the high fermentation cost of microbial lipids, in which 70–85% belongs to the raw material, is the major obstacle for its industrial development and application, making the microbial lipids less economically competitive [7,42]. *C. oleaginosus* can produce lipids from several low-cost feedstocks, including agricultural residues, food waste and industrial by-products, but often the substrate needs some pretreatment to generate the fermentable carbon sources. The specific process to achieve the final carbon source from waste products is very important since it affects the medium composition, the overall process performance, and the process costs [31,39].

One of the low-costs feedstocks that has been extensively investigated for its potential as an ecologically and economically sustainable choice is the organic fraction of municipal solid waste (OFMSW) [7,43–45]. OFMSW includes food waste, kitchen waste, leaf, grass, flower, and garden waste, etc. Food waste, kitchen waste, and leftovers from restaurants, residences, and cafeterias make up the vast majority of the organic material, whereas the amount of leaf, grass, flower and garden waste varies greatly depending on the season and region [44,45].

OFMSW is the single largest component of the waste stream by weight in the European Union where about 96 million tons are thrown away each year, and the uncontrolled decomposition of OFMSW can contribute to global warming and result in large-scale contamination of soil, water, and air. In addition, the high levels of moisture (85-90 %) content make OFMSW ineffectual for incineration [46,47]. Nevertheless, OFMSW is a lignocellulosic biomass that is abundant, sustainable, and an

inexpensive energy source. Due to the chemical composition of OFMSW, it can be utilized to produce several value-added products, including microbial lipids. Therefore, besides the environmental problems caused by the accumulation of OFMSW in the nature, the non-use of these materials constitutes a loss of potentially valuable sources [48].

2.3.1 Chemical composition of OFMSW

The organic fraction of municipal solid waste (OFMSW) can be classified based on its composition, source, and biological structure, meaning that large variations in its specific content can be observed depending on the source. This complicates the comparison of results from different scientific articles using OFMSW as a low-cost feedstock, since the components available to the microorganism differ in each case. The basis for classification may include regional, seasonal, and socio-economic impacts, but in average, the OFMSW is constituted by 30-70 % carbohydrates, 5-10 % protein, and 10-40 % lipids [44,49].

The carbohydrates constituting the majority of the OFMSW include free fermentable sugar molecules, cellulose, hemicellulose, and lignin. The cellulose, hemicellulose, and lignin are carbohydrate polymers that are closely associated with each other and often they are forming a lignocellulosic complex. Basically, cellulose forms a skeleton which is surrounded by hemicellulose and lignin as presented in Figure 2.5 [48].

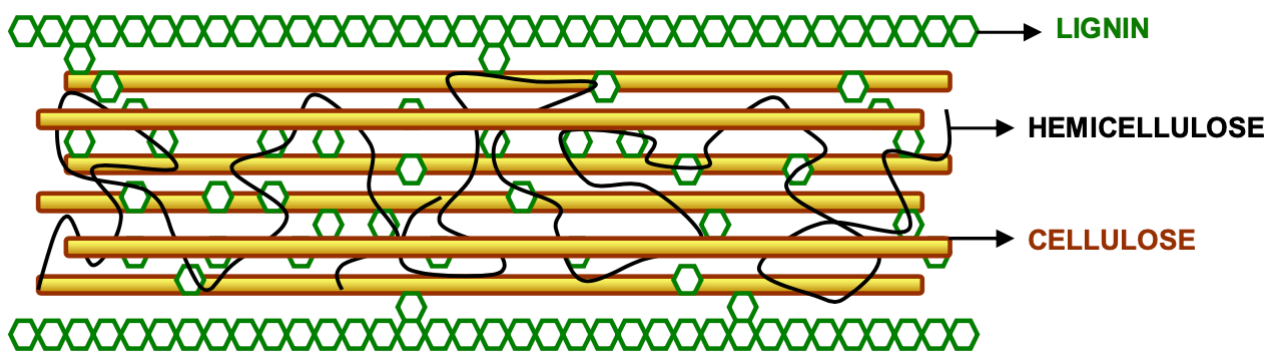


Figure 2.5: Representation of lignocellulose structure showing cellulose, hemicellulose and lignin fractions [48]

The lignocellulosic structure is very hard to degrade, due to the close packing of very complex, internally linked components. Due to this structural complexity and closely packed components, enzymes cannot easily access the components. Therefore, prior to enzymatic hydrolysis, a chemical and/or physical pretreatment is often required to break down the lignocellulosic structure sufficiently to allow for enzymatic degradation [50].

The feasibility of using waste products, such as OFMSW, for lipid production depends on the type of pretreatment needed to deconstruct the lignocellulosic backbone, enzymatic hydrolysis protocols to release the highest fermentable sugar yield from them as well as the fermentation strategies enabling maximum sugar conversion to lipids [51].

2.3.2 Pretreatment methods

Several different methods of pretreatment of lignocellulosic feedstocks have been investigated for their yield, economic feasibility, environmental impact, and industrial application [39]. And of course, the result of the pretreatment must justify its impact on the overall increase of the production costs. It is difficult to define the best pretreatment for all situations and all raw materials, but it is vital that some important features of the pretreatment method are fulfilled [52–54]:

- a) The formation of compounds that eventually can inhibit the growth of the microorganism should be minimized
- b) The energy demands should be as low as possible
- c) The pretreatment should involve a low-cost pretreatment catalyst or an inexpensive catalyst that can preferably be recycled
- d) It must be possible to implement the pretreatment method at an industrial scale
- e) Most importantly, the method should be effective in breaking down the lignocellulosic structure to allow for enzymatic hydrolysis

In general, the pretreatment processes can be divided into four classes: physical methods, chemical methods, physicochemical methods, and biological methods [39,52].

Physical methods:

Physical pretreatment methods have been utilized to enhance the accessibility to hydrolysable polymers within lignocellulosic material. Among the physical pretreatments, mechanical pretreatment is widely used for waste materials, such as agricultural residues or any other crops and forestry residues [55]. It is primarily carried out to reduce the particle size that results in an increased surface area and decreased degree of polymerization and crystallinity. Consequently, the subsequent processes become more effective and easier [56].

Some of the major advantages offered by these processes are the reduction in cellulose crystallinity, the improvement in the available surface for enzymatic hydrolysis, the reduction in the extent of cellulose polymerization, and the improvement in the mass transfer due to particle size reduction. Furthermore, these physical treatment methods are eco-friendly and rarely produce any toxic material. However, among the major disadvantages of the physical pretreatment is its high energy consumption as well as the non-removal of lignin during the process [54,56].

Since lignin present in the biomass causes reduced accessibility of the enzymes for hydrolysis of cellulose and hemicellulose, it has been investigated if chemical methods could potentially increase the success of pretreatment.

Chemical methods:

Chemical pretreatment methods are used more often than physical pretreatment methods because they are more effective and enhance the biodegradation of complex materials [55]. Among chemical pretreatment methods, pretreatment with dilute sulfuric acid is one of the most abundant methods used for breaking down the lignocellulosic material due to its high efficiency. This pretreatment method results in the disruption of the van der Waals forces, hydrogen bonds and covalent bonds that hold together the biomass components, which consequently causes the solubilization of hemicellulose and the reduction of cellulose [55,57].

Although, the concentrated acid pretreatment can highly accelerate the sugar conversion rate (higher than 90%), most of the concentrated acids are very toxic and corrosive and hence require high operational and maintenance costs [56]. Moreover, there is a need for a neutralization step after the acid treatment that in addition to sugar degradation also forms inhibitors. These inhibitory compounds include furans such as furfural from the degradation of pentoses and hydroxymethylfurfural (HMF) from the degradation of hexoses, carboxylic acids from the depolymerization of hemicellulose and further degradation of furans, and phenolic compounds from the degradation of lignin as shown in Figure 2.6. The removal of these inhibitors from the biomass adds cost to the process and generates a waste stream that can cause environmental problems, thereby limiting the use of acid pretreatment of lignocellulosic materials [57,58].

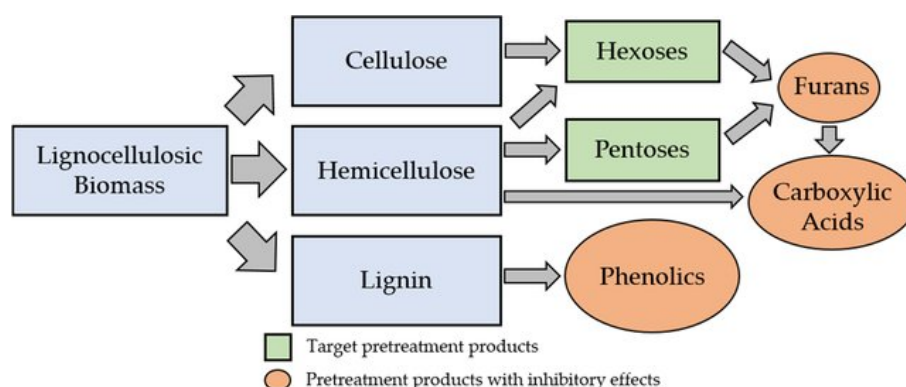


Figure 2.6: Compounds produced from acid pretreatment of lignocellulosic biomass. The green boxes represent the desired pretreatment sugar products, whereas the orange boxes represent the inhibitory compounds produced during acid pretreatment [58].

Physicochemical methods:

Using a combination of some of the physical and chemical methods described above is known as a physicochemical pretreatment method. One of the most commonly used physicochemical methods for pretreatment of lignocellulosic biomass is steam explosion [52]. During pretreatment with steam explosion, lignocellulosic material is exposed to a high-pressure saturated steam at a temperature of 160–260 °C and a corresponding pressure of 5–50 atm for a few minutes. The pressure is gradually released, and the steam expands within the lignocellulosic matrix, causing individual fibers to separate and the cell wall structure to be disrupted [55].

The steam explosion pretreatment process is a well-established technique for the pretreatment of several different biomass feedstocks. This is mainly due to the fact that it utilizes a low capital investment, it has low environmental impacts concerning the chemicals, and the process has been

industrially implemented [57,59]. Furthermore, the fact that the steam-explosion process does not require physical size reduction of the raw biomass is an important feature, considering that the energy required to reduce the particle size can represent a major part of the total energy consumption of the process [57]. Nevertheless, a major disadvantage of using steam explosion as a pretreatment method of lignocellulosic biomass is the considerable number of by-products that is generated during the pretreatment. As it was the case for the acid pretreatment, these by-products include for example furfural, HMF, carboxylic acids, and a wide range of phenolic compounds (see Figure 2.6). Several detoxification methods have been developed to reduce the inhibitory effect of these byproducts on the subsequent yeast fermentation, but this gives rise to an increased costs in the overall process [57].

Biological methods:

In comparison to the chemical and physical pretreatment methods, biological pretreatment is considered as an efficient, environmentally safe, and low-energy process. Biological pretreatments are carried out by microorganisms such as brown, white, and soft-rot fungi which mainly degrade lignin and hemicellulose and little amount of cellulose [44,52]. Furthermore, some studies have suggested that a combination of another pretreatment process with biological pretreatment process is very effective compared to a single pretreatment process [52].

There are several benefits of using a fungal pretreatment step such as it is an eco-friendly procedure, there are no chemical requirements, the energy input is very low, the unit operations are inexpensive, there is little by-product generation, and the production of inhibiting compounds are almost negligible. Nevertheless, a major drawback of fungal treatment is that it is a time-consuming process, and it requires a considerable amount of space. Furthermore, pasteurization of the substrate both prior to fungal inoculation and after pretreatment will add additional cost to the process [44].

The optimal pretreatment method for the break down of lignocellulosic biomass is individual as the composition of the biomass varies greatly. Nevertheless, the overall purpose of the pretreatment processes is to prepare the biomass by deconstructing the lignocellulosic backbone and make the polymers available for enzymatic hydrolysis.

2.3.3 Enzymatic hydrolysis

Enzymatic hydrolysis is the process in which enzymes are added to facilitate the cleavage of bonds in the pretreated biomass into fermentable sugars with the addition of the elements of water. The overall success rate of the process is influenced by the structural features of the lignocellulosic biomass as well as the composition and source of the enzymes [60,61].

As earlier mentioned, the lignocellulosic biomass is mainly composed of three polymers: cellulose $(C_6H_{10}O_5)_n$, hemicellulose $(C_5H_8O_4)_m$, and lignin $[C_9H_{10}O_3(OCH_3)_{0.9-1.7}]_x$ along with minor amounts of other compounds. In general, the cellulose, hemicellulose and lignin contents fall within the range of 30–50 %, 20–35 %, and 5–30 %, respectively. However, the composition of these major components varies depending on the source [54,56].

The enzymes needed for hydrolysis as well as the released enzymatic products from the three different polymers are very different, and collective action among several enzymes is required to break down the complicated lignocellulosic structure [50].

Cellulose

Cellulose, which is the main structural and integral part of lignocellulose, is a linear polysaccharide that consists of D-glucose subunits linked by β -(1,4)-glycosidic bonds [52]. The exceptional crystallinity, high degree of polymerization (up to 10,000 units), and presence of a network of intermolecularly and intramolecularly hydrogen bonded hydroxyl groups is responsible for the complicated structure of crystalline cellulose shown in Figure 2.7 [54].

Depolymerization of cellulose requires the combined enzymatic activities of an endoglucanase, two types of exoglucanases and one β -glucosidase. It is generally an accepted theory that the cellulases act sequentially and synergistically. First, the endoglucanase randomly cleaves the cellulose backbone at amorphous sites along the cellulose fiber. This leads to a decreased degree of polymerization and exposes new reducing and non-reducing chain ends on which exoglucanases act to release mainly cellobiose. And lastly, a β -glucosidase hydrolyze the β -1,4 glycosidic bond of cellobiose to release glucose units [20,50]. However, it is commonly known that glucose exert inhibitory effects, directly affecting β -glucosidase activity. Inhibition of β -glucosidase results in an increased cellobiose concentration that subsequently act as a strong inhibitor of exoglucanase enzymes as it is illustrated in Figure 2.7. This common biological process is known as feedback inhibition [62]. Strategies to overcome feedback inhibition includes the use of high concentration of enzymes, addition of extra β -glucosidases and continuous removal of sugars during enzymatic hydrolysis. Moreover, to minimize the feedback inhibition due to the accumulation of cellobiose, the system can be supplemented by an additional amount of exoglucanases to enhance the activity of these enzymes [62].

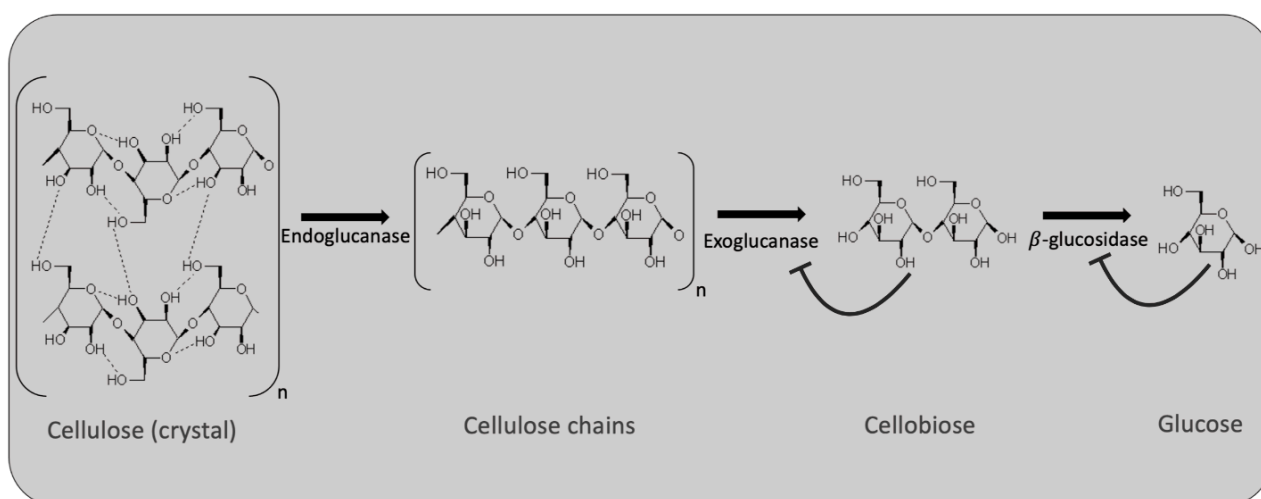


Figure 2.7: The enzymatic hydrolysis of crystalline cellulose and the cellulase enzymes involved in each step. An endoglucanase is needed to break down the crystalline structure and produce polymer chains of cellulose, two types of exoglucanases (one acting at the reducing end and one acting at the non-reducing end) are needed to convert the polymer chains to cellobiose and lastly, a β -glucosidase is needed to cleave the β -1,4-glycosidic bond in cellobiose to produce glucose monomers.

Hemicellulose

Hemicellulose is the second major component of lignocellulose that mainly consists of pentoses, such as xylose and arabinose, and hexoses, such as mannose, glucose, and galactose, that are held together by β -(1,4)- and/or β -(1,3)-glycosidic bonds as shown in Figure 2.8. In addition, hemicellulose often also has considerable side chain branching consisting of hydrolysable polymers [56,59]. Among different hemicellulose structures, xylans are the most abundant polysaccharides that often form a backbone with branching side chain polymers [63]. The hemicellulose fraction acts as a binding agent between the cellulose and lignin fractions and adds rigidity to the overall biomass matrix [54,64].

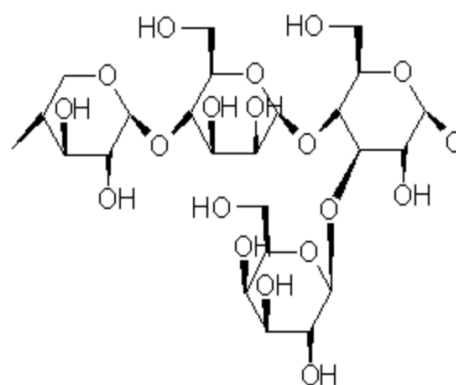


Figure 2.8: A typical chemical structure of hemicellulose could be xylose- β (1,4)-mannose- β (1,4)-glucose- α (1,3)-galactose [64].

The depolymerization of heavily branched and substituted hemicellulose structures also requires an entire complement of enzymes. At least one kind of endoxylanase is needed to break the xylan backbone. The endoxylanase activity is assisted by a range of other hemicellulases (acetyl xylan esterase, arabinofuranosidase, and ferulic acid esterase), usually with synergistic activity. Many of the hemicellulase enzymes are not always included in commercialized enzyme blends for lignocellulosic materials because many of the linkages cleaved by these enzymes are already broken down during the pretreatment processing due to the amorphous structure of hemicellulose [50].

Lignin

Lignin is the third polymeric organic component of lignocellulose. It is a complex chemical compound mostly derived from wood, and an integrated part of the secondary cell walls of plants. It is a complex, three-dimensional cross-linked polymer that consists of phenyl propane structural units that can vary depending on the substitute of the methoxy groups present in the aromatic rings. The units are linked to each other by ether linkages and carbon-carbon bonds as shown in Figure 2.9 [56,65]. As a biopolymer, the handling of lignin is more difficult due to its lack of defined primary structure, and the random, high degree of polymerization of lignin has made it an intensive field of study [65].

The most prominent types of enzymes active in lignin degradation are the laccases and peroxidases (both types are oxidative enzymes). However, such enzymes do not react independently, and compounds of small molecular weight (redox mediators) are needed to act as electron shuttles performing the oxidation of lignin that do not have access to the enzyme's active site [50,66].

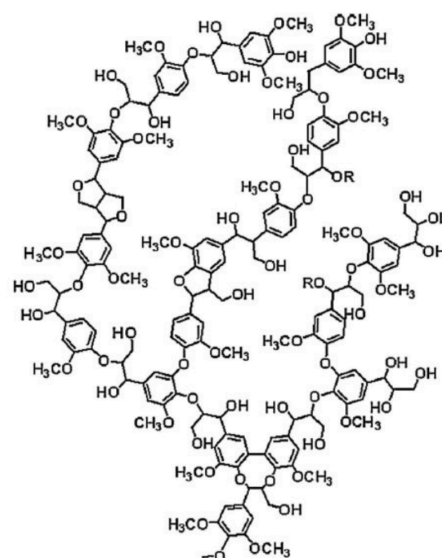


Figure 2.9: Chemical structure of lignin linked by ether linkages and carbon-carbon bonds [64].

The concentration of different enzymes as well as the composition of the enzyme mix needed for the enzymatic hydrolysis of the lignocellulosic material of interest can be investigated in an infinite number of combinations. However, optimization of the overall conversion from OFMSW to lipids is not limited to the pretreatment.

2.4 Improving the fermentation strategy

As previously mentioned, several improvements must be implemented to lower the financial expenses and thereby make the overall microbial lipid-producing fermentation process economically feasible [7,17]. Several different ways to improve the economic aspect of the process exist, both upstream, during fermentation, and downstream [67]. The area of interest to achieve this improvement in this thesis is within the fermentation setup which includes both the enzymatic hydrolysis and the fermentation strategy as well as the genetic engineering of the yeast strain of interest, which in this case is *C. oleaginosus*.

2.4.1 Mode of enzymatic hydrolysis and fermentation

The use of a lignocellulosic feedstock for the lipid production requires an enzymatic hydrolysis to convert cellulose and hemicellulose to free fermentable sugars that can then be converted to lipids by a yeast fermentation. If the enzymatic hydrolysis and fermentation is conducted separately, the process is called separate hydrolysis and fermentation (SHF) and a schematic is presented in Figure 2.10A [68–70]. When performing the two processes separately, it is possible for the enzymes and the yeast to work at their optimal conditions with respect to temperature in each of their tank [68]. However, the SHF has the disadvantage that inhibitory products of the hydrolysis accumulate which reduces the reaction rate and eventually makes the overall product formation stop. To overcome the feedback inhibition of the product during enzymatic hydrolysis, it has been suggested that saccharification and fermentation can be conducted in the same fermentation tank [71]. This process is known as a simultaneous saccharification and fermentation (SSF), and it is illustrated in Figure 2.10B. When enzymatic hydrolysis of cellulose and fermentation are conducted in the same reactor, the glucose generated during cellulose hydrolysis is rapidly utilized by the microorganisms. Feedback inhibition of glucose is in this way reduced, which potentially improves the efficiency of enzymatic hydrolysis and reduces the amount of enzymes needed for the hydrolysis [69].

Some of the advantages of using SSF compared to SHF are the use of a single container for fermentation and hydrolysis, which reduces both residence times and the cost of capital of the process. Another prominent benefit is the reduction of product inhibition from enzymatic hydrolysis, which can potentially improve the overall performance of the process [8,67,70].

On the other hand, SSF also has disadvantages that limit its use at an industrial level compared to SHF. Among the disadvantages are the optimal pH and temperatures of the processes, as the optimal temperature for enzymatic hydrolysis is typically much higher than the fermentation temperature. Thus, it is necessary to find a compromise that provides the optimal conditions for both processes resulting in the maximum possible lipid production. However, this maximum lipid production that can be achieved using SSF is not necessarily higher than the maximum lipid

production that can be achieved using SHF [70]. The best method can vary for each individual process which means that laboratory experiments must be conducted to determine whether SHF or SSF is the best choice in each case.

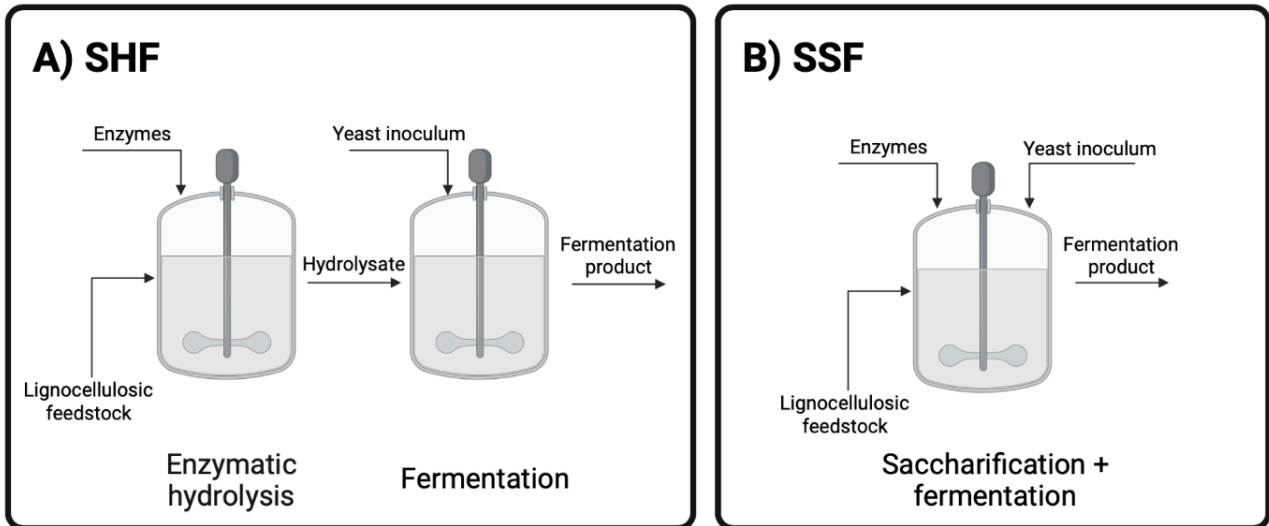


Figure 2.10: Schematic of the principle behind separate hydrolysis and fermentation, SHF (A) and simultaneous saccharification and fermentation, SSF (B) including the timepoint for addition of enzymes and yeast inoculum. The figure was adapted from [72] and created with Biorender.com.

The mode of fermentation can potentially lower the expenses of the process since less time may be needed to achieve the optimal lipid production. It could possibly also increase the overall lipid production even when the yeast strain is consistent throughout the fermentations due to a reduction in the product inhibition during enzymatic hydrolysis. However, if it is intended to increase the overall lipid production significantly, it may be worth exploring the possibilities of genetic manipulation of the biological lipid producing pathways within the yeast. Genetic engineering of the yeast could possibly also lower the costs associated with the addition of commercial enzymes to hydrolyze the complex feedstock if a genetically engineered yeast strain is able to produce the necessary enzymes during fermentation.

2.4.2 Genetic engineering for enhanced lipid production

Most of the published genetic engineering studies in oleaginous yeasts have focused on species within the *Yarrowia* genus since tools, recommendations, and protocols for genetic engineering in *Yarrowia* already have been developed and optimized [73,74]. Researchers have successfully modified endogenous gene expression in *Yarrowia lipolytica* to enhance lipid biosynthesis, mainly using glucose as sole carbon source [74]. Overexpression of the genes directly involved in fatty acid or TAG synthesis [75,76], or deletion of the genes involved in competing pathways, such as beta-oxidation or TAG remobilization [77], has generated strains that can accumulate up to 90% of their DCW as fatty acids [78] or that can reach a yield of 84.7% of the theoretical maximal yield [73]. Furthermore, mutant strains of *Y. lipolytica* have been shown to be able to grow on several different carbon sources, including xylose, even though the wild type of *Y. lipolytica* does not utilize xylose [79,80]. This is of interest when it is intended to use cheap lignocellulosic materials as the feedstock

since up to 50 % of the lignocellulosic material can be xylose [79,81]. In another article [82], they showed that they were able to engineer *Y. lipolytica* in such a way that it enabled lipid secretion into the culture media, which allowed them to go beyond the maximum lipid accumulation capacity and to facilitate the recovery of the lipids; these downstream processes can be up to 40-80 % of the total costs of the process [82].

Even though there is plenty of researchers working on the genetic engineering of *Y. lipolytica* aiming at increasing the lipid production, there is still a doubt among other researchers whether this yeast is the optimal candidate for an industrial lipid production site. If it is possible to genetically engineer some of the yeast strains that naturally accumulate higher amounts of lipids in such a way that the expenses of the process can be lowered from an industrial point of view, it is believed that it would outcompete even the best mutated strains of *Y. lipolytica*.

2.5 Methods for genetic engineering of *C. oleaginosus*

Compared to *Yarrowia*, the genetic engineering of other oleaginous yeasts is still limited due to the lack of genetic tools and generally insufficient knowledge of the cellular genetics within these yeasts [16]. However, recent studies focusing on the establishment of the genetic availability have improved the possibilities for developing a more economically feasible lipid production process in these yeast species [83,84]. But more advanced genetic tools and a better understanding of the genetics are still in demand if the full potential of these yeast species as a platform for lipid production is to be exploited [16].

Only two groups of researchers have published articles in which they have successfully transformed *C. oleaginosus* [17,19], which indicates that this area of research is crying out for improvements, but it is also clear that it is challenging to develop an efficient and successful transformation protocol for this yeast. In the study by Görner et. al. [17], an *A. tumefaciens* mediated transformation (ATMT) protocol for *C. oleaginosus* was established. Transformants were successfully selected, and it was demonstrated that *C. oleaginosus* can be engineered to produce significant concentrations of high value fatty acids. This was shown by random integration of codon optimized synthetic versions of the $\Delta 9$ elongase IgASE2 gene from *Isochrysis galbana*, the $\Delta 12/\omega 3$ desaturase Fm1 gene from *Fusarium moniliforme* and the linoleic acid isomerase PAI gene from *Propionibacterium acnes* [17]. In the study by Koivuranta et.al. [19], they established a PDH (pyruvate dehydrogenase) bypass by expressing codon optimized versions of PDC (pyruvate decarboxylase), ALD (acetaldehyde dehydrogenase) and ACS (acetyl-CoA synthetase) encoding genes in various combinations in *C. oleaginosus* by transformation with electroporation and demonstrated that the yield of lipids was improved both when using glucose and xylose as the carbon source. Furthermore, it was found that expression of a PDAT (phospholipid:diacylglycerol acyltransferase) encoding gene together with the PDH bypass enhanced the lipid production even further [19].

There are many other interesting genes involved in the lipid biosynthesis pathway that could increase the production of lipids in *C. oleaginosus* and there is no doubt that several researchers will investigate the effect of integrating these different genes in the following years. However, since

it has already been shown that it is possible to manipulate the biosynthetic pathway of lipid production and thereby increase the lipid yield, it might be even more interesting to look in another direction.

2.5.1 Interesting possibilities for genetic engineering of *C. oleaginosus*

As previously mentioned, *C. oleaginosus* has been shown to be able to utilize pentoses as a carbon source [85] which means that it is not necessary to genetically engineer the wild-type strain to utilize the xylose released from the hemicellulose present in lignocellulosic feedstocks as it was the case for *Y. lipolytica* [79,80]. Furthermore, other studies have verified that *C. oleaginosus* can tolerate lignocellulosic hydrolysis byproducts which is a key feature if it is intended to use lignocellulosic materials for the yeast fermentation [86]. However, there are other ways in which genetic engineering can potentially optimize the ability of this yeast strain to use lignocellulosic materials as the feedstock from an economical and industrial point of view.

The high cost of the addition of purchased enzymes remains the main barrier in the process of bioconversion of lignocellulosic biomass [87]. Thus, a variety of methods have been suggested to achieve a reduction in the amount of enzymes required for the enzymatic hydrolysis including gradual loading of substrate, minimal loading of enzyme, recycling or recovery of enzyme and avoiding product inhibition by continuous product removal [88–91]. However, there is very little published literature investigating the possibility of genetically engineering an oleaginous yeast strain to be able to produce the enzymes necessary for the conversion of lignocellulosic biomass. Around 50 % of the industrial enzymes used globally are of fungal origin. This is mainly because fungal enzymes have a sufficient protein stability to give the enzyme products an acceptable shelf life and that they meet regulatory approval requirements [50]. Most industrial cellulases are produced using either *Trichoderma* or *Aspergillus* species as expression and production hosts [92]. Interestingly, *Trichoderma* and *Aspergillus* species also function well as production hosts for a broad spectrum of enzyme genes derived from other parts of the fungal kingdom, including species of Basidiomycota. However, production of basidiomycete genes in ascomycetous hosts still result in lower yields compared to ascomycetous genes [50].

Considering the above, it may also be possible to introduce a cellulase-encoding gene of fungal origin into the genome of the yeast *C. oleaginosus* to reduce the need for addition of expensive industrial enzymes during lipid fermentation.

2.5.2 Choosing a cellulase-encoding gene for expression in *C. oleaginosus*

To choose the most interesting cellulase-encoding gene for expression in *C. oleaginosus* aiming at reducing the need for addition of industrial enzymes, it is essential to investigate the natural enzyme production in *C. oleaginosus*. Unfortunately, there is a limited number of published scientific studies considering the enzyme production in *C. oleaginosus*. However, Fuchs et. al. recently published an article [30] in which they conducted a proteomic analysis of the secreted, cell wall-associated, and cytoplasmatic hydrolases produced by the yeast when grown on different mono- or disaccharides. They were able to detect 58 different enzymes and their functions during growth on either glucose,

cellobiose, lactose, maltose, sucrose, or trehalose. Each of the detected enzymes were either down- or up-regulated depending on the cultivation media. For example, when *C. oleaginosus* was grown on cellobiose, the secreted hydrolase with the second highest activity was determined to be an exoglucanase (enzyme number in article: H12) acting on the non-reducing end, but the level of expression was found to be very low. In addition, a significant activity of an endoglucanase (H18) and a β -galactosidase (H48) was observed. On the other hand, when grown on maltose, high activities of α -glucosidases (H2 and H14) were observed, and expression of an α -amylase (H5) was upregulated nine-fold compared to that of glucose. And when grown on lactose, the activity of a β -galactosidase (H28) that cleaves the terminal bound β -D-galactose from molecules were highly upregulated. Thus, it was concluded that the secretion and expression of hydrolases in *C. oleaginosus* are highly dependent on the cultivation media.

However, as previously mentioned, the depolymerization of cellulose requires an endoglucanase, exoglucanases and a β -glucosidase [50]. And since the growth pattern on cellobiose and glucose was found to be very similar [30], *C. oleaginosus* must be able to either cleave the β -1,4-glycosidic bond on its own using a β -glucosidase or be able to transport the cellobiose through the cell wall for metabolic utilization. But for the yeast to grow on cellulose, it must be able to release the cellobiose from the ends of the cellulose chains using an exoglucanase. In the article by Fuchs et. al. [30] an exoglucanase (H12) was found to have high activity but very low level of expression, and therefore, it would be interesting to investigate the possibilities of expressing a fungal gene encoding an exoglucanase in *C. oleaginosus* to determine if that improves the ability of the yeast to grow on a lignocellulosic material comprising cellulose.

The most studied cellulolytic fungus, *Trichoderma reesei*, produces up to about 80% of the total secreted protein as exoglucanases, and the best production strains can secrete tens of grams per liter of these enzymes [93]. There are two fungal exoglucanase classes, separated into CBH1 and CBH2 based on their sequence similarity and predicted structural and functional relationships. The catalytic domains of these two enzyme classes are structurally different but both share a tunnel-like active site [93]. An advantage of introducing *cbh1* or *cbh2* genes encoding exoglucanases from *T. reesei* into the genome of *C. oleaginosus* is that they have been shown to be able to hydrolyze crystalline cellulose in the absence of endoglucanases [94]. Furthermore, both *cbh1* and *cbh2* genes have previously been successfully expressed in the ascomycetous yeasts *S. cerevisiae* [95,96], *P. pastoris*, [97] and *Y. lipolytica* [98] and secreted into the cultivation media. However, in the study by Wei et. al. [98] they say that expression of the *cbh1* gene from *T. reesei* in *Y. lipolytica*, *S. cerevisiae* and *P. pastoris* is notoriously difficult and they suggest that it may be explained by the fact that the folding or post-translation modification of heterologous CBH1 in yeast cannot completely mimic that in the original source strain, *T. reesei*. To solve this problem, they investigated the possibility of introducing a Tr-Te chimeric CBH1 containing the catalytic domain from *Talaromyces emersonii*, the linker and carbohydrate-binding molecule (CBM) from *T. reesei* and the XPR2 signal peptide from *Y. lipolytica*. Interestingly, the measured activity of the Tr-Te chimeric CBH1 was found to be nearly the same as the native CBH1 produced in *T. reesei*.

Based on this study by Wei et. al. [98], it would be interesting to introduce the same Tr-Te chimeric CBH1 into *C. oleaginosus* but to exchange the signal peptide from *Y. lipolytica* with a signal peptide from *C. oleaginosus*. In the previously mentioned study by Fuchs et. al. [30] in which they investigated the natural production of hydrolases in *C. oleaginosus*, they identified several glycosylated peptides in the secreted enzyme fraction and discovered numerous carbohydrate-related proteins that are potentially involved in the cellular export. Adding one of these potential signal peptides to the Tr-Te chimeric CBH1 may increase the chance of correct post-translational modifications of the enzyme as well as successful secretion of the enzyme into the lignocellulosic cultivation media.

However, to obtain an acceptable enzyme yield and for successful expression in the basidiomycete host *C. oleaginosus*, codon-optimized synthetic versions of the ascomycetous genes are required. The codon usage in *C. oleaginosus* was only briefly described by Meesters et. al [99] from cloning of the $\Delta 9$ fatty acid desaturase gene. The $\Delta 9$ fatty acid desaturase gene in *C. oleaginosus* was found to have a GC-content of 61 % and display a codon usage different from that of *S. cerevisiae*, but closely related to that of basidiomycete fungi. For example, in the case of the amino acids Gln, Cys and Glu, they concluded that *C. oleaginosus* prefers the codons CAG, TGC and GAG respectively, while *S. cerevisiae* prefers CAA, TGT and GAA. In general, it was found that *C. oleaginosus* prefer to have a C at third positions of codons and generally it is avoided to have an A in the third position [99].

This codon usage also indicates that *C. oleaginosus* is more related to basidiomycete fungi than to *S. cerevisiae*. Therefore, tools available for basidiomycete fungi, may be useful for the development of transformation and expression systems for *C. oleaginosus* [99]. Although there exist transformation methods that can be used to edit target genes at the genomic level in basidiomycete fungi, the low editing efficiency and the consequently large amount of necessary labor time limit the further development of these technologies [100]. Consequently, the development of a simple, fast, and cheap transformation system with high efficiency is in high demand.

2.5.3 Improving the transformation system for *C. oleaginosus*

It can be a good strategy to implement previously established successful transformation systems when looking for new and improved methods. In the study by Görner et. al [17], several plasmids containing the left and right T-DNA border sites (LB and RB) for *Agrobacterium tumefaciens* mediated transformation (ATMT) was constructed, and the plasmid pRF-HU2-hyg-yfp from the article illustrated in Figure 2.11 (Figure S5 in the original article) could potentially be used as the template for constructing a new successful transformation system for *C. oleaginosus*.

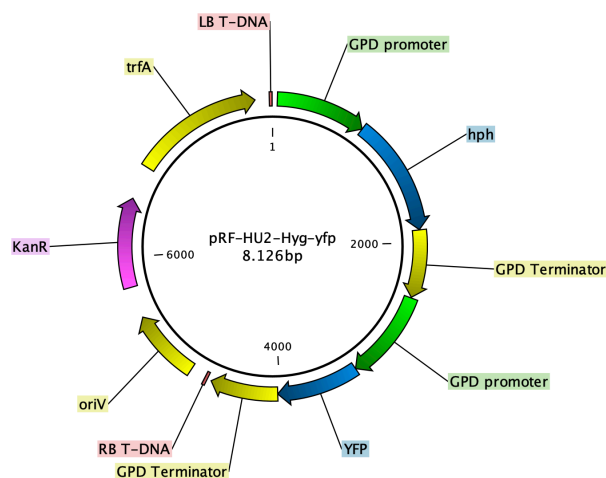


Figure 2.11: Plasmid map of the pRF-HU2-hyg-yfp plasmid from the study by Görner et. al. [17].

Agrobacterium tumefaciens mediated transformation (ATMT)

It is well known that *A. tumefaciens* has the ability to transfer a fragment of DNA (T-DNA) from its tumor-inducing (Ti) plasmid to a recipient's genome by infecting the receiving cell [101–103]. The boundaries of the T-DNA region are defined by two imperfect repeats (25 bp long) called the right and left borders (RB and LB), and it was quickly realized that any genetic material placed between the RB and LB sequences would be introduced into the genome of the targeted cells [101]. However, the large size of the Ti-plasmid, the low copy number, and the inability to replicate in *E. coli*, etc. initially made it very difficult to genetically manipulate by standard techniques [102]. Therefore, the laboratory strains that are used for ATMT have been disarmed by erasing the genes responsible for creating tumors, while the virulence genes that cause the infection and mediate the transfer of T-DNA are still unaffected (the *vir* helper plasmid) [102,103].

The transformation technique that has been used for the last two decades relies on a binary vector system in which the virulence genes and the T-DNA regions are split onto two separate replicons (Figure 2.12) [102,104]. As long as both of these replicons are located within the same *Agrobacterium* cell, proteins encoded by virulence genes can transact upon T-DNA to mediate its processing and export to the recipient cell [102]. By including the RB and LB boundaries of the T-DNA on the small shuttle vector (the binary plasmid) used for transformation, it is possible to integrate any foreign genes or DNA sequences placed between the two borders into the recipient's genome by ATMT [103].

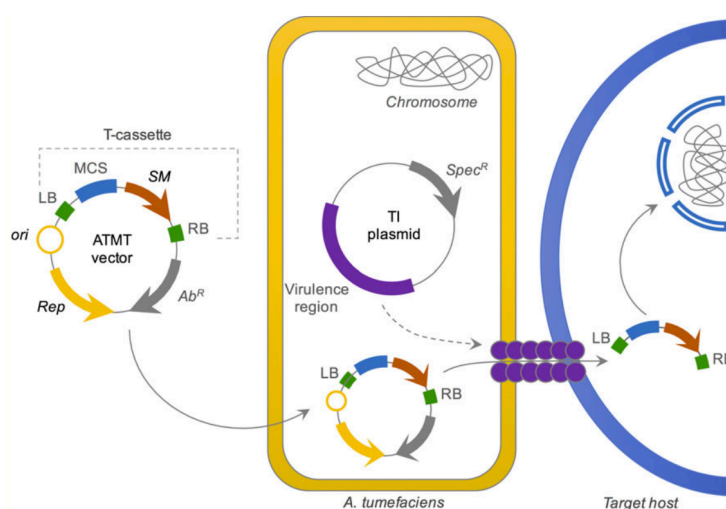


Figure 2.12: *Agrobacterium tumefaciens* mediated transformation (ATMT) is based on a binary vector system, where the shuttle vector harbors a T-cassette which may be composed of a multiple cloning site (MSC) and a selection marker (SM) flanked by the left and right border sites (RB and LB). Once inserted into the *A. tumefaciens* strain containing the Ti plasmid expressing the virulence genes necessary for transfer of the T-DNA, the DNA sequence located between RB and LB can be integrated into the recipients genome [104].

Based on the established protocol for ATMT of *C. oleaginosus* presented by Görner [27], it is a good idea to keep the RB and LB sequences in the plasmid. However, it may be possible to make several other improvements to increase the robustness of the transformation system. Complex molecular genetic techniques demand efficient and cost-effective DNA cloning methods and the increasing size and complexity of today's constructs in metabolic engineering has made design and construction of plasmids increasingly complicated and time consuming [105,106].

Several *in vitro* techniques have been developed to overcome these issues and methods such as Gibson assembly and USER cloning enable efficient assembly of up to five or six overlapping DNA fragments into a plasmid [105,107]. However, the efficiencies of these systems decrease at higher numbers of fragments and commercial kits are required to obtain the necessary recombinases. In contrast, *in vivo* assembly of multiple overlapping DNA fragments by homologous recombination in *Saccharomyces cerevisiae* does not exhibit these limitations [105].

Plasmid assembly by homologous recombination in *S. cerevisiae*

The popular and highly efficient cloning method utilizes the ease and simplicity of homologous recombination in *S. cerevisiae* as shown in Figure 2.13 [108]. Yeast recombination cloning allows assembly of multiple DNA fragments in a single step and many variations of transformation protocols have been described [109–111]. It is extremely efficient and requires only 30 nucleotides of overlapping sequences, however, it is important to remember that plasmid assembly by yeast homologous recombination needs a yeast compatible shuttle vector [106]. There are two elements that are essential for survival: i) a yeast centromere sequence (CEN) and an autonomously replicating sequence (ARS) and ii) a selection marker gene. Presence of these survival elements are essential for replication and selection of the plasmid [105].

ARS contains the origin of replication in the yeast genome and plasmids containing ARS elements are normally present in multiple copies and replicate once per cell cycle. However, during cell division, such plasmids segregate preferentially into mother cells and this bias leads to continuous plasmid loss. However, if a CEN sequence is grafted onto a plasmid already containing an ARS, the resulting vector plasmid is stabilized and segregates accurately [112]. The other important element of a yeast vector is the incorporation of selectable marker which allows selection of vector harboring-transformants. The currently most commonly used yeast selectable markers include the auxotrophic marker genes *LEU2*, *HIS3*, *URA3* and *TRP1* [113]. Auxotrophic markers are single gene perturbations of essential metabolic pathways, that are exploited in the efficient selection of plasmids. For a metabolic gene to function as an auxotrophic marker, it needs to be part of a metabolic pathway for which the cells possess an extracellular uptake. Auxotrophic marker mutations are hence associated with metabolites that are readily taken up from the environment, in particular amino acids [114].

Since homologous regions of the plasmid will recombine with each other during cloning procedures, it is not optimal to reuse the same promoter and the same terminator twice in a plasmid. Therefore, replacing the promoter and terminator in one of the cassettes with another promoter and terminator will definitely increase the robustness of the transformation system. That could potentially be the well-known constitutive promoter of the translation elongation factor α gene (*TEF1- α*) from *C. oleaginosus* and the associated terminator.

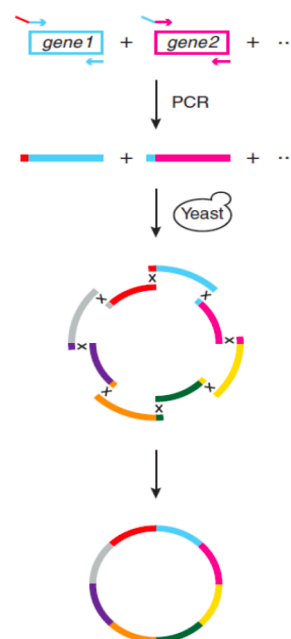


Figure 2.13: *In vivo* recombination of multiple fragments in *S. cerevisiae* using homologous double-stranded DNA sequences introduced by PCR [108].

3 Problem formulation

As described in the previous literature review, biodiesel derived from lipids has proven to be a promising alternative when it comes to transportation fuels. However, its development and use have been hindered by low lipid yields and high production costs when compared to e.g., fossil fuels. This means that there is an increasing interest in investigating new and economically favorable methods for producing lipids that can be used for biodiesel production.

Therefore, the objective of this master thesis is to examine the lipid production during fermentation with the yeast *Cutaneotrichosporon oleaginosus* using the organic fraction of municipal solid waste (OFMSW) as the feedstock. As part of this investigation, two time-studies are conducted to determine the optimal time for fermentation and whether separate hydrolysis and fermentation (SHF) or simultaneous saccharification and fermentation (SSF) results in the highest lipid production with a predefined mix of enzymes.

The need for these enzymes that can break down the cellulose and hemicellulose present in the OFMSW into free fermentable sugar molecules is a major expense in the production process. Therefore, it is very interesting to explore the possibilities of reducing the need for these enzymes in the fermentation process. This thesis aims to genetically engineer *C. oleaginosus* by inserting a codon optimized version of a *cbh1* gene responsible for the production of an exoglucanase into the genome of the yeast by *Agrobacterium tumefaciens* mediated transformation (ATMT). More specifically, it is intended to produce a Tr-Te chimeric CBH1 exoglucanase containing the catalytic domain from *Talaromyces emersonii*, the linker and carbohydrate-binding molecule (CBM) from *Trichoderma reesei*, as well as a signal peptide from an endoglucanase from *C. oleaginosus*.

Lastly, it is intended to investigate the effect of random integration on the level of expression by measuring the yfp fluorescence over time of several different *C. oleaginosus* mutants obtained during the laboratory work conducted in this master thesis.

4 Materials and methods

The experimental work during this thesis project was designed to optimize the production of lipids by the oleaginous yeast *Cutaneotrichosporon oleaginosus* using OFMSW as the feedstock. This was done by conducting time studies of fermentation, genetically engineering the yeast strain to reduce the need for the addition of enzymes and testing the performance of the produced mutant strains in a fermentation setup.

4.1 Time studies on yeast fermentations using OFMSW as the feedstock

A general workflow of laboratory work performed during the time studies of the yeast fermentations using OFMSW as the feedstock is presented in Figure 4.1. The different setups and conditions for the separate hydrolysis and fermentation (SHF) and the simultaneous saccharification and fermentation (SSF), respectively, is presented in the following subsections and are not included in the figure.

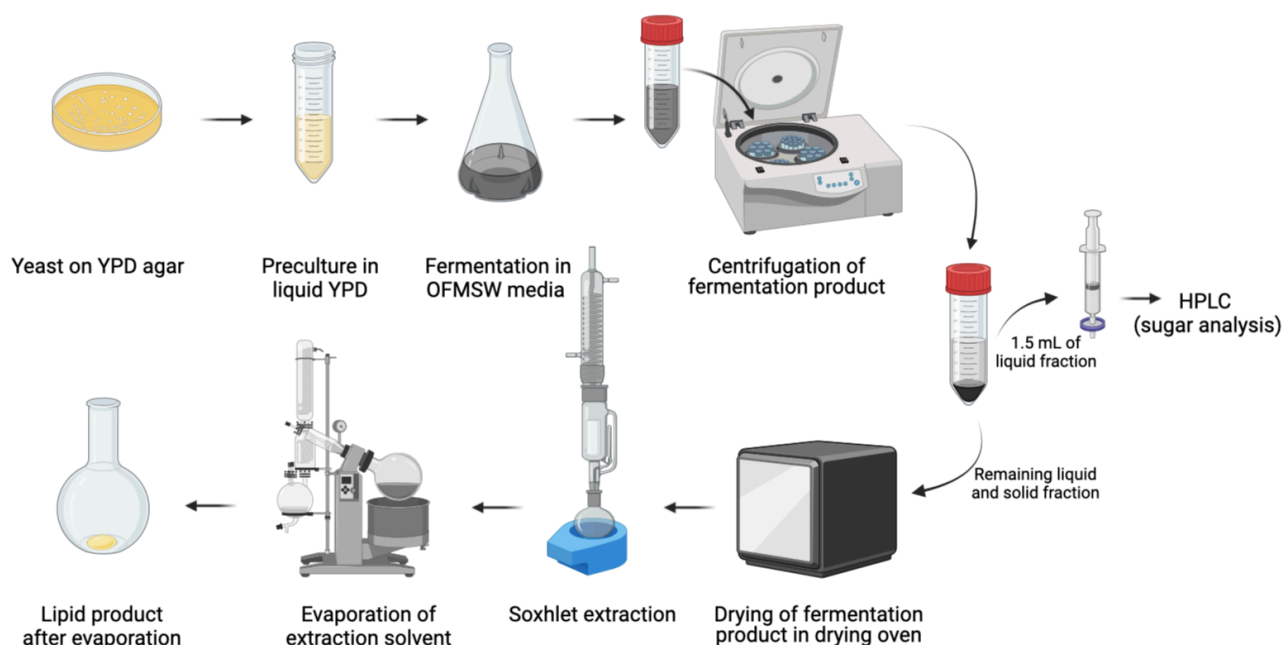


Figure 4.1: General workflow presenting each of the steps in the laboratory work that was conducted during the time studies of the yeast fermentation with OFMSW media. The figure was created with BioRender.com.

4.1.1 Preparation of OFMSW

The experimental OFMSW was prepared in the laboratories at AAU Esbjerg and contains the ingredients that are listed in Table 4.1 below.

The composition of the experimental OFMSW was based on a study by Edjabou M. et al. [115] in which they evaluated the average weighted composition of Danish household food waste. They found that the dominant food products (% mass pr wet basis) were fresh vegetables and salads (30 %) and fresh fruit (17 %), followed by bakery (13 %) and drinks, confectionery, and desserts (13 %).

Table 4.1: The composition of the experimental OFMSW used for the experimental work conducted in this master thesis. The experimental OFMSW was prepared at the laboratories of AAU, Esbjerg.

Category	Percentage (%)	Ingredients	Total mass for preparing 50 kg of OFMSW
Vegetables, salads	30	Carrots, potatoes, cucumber, tomatoes, peppers, iceberg, broccoli, pointed cabbage, avocado, onion, spring onions, champignons, garlic	15 kg
Fresh fruits	17	Banana, grapes, apples, pears, blueberries, melon, oranges	8.5 kg
Bakery	13	Baker's yeast, danish "rugbrød", roasted onions, toast bread, buns	6.5 kg
Drinks, snacks, dessert	13	Tea bags, coffee grounds, chocolate, candies, frozen pizza, nuts, chips, biscuits	6.5 kg
Meat and fish	8	Liver pâté, ground beef, bacon, salmon, chicken, sausage, shrimps	4 kg
Dairy, eggs	7	Milk, eggs, cheese, butter, creme fraiche, whipped cream	3.5 kg
Herbs, sauces, spices	2	Tomato sauce, ketchup, mayonnaise, honey, jam, parsley, peanut butter	1 kg
Canned food	2	Beans, corn, tuna, mackerel, cod, chopped tomatoes, peas, olives	1 kg
Stable	8	Rice, pasta, flour, oats, cereals	4 kg

The ingredients were mixed and blended to the best of our ability to make the experimental OFMSW as homogenous as possible. The prepared OFMSW was sealed in plastic bags and stored at -80 °C until further use. When needed, a plastic bag with OFMSW was thawed in the fridge at 5 °C and prepared for experiments. In all hydrolysis and fermentation experiments, the OFMSW was mixed with demineralized water at a solid loading of 50 % (w/v) and stirred to get a more liquified waste media. The waste media was autoclaved (121 °C for 20 min) prior to use in all experiments.

4.1.2 Enzymatic hydrolysis of OFMSW

Enzymatic hydrolysis of OFMSW was carried out in 250 mL Erlenmeyer flasks, containing 50 mL of autoclaved waste media (50 % w/v) as well as the enzyme complex (see section 4.1.2.1), placed in a shaking incubator (150 rpm) for different periods of time at 30 °C or 50 °C, respectively. Medium without enzymes were used as control for the hydrolysis experiments.

After hydrolysis, the media was centrifuged, and 1.5 mL of the supernatant was used for analyzing the sugar concentration with HPLC. The weight of the biomass was determined by drying the remaining content, including both solids and liquids, in an oven for at least 24 h at 105 °C.

4.1.2.1 Enzyme complex:

An enzyme complex with the following ratio was used for all experiments that required the addition of enzymes. This ratio was recommended by Novozymes A/S Denmark based on the composition of the experimental OFMSW.

amylase : cellulase : hemicellulase : pectate lysase : lipase : protease 1 : 1 : 0.2 : 0.2 : 0.2 : 0.2

The volume of amylase added to the fermentation flasks was set to 1 kg pr 77 kg of OFMSW based on the activity of amylase determined in our laboratories (620 U/ml) and the suggestion by Yan et. al. [116] to use 8 units of enzyme pr g of OFMSW. The amount of the other enzymes in the enzyme complex were measured accordingly, which means that the volumes listed in Table 4.2 were used for 50 mL waste media (50 % w/v) in all experiments that included enzymes.

Table 4.2: Names and manufacturer of enzymes as well as the volumes used for fermentations with 50 mL waste media (50 % w/v)

Enzyme	Manufacturer	Volume (µL)
Cellic (cellulase mix)	Novozymes, Cellic CTec2	320
Amylase	Novozymes, NS22028	320
Hemicellulase	Novozymes, NS22240	65
Pectate lyase	Novozymes, NS22185	65
Lipase	Novozymes, NS22031	65
Protease	Novozymes, NS22167	65

4.1.3 Yeast strain and media

The yeast strain *Cutaneotrichosporon oleaginosus* (ATCC 20509) was maintained on plates of YPD agar (20 g/L agar, 20 g/L peptone, 10 g/L yeast extract, 20 g/L glucose) at 4 °C. For activation, the yeast was streaked on a new YPD agar plate and incubated at 30 °C for 48 h. The grown colonies were inoculated into 50 mL centrifuge tubes containing 35 ml of liquid YPD medium (20 g/L peptone, 10 g/L yeast extract, 20 g/L glucose) and incubated in a shaking incubator (150 rpm) at 30 °C for 48 h to prepare a preculture of the yeast. Finally, the resultant cell pellet was resuspended in 1 mL autoclaved water to prepare for inoculation in fermentation flasks for SHF and SSF, respectively.

4.1.4 Separate hydrolysis and fermentation (SHF)

For the separate hydrolysis and fermentation (SHF) process, 250 mL Erlenmeyer flasks containing 50 mL of waste media (50 % w/v) and the enzyme complex was left in a shaking incubator (150 rpm) at 50 °C for 24 h, which was found in the previous experiments to be the enzymatic hydrolysate with the highest concentration of glucose and the most time efficient settings. After the enzymatic hydrolysis, the temperature of the shaking incubator was lowered to 30 °C and the resuspended yeast cells were added to the flask to start the fermentation.

The fermentation was left running for 1-9 days, after which the flasks were removed from the shaking incubator and the broth was centrifuged. 1.5 mL of the supernatant was used for analyzing the sugar concentration with HPLC.

The remaining content in the fermentation flask (both solids and liquids) was left to dry in an oven for at least 24 h at 105 °C, resulting in the solid residue of the fermentation used for biomass determination. The solid residue was mechanically reduced to powder with a hand mortar and used for the Soxhlet extraction of lipids.

4.1.5 Simultaneous saccharification and fermentation (SSF)

For the simultaneous saccharification and fermentation (SSF) process, the resuspended yeast cells and the enzyme complex were added to 250 mL Erlenmeyer flasks containing 50 mL of autoclaved waste media (50 % w/v) at the same time. The fermentation flasks were incubated in a shaking incubator (150 rpm) at 30 °C for 1-9 days. Medium without enzymes and yeast was used as control.

The sugar concentration, the lipid content, and the weight of biomass was determined as described for the SHF process.

4.1.6 Analytical methods

The concentrations of glucose, xylose, galactose, cellobiose and fructose in the hydrolysate and fermentation samples were determined by HPLC equipped with a Bio-Rad Aminex HPX-87P column (300 × 7.8 mm, 9 µm) at 85 °C and a refractive index detector. The samples were filtered through 0.45 µm syringe filters to remove impurities and injected into the HPLC. The mobile phase was distilled water with flow rate of 0.6 mL/min and the injection volume was 20 µL.

For the Soxhlet extraction (figure 4.2) of lipids, the dried sample is introduced in the thimble and clogged with cotton to avoid overflowing. The organic solvent evaporates in the bottom and is cooled down in the top by the condenser, causing it to flow into the sample chamber. When the volume of solvent is large enough, it follows Pascal's Law and drains into the round flask, accumulating the extract and starting the extraction cycle again. A volume of 200 mL of hexane was used as the organic solvent and the process was left running for 4 h to ensure sufficient lipid extraction.

The hexane was recovered by means of the rotary evaporator (130 rpm) with a 40 °C water bath.

The weight of the extract was compared against the weight of the lipids determined to be present in the waste media. Subtracting the lipids in the waste media, allows to calculate the lipid production by the yeast.

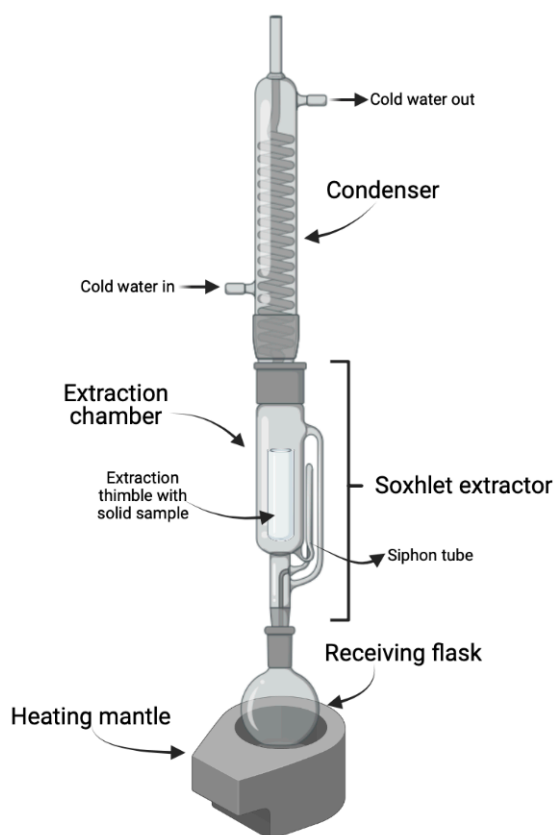


Figure 4.2: Soxhlet extraction setup used for the extraction of lipids from the dried biomass. The figure was created with BioRender.com.

4.2 Genetic engineering of *Cutaneotrichosporon oleaginosus*

As previously mentioned, this thesis aims to genetically engineer *C. oleaginosus* by inserting a codon optimized version of a *cbhl* gene responsible for the production of an exoglucanase into the genome of the yeast by ATMT. A general laboratory workflow of the genetic engineering of *C. oleaginosus* conducted during this master thesis is presented in Figure 4.3.

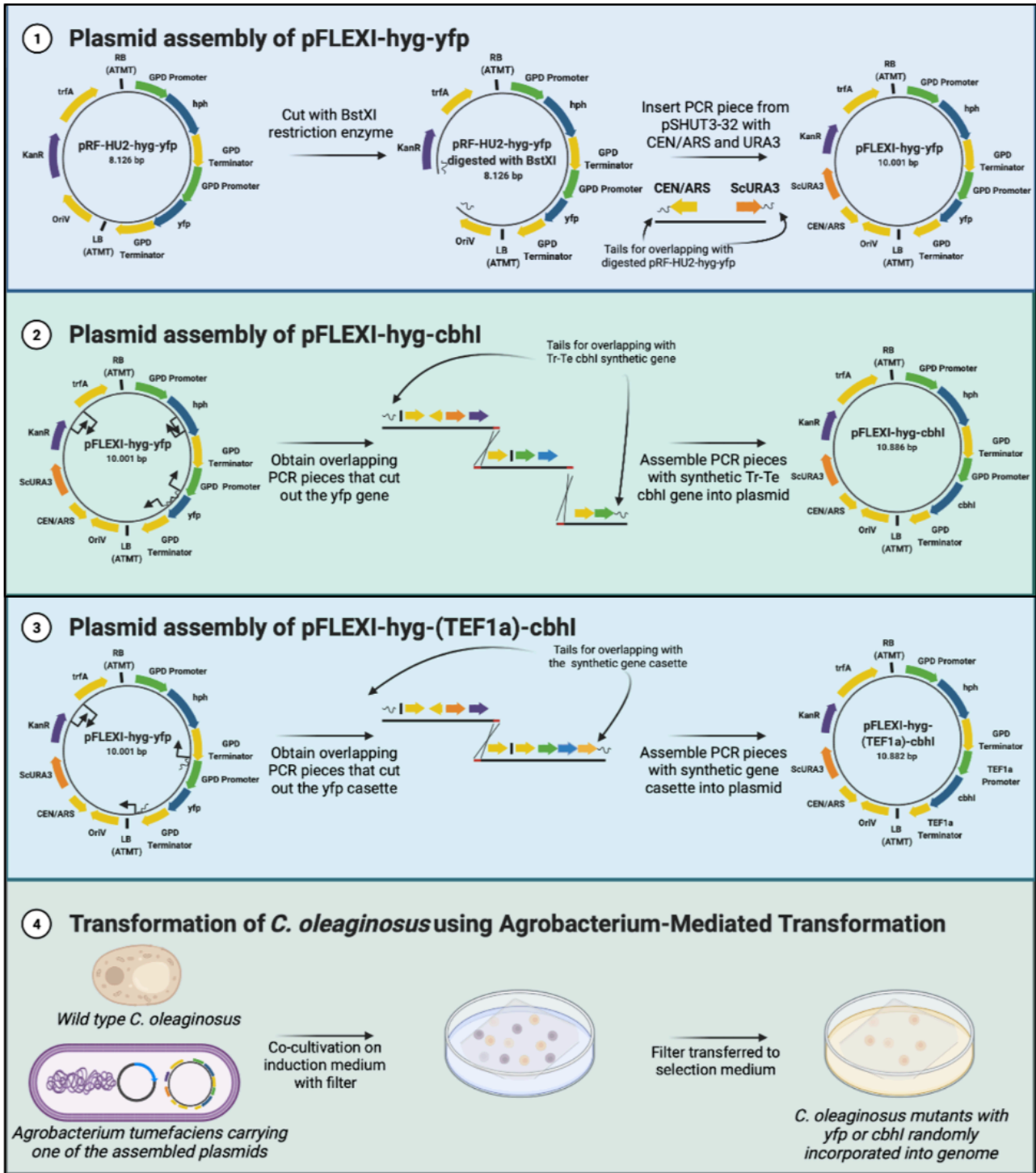


Figure 4.3: General workflow of the laboratory work conducted during the genetic engineering of *C. oleaginosus*. (1) Plasmid assembly of pFLEXI-hyg-yfp, (2) plasmid assembly of pFLEXI-hyg-cbhl, (3) plasmid assembly of pFLEXI-hyg-(TEF1a)-cbhl and (4) transformation of *C. oleaginosus* with the assembled plasmids using *Agrobacterium tumefaciens* mediated transformation (ATMT).

The overall purpose of each task in the laboratory workflow is given in the section below:

1) Plasmid assembly of pFLEXI-hyg-yfp

The CEN/ARS sequence and a selection marker (URA3) was inserted into the backbone of the pRF-HU2-hyg-yfp plasmid from Görner et. al. [17] to allow for plasmid assembly by yeast recombination. As described in the literature background (section 2.5.3), the efficiency of plasmid assembly of multiple overlapping DNA fragments is typically higher by homologous recombination in *Saccharomyces cerevisiae* compared to *in vitro* methods such as USER cloning and Gibson assembly. By inserting the necessary components to the shuttle plasmid, the assembly can be performed with several different methods which overall increases the robustness of the transformation system.

2) Plasmid assembly of pFLEXI-hyg-cbhl

The yfp gene of the pFLEXI-hyg-yfp plasmid were exchanged with a synthetic codon optimized version of a *cbhl* gene responsible for the production of an exoglucanase. The promoter and terminator from the original plasmid were kept unchanged since it was proven by Görner et. al. [17] that this cassette system could be successfully expressed by *C. oleaginosus* after transformation.

3) Plasmid assembly of pFLEXI-hyg-(TEF1a)-cbhl

Since homologous regions of a plasmid will recombine with each other during cloning procedures, it is not optimal to reuse the same promoter and the same terminator twice. Replacing the promoter and terminator in one of the cassettes with another promoter and terminator will increase the robustness of the transformation system. Therefore, the entire yfp cassette from the pFLEXI-hyg-yfp plasmid was exchanged with a synthetic cassette containing the constitutive promoter of the translation elongation factor α gene (TEF1- α) from *C. oleaginosus*, the codon optimized *cbhl* gene and the TEF1- α terminator from *C. oleaginosus*.

4) Transformation of *C. oleaginosus* using *Agrobacterium*-mediated transformation

The successfully assembled plasmids were transformed into *C. oleaginosus* with ATMT using the RB and LB boundaries of the T-DNA on the shuttle plasmids as described in section 2.5.3.

4.2.1 Yeast and bacterial strains

Saccharomyces cerevisiae (strain BY4743) was used for plasmid assembly by yeast transformation, after which the DNA extracts were transformed into *Escherichia coli* (strain DH5 α) by electroporation. Plasmids that were assembled by Gibson assembly were transformed into NEB #C2987 5-alpha competent *E. coli* cells (New England Biolabs (NEB), Ipswich, Massachusetts, USA) by heat shock. The successfully assembled plasmids were electroporated into *Agrobacterium tumefaciens* (strain AGL1) after which the transformed cells were used for ATMT of the oleaginous yeast *Cutaneotrichosporon oleaginosus* (strain ATCC 20509).

4.2.2 Growth and selection media

For plasmid assembly by yeast transformation, *S. cerevisiae* was grown in 2X YPAD liquid medium. Additional reagents used for the yeast transformation include 1.0 M lithium acetate, PEG MW 3350 (50 % w/v), frozen competent cell solution, and single stranded carrier DNA (2.0 mg/ml) as described in the protocol by Gietz and Schiestl [110]. For selection of successful yeast transformants, the cell suspension was plated on synthetic complete (SC) drop out medium without uracil (6.7 g/L yeast nitrogen base without amino acids, 1.92 g/L yeast synthetic drop-out medium supplement without uracil, 20 g/L agar).

E. coli and *A. tumefaciens* was generally cultivated in LB liquid medium (10 g/L tryptone, 5 g/L yeast extract, 10 g/L NaCl). When carrying the plasmid of interest, the medium was supplemented with 50 µg/ml kanamycin to select for successful transformants.

C. oleaginosus was routinely streaked and maintained on YPD agar plates (20 g/L agar, 20 g/L peptone, 10 g/L yeast extract, 20 g/L glucose) and precultures of the yeast was obtained by growth in 35 ml of liquid YPD medium (20 g/L peptone, 10 g/L yeast extract, 20 g/L glucose). For selection of successful transformants of *C. oleaginosus* after ATMT, the YPD agar plates was supplemented with 200 µg/ml hygromycin B and 300 µg/ml cefotaxime, respectively. Additional media used for *A. tumefaciens* mediated transformation of *C. oleaginosus* were liquid induction medium with acetosyringone (L-IMAS) (2.05 g/L K₂HPO₄, 1.45 g/L KH₂PO₄, 0.15 g/L NaCl, 0.5 g/L MgSO₄ · 7H₂O, 67 mg/L CaCl₂ · 2H₂O, 7.8 g/L 2-4-morpholineethanesulfonic acid monohydrate (MES), 1.8 g/L glucose, 39.24 mg/L acetosyringone, 2.5 mg/L FeSO₄ · 7H₂O, 0.5 g/L (NH₄)₂SO₄, 5 % (v/v) glycerol, 5 % (v/v) trace elements solution (100 mg Na₂MoO₄, MnSO₄ · H₂O, ZnSO₄ · 7H₂O, CuSO₄ · 5H₂O, H₃BO₃ in 1 L distilled water, pH = 5.6)) and solid induction medium with acetosyringone (S-IMAS) (equivalent to L-IMAS, without glucose, supplemented with 20 g/L agar) (see section 4.2.5 for a thorough description of the ATMT procedure).

4.2.3 Cloning methods

4.2.3.1 Polymerase chain reactions and DNA purifications

Polymerase chain reactions were mixed with the following ingredients and concentrations: 1X Phusion GC Buffer including 1.5 mM MgCl₂ (Thermo Scientific™, Waltham, MA, USA), 0.2 mM dNTPs, 0.5 µM of each primer, 1 µL template and 1 U polymerase per 50 µL reaction (Phusion Hot Start II DNA Polymerase (Thermo Scientific)). The PCR reactions were carried out on a T100™ thermal cycler (Bio-Rad, Hercules, CA, USA) with primer pairs specific for each reaction. Generally, all primer sequences and the program used for each reaction is given in Appendix D.

All PCR pieces were purified using the QIAquick PCR Purification Kit (Qiagen, Hilden, Düsseldorf, Germany) to remove primers, nucleotides, and other impurities from the DNA samples by following the manufacturer-supplied protocol. Occasionally, the DNA was also gel purified using the QIAquick Gel Extraction Kit (Qiagen) to remove unspecific DNA bands. The sample was loaded on a 2 % agarose gel, after which the DNA fragment was excised from the gel and the enclosed protocol from the manufacturer was followed.

4.2.3.2 Plasmid templates

As described in the literature review and illustrated in the laboratory workflow (Figure 4.3), the plasmid used as the main template for cloning of the new pFLEXI plasmids in this master thesis was the pRF-HU2-hyg-yfp plasmid from Görner et. al. [17] as shown in Figure 4.4A (Figure S5 in the original article). Furthermore, the CEN4/ARSH6 sequence and the URA3 selection marker was cut out of the in-house shuttle vector pSHUT3-32 from Nielsen et. al. [117] illustrated in Figure 4.4B (Figure 1C in the original article) and inserted into the backbone of the pFLEXI plasmids to allow for plasmid assembly by *S. cerevisiae*.

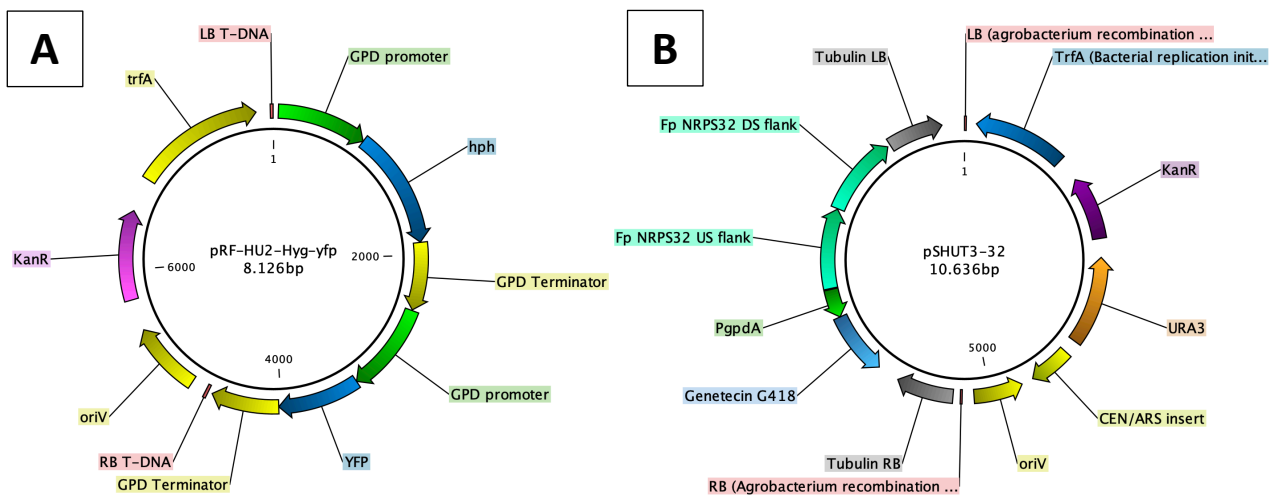


Figure 4.4: Plasmid maps of the two templates used to construct the new pFLEXI plasmids. (A) The pRF-HU2-hyg-yfp plasmid from Görner et. al. [17] and (B) the pSHUT3-32 plasmid from Nielsen et. al. [117].

4.2.3.3 Cloning of the pFLEXI-hyg-yfp plasmid

The pRF-HU2-hyg-yfp plasmid template was linearized by digestion with the restriction enzyme BstXI. Simultaneously, the CEN4/ARSH6 sequence and the URA3 selection marker was amplified from the pSHUT3-32 plasmid using the primer set CA-Ura3-Fw and CA-Ura3-Rv. The settings used for the PCR including temperature and time as well as the primer sequences are given in Appendix D. The primers were designed with tails that overlap with the linearized pRF-HU2-hyg-yfp plasmid. Assembly of these two DNA fragments yielded the plasmid pFLEXI-hyg-yfp seen in Figure 4.5.

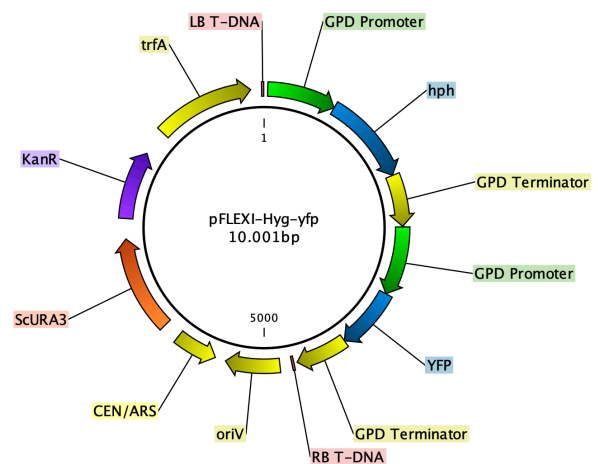


Figure 4.5: Plasmid map of the pFLEXI-hyg-yfp plasmid

The two DNA fragments were assembled using the frozen yeast transformation protocol described in the paper by Gietz and Schiestl [110]. The optimal transformation efficiency was obtained with an incubation time and temperature at 42 °C for 40 min. After incubation, the transformed cells

were resuspended in 500 μ L of sterile water after which the full volume was plated onto the uracil drop-out selection plates and incubated for 4 days at 30 °C. To extract DNA from the freshly grown yeast cells, the reagents, and buffers from QIAprep Spin Miniprep Kit (Qiagen) were used with a modified protocol. A loop of cells was scraped off from the plate and resuspended in 250 μ L of Buffer P1 and 3 μ L of Zymolyase; the suspension was incubated for 1 hour at 37 °C, after which the steps 3-9 from the Qiagen miniprep protocol was followed. The extracted DNA was electroporated into *E. coli* using a MicroPulser Electroporator (Bio-Rad) and following the manufacturer's protocol.

4.2.3.4 Cloning of the pFLEXI-hyg-cbhl plasmid

The *yfp* gene of the pFLEXI-hyg-*yfp* plasmid was exchanged with a codon-optimized gene (referred to as *Tr-Te cbhl*) encoding a chimeric CBH1 exoglucanase containing the catalytic domain from *Talaromyces emersonii*, the linker and carbohydrate-binding molecule (CBM) from *T. reesei* and a signal peptide from an endoglucanase from *C. oleaginosus* to construct the pFLEXI-hyg-CBHI plasmid. The *Tr-Te cbhl* gene was codon optimized based on the preferred codon usage table for the glyceraldehyde-3-phosphate dehydrogenase (GPD) in *C. oleaginosus* (Genebank AF126158.1) and the protein sequence as

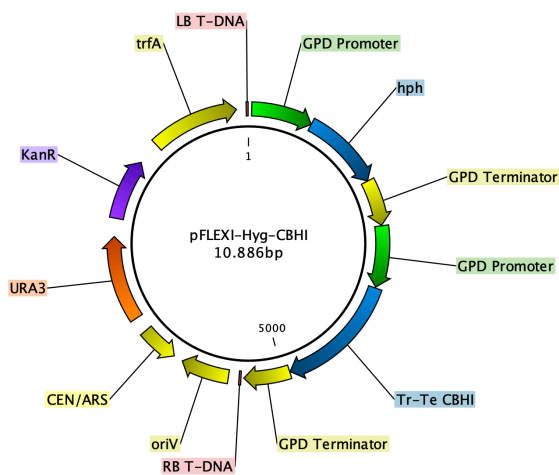


Figure 4.6: Plasmid map of the pFLEXI-hyg-cbhl plasmid

well as the codon optimized gene sequence is presented in Appendix A and Appendix B, respectively. The synthetic *Tr-Te cbhl* gene was inserted into the multiple cloning site of the pUC57 plasmid by the suppliers (Genscript Biotech, Piscataway, New Jersey, USA) and the restriction enzyme Anza 26 Eco32I (Thermo Scientific) was used to cut out the gene.

Three sets of primers (T1-bb1, bb2-Hyg and Hyg-P1) were used to amplify the backbone of the pFLEXI-hyg-*yfp* plasmid as it was described in the general laboratory workflow in Figure 4.3. All PCR settings and primer sequences used are given in Appendix D. Two of the primers were designed with a tail that overlaps with the synthetic *Tr-Te cbhl* gene and one of these primers also includes a stop codon for the gene. Assembly of these three DNA fragments as well as the synthetic *Tr-Te cbhl* gene should yield the pFLEXI-hyg-cbhl plasmid seen in Figure 4.6.

Several attempts to assemble the plasmid were performed using yeast transformation and Gibson Assembly, respectively. For the yeast transformation, the same protocol as for the cloning of the pFLEXI-hyg-*yfp* plasmid was followed and several different concentrations of DNA were used without obtaining any successful transformations. Subsequently, it was attempted to assemble the DNA fragments into the pFLEXI-hyg-cbhl plasmid using the Gibson Assembly Master Mix (NEB) by following the manufacturer's protocol. Again, different concentrations of DNA and longer incubation times were tested but without any successful plasmid assemblies.

4.2.3.5 Cloning of the pFLEXI-hyg-(TEF1 α)-cbhl plasmid

The entire yfp gene cassette of the pFLEXI-hyg-yfp plasmid was exchanged with a synthetically synthesized cassette. The codon-optimized *Tr-Te cbhl* gene were synthesized containing 800 bp upstream of the *C. oleaginosus* TEF1- α gene as the promoter and 600 bp downstream of the *C. oleaginosus* TEF1- α gene as the terminator (NCBI genome ID: 38460, NCBI Gene Reference Sequence: XP_018277688.1). The sequence of the entire cassette is presented in Appendix C. The cassette was inserted into the multiple cloning site of the pUC57 plasmid by the suppliers

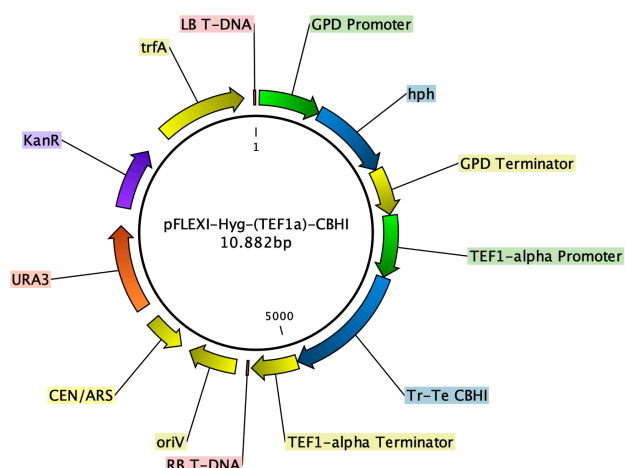


Figure 4.7: Plasmid map of the pFLEXI-hyg-(TEF1 α)-cbhl plasmid

(Genscript Biotech) but was amplified by using the primer set TEF1a-Fw and TEF1a-Rv. The primers include tails that overlap with the backbone DNA pieces from the template. To amplify the backbone of the pFLEXI-hyg-yfp plasmid, two sets of primers (bb1 and bb2) were used as it was described in the general laboratory workflow in Figure 4.3. All PCR settings and primer sequences used are given in Appendix D.

Assembly of the plasmid was attempted using the Gibson Assembly Master Mix (NEB) following the manufacturers protocol without success. Subsequently, the plasmid was successfully assembled using the frozen yeast transformation protocol described in the paper by Gietz and Schiestl [110]. The DNA was extracted from the yeast and electroporated into *E. coli* as it was described in section 4.2.3.3. for the pFLEXI-hyg-yfp plasmid.

4.2.4 Plasmid validation

The successful assembly of all plasmids were validated with colony PCR reactions using the primer set cPCR-Fw and cPCR-Rv. The primers were designed to be backbone-specific meaning that they anneal to sites that flank the insert site. All PCR settings and primer sequences used are given in Appendix D. The three plasmids pRF-HU2-hyg-yfp, pFLEXI-hyg-yfp and pFLEXI-hyg-(TEF1 α)-cbhl were also validated by digestion with the restriction enzyme FastDigest PstI (Thermo Scientific™) for 30 min at 37 °C in 1X FastDigest buffer.

4.2.5 Transformation of *Cutaneotrichosporon oleaginosus*

The validated plasmids were electroporated into *Agrobacterium tumefaciens* to prepare for ATMT using a MicroPulser Electroporator (Bio-Rad) by following the manufacturer's protocol. To select for successful transformants, the cell suspensions were plated onto LB agar supplemented with 50 μ g/ml kanamycin and 20 μ g/ml rifampicin. The plates were incubated at 28 °C for 72 hours after which individual colonies were isolated on new selection plates.

4.2.5.1 *Agrobacterium tumefaciens* mediated transformation

An individual transformed *A. tumefaciens* colony was cultured in LB medium supplemented with 30 µg/mL kanamycin at 28 °C for 18 hours after which the cell pellet was transferred to a shake flask containing 10 mL of L-IMAS medium and cultured for 6 hours at 28 °C. At the same time, a culture of the wild-type *C. oleaginosus* was grown in YPD medium at 28 °C for 24 hours. The overnight culture was centrifuged, the supernatant discarded, and the cell pellet was resuspended in 10 mL of L-IMAS medium. 500 µL of the *C. oleaginosus* in L-IMAS medium was mixed with 500 µL of the *A. tumefaciens* cell solution. In the next step, 500 µL of the *A. tumefaciens* and *C. oleaginosus* cell mixture was plated on top of a black filter paper that was placed on S-IMAS agar plates. The plates were incubated at 24 °C for 48 hours, after which the filter was transferred to YPD agar plates supplemented with 200 µg/mL hygromycin B and 300 µg/mL cefotaxime. Incubation of the agar plates was carried out over 3 days at 28 °C. A day-by-day protocol for the ATMT procedure of *C. oleaginosus* is given in Appendix E.

4.2.6 Validation of the *C. oleaginosus* mutants

Individual colonies of the *C. oleaginosus* mutants that appeared on the black filter paper after ATMT were picked with a sterile inoculation loop and isolated on new YPD agar plates supplemented with 200 µg/mL hygromycin B. To validate the mutants for successful integration of the DNA by ATMT, a colony PCR of the individual colonies was performed using primers Co-cPCR-Fw and Co-cPCR-Rv. The primers were designed to yield a 579 bp PCR product within the hygromycin cassette. A list of primers and PCR settings are given in Appendix D.

The colony PCR was performed by inoculating a single colony in 300 µL of lysis buffer (0.2 M NaCl, 0.1 % Triton X-100, 0.2 % SDS, 10.2 mM Tris-HCl solution, 48 mM EDTA solution) after which the tubes were vortexed to resuspend the yeast cells. Subsequently, the tubes were centrifuged and 1 µL of the supernatant was used as template DNA for the PCR reaction.

4.2.7 Level of yellow fluorescent protein expression in *C. oleaginosus* mutants

To test for the level of expression of the yellow fluorescent protein, the wild type and 7 randomly chosen mutants of *C. oleaginosus* were inoculated in 10 mL of YPD liquid media and incubated for 24 hours at 30 °C. The 24 overnight cultures (1 wild type + 7 mutants in triplicates) were diluted to an OD₆₀₀ = 0.8 after which 2 mL of each culture was transferred to a sterile 24-well culture plate. The culture plate was incubated at 30 °C while the absorbance (600 nm) and the YFP fluorescence (Excitation: 514 nm, 5nm bandwidth; Emission: 527 nm, 5nm bandwidth) were monitored using a Tecan M1000 Pro at different time points during the following days. MQ-water and YPD medium was used to blank the measurements.

5 Results and discussion

5.1 Time studies on the yeast fermentations using OFMSW as the feedstock

The optimal operating conditions of biological processes varies with the type of microorganism and the characteristics of the substrate used in the process. Therefore, a series of time studies was conducted on the enzymatic hydrolysis of OFMSW as well as the fermentation process with *C. oleaginosus* to find the optimal operating conditions regarding time and temperature. For the fermentation setup, time studies were conducted using separate hydrolysis and fermentation (SHF) and simultaneous saccharification and fermentation (SSF), respectively.

5.1.1 Enzymatic hydrolysis

The efficiency of the enzymatic hydrolysis is mostly dependent on the operating conditions of the enzyme involved; e.g. the rate of mixing in the reactor, the type of substrate and the concentration of enzyme [118]. Nevertheless, if these factors are kept constant when conducting experiments, it is possible to investigate the effect of other external factors such as temperature and time on the efficiency of the enzymatic hydrolysis and thereby also on the release of residual sugars available for subsequent fermentation.

The concentration of glucose, fructose, and cellobiose are shown in Figure 5.1 as a function of time at two different constant temperatures (30 °C and 50 °C) of enzymatic hydrolysis on OFMSW using the fixed enzyme mix described in the materials and methods. The concentration of xylose, galactose, and arabinose were also monitored but no detectable amounts of these sugars were obtained at any point during enzymatic hydrolysis.

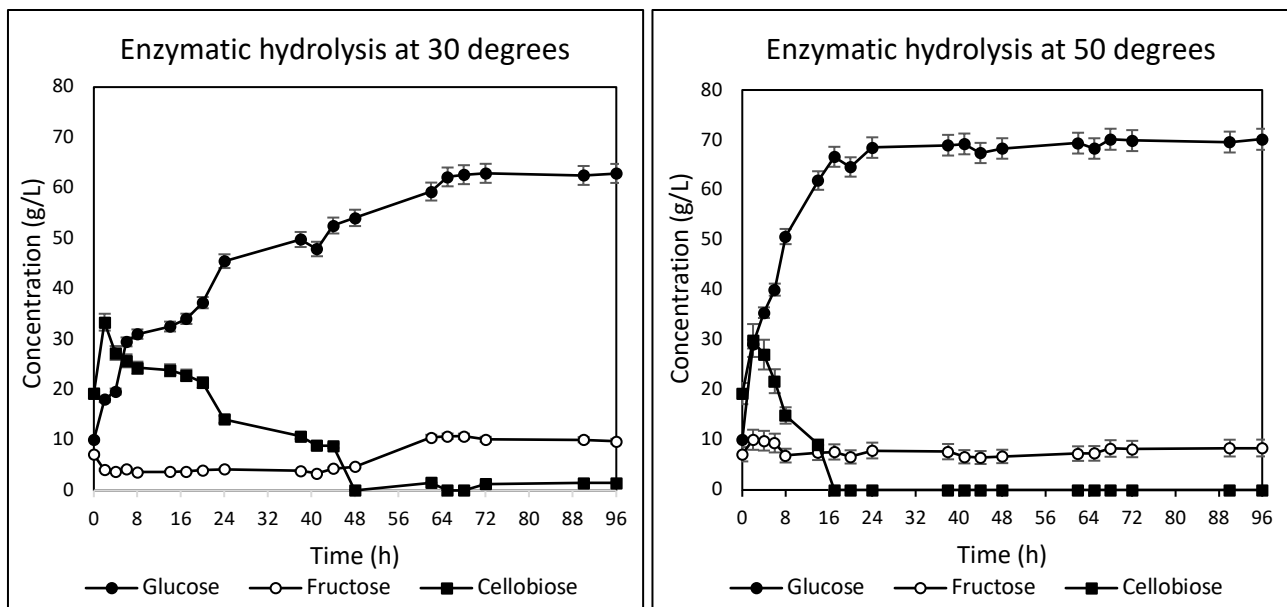


Figure 5.1: Enzymatic hydrolysis at 30 °C (left) and 50 °C (right). The concentration of glucose (black circle), fructose (white circle), and cellobiose (black square) are given in g/L as a function of time at the two different temperatures.

The glucose release during enzymatic hydrolysis increased with time up to 64 h at 30 °C and up to 16 h at 50 °C, after which product feedback inhibition of the enzymes occurred and the maximum glucose release of 61.19 g/L and 70.22 g/L, respectively, was obtained. The faster release of glucose during enzymatic hydrolysis at 50 °C compared to enzymatic hydrolysis at 30 °C can be attributed to the fact that the optimal temperature of the enzyme mix is very close to 50 °C. This means that the activity of the enzymes present in the mix was higher at 50 °C which can also explain the higher amount of glucose released at 50 °C compared to 30 °C before reaching the level of product feedback inhibition.

The concentration of cellobiose was found to decrease with time up to 48 h at 30 °C and up to 16 h at 50 °C after which all cellobiose had been converted to glucose by the β -glucosidases present in the mix of enzymes. Again, the lower temperature during enzymatic hydrolysis leads to a decrease in the activity of the enzymes.

The amount of fructose present in the samples was quite stable and no fructose was being released by the enzymatic hydrolysis at any time point. The small deviations in the concentrations of fructose seen in the graph can be explained by the fact that it was not possible to make the OFMSW media completely homogenous.

5.1.2 Separate hydrolysis and fermentation (SHF)

As described in the literature review, the mode of fermentation chosen for the reaction can influence the overall yield of lipids and the best method can vary for each individual process which means that laboratory experiments must be conducted to determine whether it is best to have a separate hydrolysis and fermentation (SHF) or a simultaneous saccharification and fermentation (SSF). For the SHF process in this setup, a pre-hydrolysis of 24 h at 50 °C was conducted after which the temperature was decreased to 30 °C and the yeast was added to start the fermentation process. The total production of lipids (left) as well as the concentration of glucose, fructose, and cellobiose (right) are shown in Figure 5.2 as a function of time during the SHF process.

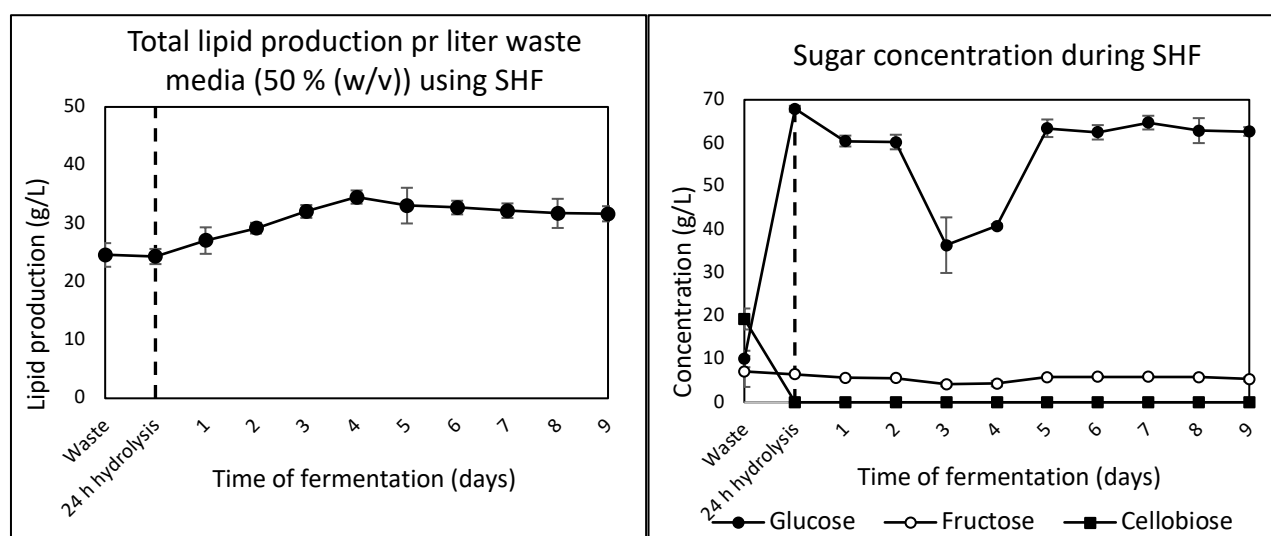


Figure 5.2: Total lipid production (left) during separate hydrolysis and fermentation (SHF) and the concentration of glucose (black circle), fructose (white circle), and cellobiose (black square) (right) are given in g/L as a function of time.

As it was the case for enzymatic hydrolysis, the level of fructose was found to be quite stable throughout the fermentation process, meaning that no fructose was being released by the enzymes and no fructose was utilized by the yeast for survival or metabolic processes. On the other hand, cellobiose was almost nonexistent in the media after 24 h of hydrolysis, which indicates that inhibition of β -glucosidase at the maximum glucose level did not result in an increased cellobiose concentration at any time point and as a result, all cellobiose was converted to glucose by the cellulolytic enzymes.

After 24 h of pre-hydrolysis at 50 °C, the level of glucose was at ≈ 70 g/L which was found to be the maximum amount of glucose that could be released in the enzymatic hydrolysis time studies. After the addition of yeast to the fermentation flask, the level of glucose decreased until 3-4 days of fermentation had passed. During this period (from day 1 to day 4 of fermentation), the yeast must have been consuming more glucose than there was released from enzymatic hydrolysis of the lignocellulosic materials. From day 5 of fermentation, the glucose reraised to the maximum level and stayed there until day 9 of fermentation after which the fermentation was stopped. During this period (from day 5 to day 9 of fermentation), the yeast either stopped consuming glucose or the activity of the cellulolytic enzymes increased significantly. To answer that question, it may be interesting to look at the production of lipids in Figure 5.2 (left), where it is quite clear that the maximum production of lipids at 34.53 g/L occurred after 4 days of fermentation. From day 5 to day 9 of fermentation, the production of lipids slowly decreased which may indicate that the metabolism of the yeast had shifted, and the yeast started metabolizing lipids for its survival.

In other oleaginous yeasts such as *Yarrowia Lipolytica* [119] and *Lipomyces Starkeyi* [120], accumulated lipids have been found to be mobilized through β -oxidation on exit from the exponential phase of growth. Presumably, by the time the cellulolytic enzymes had broken down more of the lignocellulose to fermentable sugars, the enzymes for β -oxidation of lipids had already been built to a level that hydrolysis of lipids occurred. The lipid content of the biomass continued to decline hereafter even though the concentration of glucose was reraised to the maximum level in the medium. This issue may be avoided by using a SSF process where feedback inhibition of the cellulolytic enzymes is minimized due to the rapid utilization of sugars by the microorganism from the beginning.

5.1.3 Simultaneous saccharification and fermentation (SSF)

The reduction of product inhibition from enzymatic hydrolysis can potentially improve the overall performance of the process. However, the optimal temperatures of the two combined processes are different, as the optimal temperature for enzymatic hydrolysis is typically much higher than the fermentation temperature. Thus, it is necessary to find a compromise that provides the optimal conditions for both processes resulting in the maximum possible lipid production.

For the SSF process in this thesis, the optimal temperature of the yeast at 30 °C was used throughout the fermentations since it was believed that the lower activity of the enzymes would not affect the lipid yield as much as a higher temperature would affect the survival of the yeast. This means, that the yeast and the cellulolytic enzymes were added to the OFMSW media at the same time to start

the SSF process at 30 °C. The total production of lipids (left) as well as the concentration of glucose, fructose, and cellobiose (right) are shown in Figure 5.3 as a function of time during SSF.

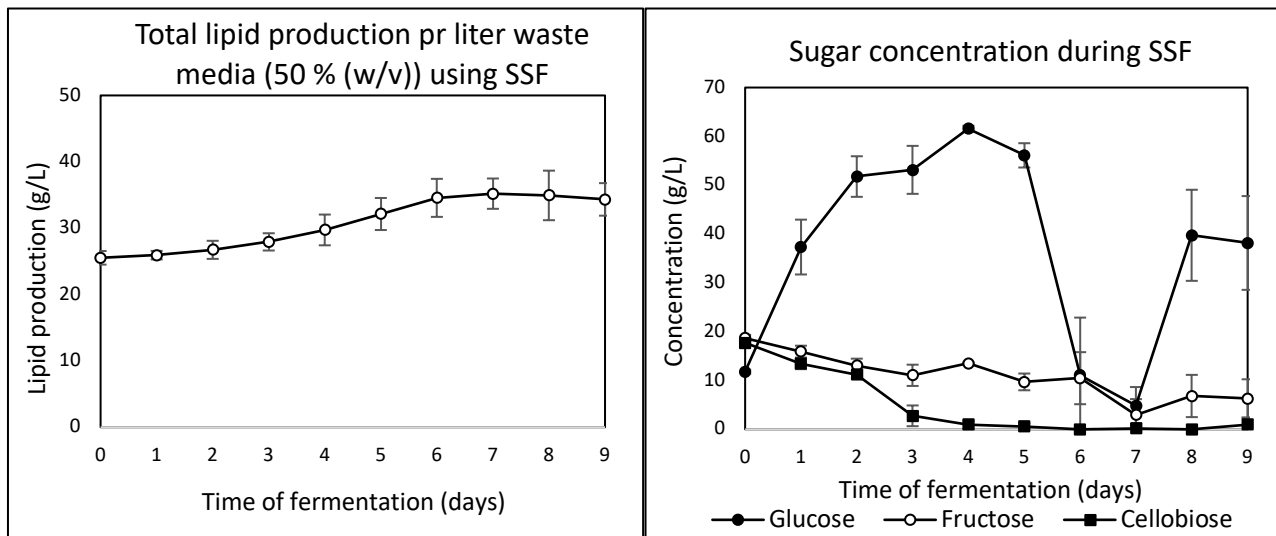


Figure 5.3: Total lipid production (left) during simultaneous saccharification and fermentation (SSF) and the concentration of glucose (black circle), fructose (white circle), and cellobiose (black square) (right) are given in g/L as a function of time.

Unlike, the SHF process where the level of fructose was found to be quite stable throughout the fermentation, it seems as if the fructose was being utilized to some extent by the yeast during SSF. This could possibly be explained by the much lower amount of glucose available in the media in the beginning where the cellulolytic enzymes were still working flat out to break down the starch and cellulose in the lignocellulosic feedstock. This lower amount of glucose may have provoked the use of fructose by the yeast even though *C. oleagnosus* usually prefer to grow on glucose [29]. However, it should be noted that the fructose level in the samples varied a little bit depending on the homogeneity of the OFMSW media.

Due to the low temperature throughout the SSF process, the concentration of cellobiose decreased slowly and 3-4 days of hydrolysis and fermentation was needed to convert the cellobiose to glucose by the β -glucosidases added to the media. An increase in the concentration of cellobiose was not observed at any point since the product inhibition limit of glucose was never reached during SSF and inhibition of the β -glucosidases could not occur. However, the concentration of glucose did slowly increase during the first 3-4 days of the SSF process. In this phase, the cellulolytic enzymes must have released more glucose from the lignocellulosic biomass than the yeast consumed even though the temperature of the process reduced the activity of the enzymes. From day 5 to day 7 of fermentation, the glucose level decreased drastically after which it reraised to a higher level on day 8 and day 9 of fermentation.

A comparison of the lipid production (left in Figure 5.3) and the glucose concentration (right in Figure 5.3) during SSF reveals that the maximum lipid production at 35.30 g/L was reached after 7 days of fermentation, where the concentration of glucose was decreasing significantly. Shortly hereafter, the total amount of lipids that could be extracted after fermentation decreased, while the glucose level reraised. This situation was also observed for the SHF process in Figure 5.2, where

it was assumed that the accumulated lipids were mobilized through β -oxidation on exit from the exponential phase of growth and it was believed that SSF could solve this issue due to the minimized effect of feedback inhibition. However, the issue was not avoided by using a SSF process and furthermore, the time needed to reach the maximum total lipid production was increased compared to the SHF process due to the lower enzyme activity.

5.1.4 SHF vs. SSF

The best fermentation setup (SHF or SSF) varies for each individual process and a comparison of the lipid production during the time-studies conducted in this master thesis is presented in Figure 5.4. The dry weight (DW) of the biomass after fermentation was also monitored during both SHF and SSF (Figure 5.4 right) to follow the formation of new yeast biomass as well as the performance of the cellulolytic enzymes breaking down the lignocellulosic feedstock.

The total lipid production increased significantly faster with time using the SHF process where a pre-hydrolysis step at 50 °C was included, compared to SSF where the process was started at 30 °C. When performing the two processes separately using SHF, it is possible for the enzymes and the yeast to work at their optimal conditions with respect to temperature. This is one of the large disadvantages of the SSF process, as it is necessary to find a compromise that provides the optimal conditions for both enzymatic hydrolysis and yeast fermentation resulting in the maximum possible lipid production. The use of a higher temperature could potentially have decreased the time needed to reach the maximum total lipid production during SSF since the activity of the cellulolytic enzymes would be higher and more glucose would have been rapidly available to the yeast. However, this higher temperature would most likely influence the growth of the yeast negatively, but that is a compromise that would have to be investigated using laboratory experiments.

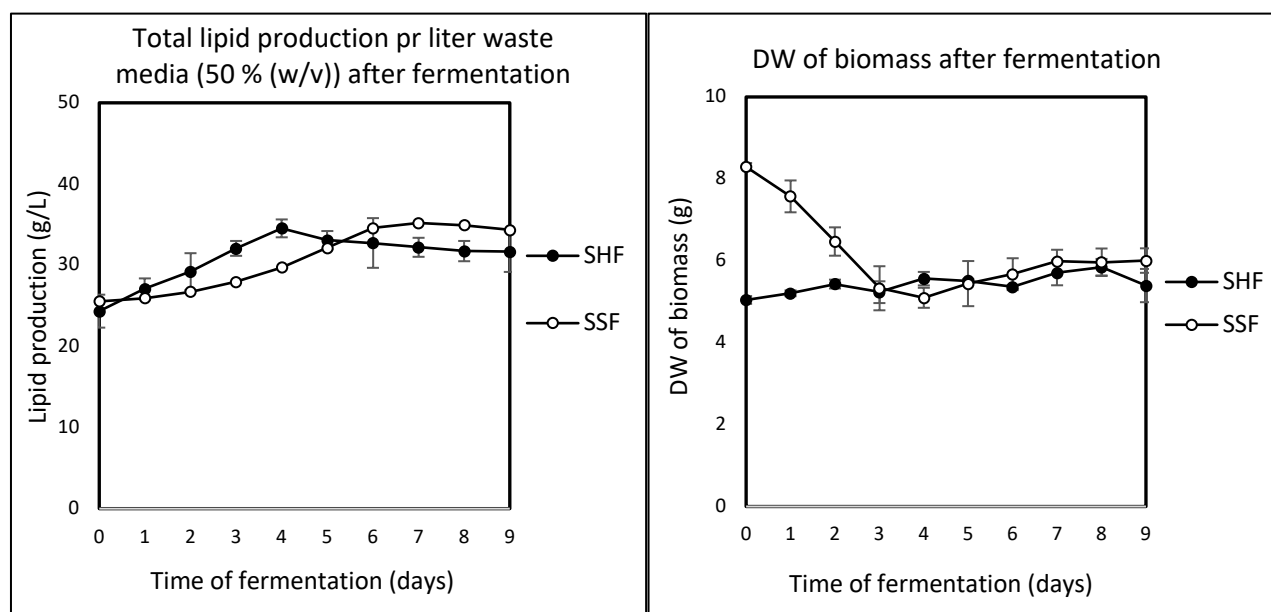


Figure 5.4: Comparison of the total lipid production (left) and the dry weight of the biomass after fermentation (right) during the time-studies using SHF and SSF, respectively.

The dry weight of biomass during SSF decreased drastically during the first 4 days of fermentation after which a small increase was observed. This indicates that the enzymes converted more lignocellulosic biomass to water-soluble sugars per weight than the weight of yeast increased during the first 4 days of fermentation. In comparison, the dry weight of biomass during SHF was already low from the beginning, which can be explained by the pre-hydrolysis step conducted before fermentation. Once the cellulolytic enzymes had broken down most of the lignocellulosic biomass, the overall dry weight of biomass stabilized in both processes. This indicates that the extra biomass gained from the formation of new yeast cells were comparable to the weight of biomass broken down by the enzymes.

An overview of the outputs from the most important results regarding lipid production and dry weight during the time-studies conducted with SHF and SSF, respectively, are given in Table 5.1.

Table 5.1: The outputs of the DW of biomass, total amount of lipids extracted and the lipid content in both SHF and SSF processes.

Time (days)	SHF			SSF		
	DW (g/L)	Lipids extracted (g/L)	Lipid content (%)	DW (g/L)	Lipids extracted (g/L)	Lipid content (%)
0	100.8	24.33	24.12	165.8	25.53	15.40
1	104.2	27.07	26.03	151.4	25.93	17.14
2	108.6	29.20	26.94	129.4	26.73	20.69
3	104.6	32.07	30.65	106.6	27.93	26.31
4	111.2	34.53	31.03	102.0	29.73	29.28
5	111.0	33.07	29.99	108.8	32.13	29.69
6	107.2	32.73	30.57	113.4	34.57	30.57
7	114.2	32.20	28.24	119.8	35.20	29.46
8	116.8	31.73	27.30	119.2	34.93	29.27
9	108.0	31.67	29.36	120.2	34.33	28.60

As shown in Table 5.1, the maximum total lipid production that was extracted per liter waste media was 34.53 g/L after 4 days of fermentation for SHF and 35.30 g/L after 7 days of fermentation for SSF, respectively. Since there was 24.33 g/L of lipids in the batch of waste media used for the SHF process and 25.53 g/L of lipids in the batch of waste media used for the SSF process, the production of lipids by *C. oleaginosus* was 10.20 g/L and 9.67 g/L using SHF and SSF, respectively. This corresponds to 61.41 g of lipids produced from each kg of dry OFMSW for SHF and 57.80 g of lipids per kg dry OFMSW for SSF. These results are comparable to a study performed by Ghanavati et. al. [7] in which they investigated the lipid production by *Cryptococcus aerius* on an OFMSW feedstock using several different conditions. At the optimal conditions, 8.19 g/L of lipids were obtained with detoxified pre-hydrolysate and enzymatic hydrolysate of OFMSW as the substrate. This corresponds to 39.6 g of lipids produced from each kg of dry OFMSW in that study due to the much lower moisture content in their OFMSW waste substrate. Similarly, Ma et. al. [121] produced 6.4 g/L with

Rhodosporidium toruloides using an enzymatic hydrolysate of food waste as the substrate. The lipid production in several other studies [27,73,119,120 etc.] with different oleaginous yeasts was higher, but it is worth mentioning that synthetic media or pure lignocellulosic materials were used in all those studies. In this master thesis and in the studies by Ghanavati et. al. and Ma et. al. [7,121], very complex and heterogeneous feedstock (OFMSW or food waste) was employed as the substrate for the yeast fermentation and to my knowledge, no studies have reported higher lipid production on OFMSW feedstocks than presented in this work.

A summary of the most important results obtained in the time-studies conducted on OFMSW is given in Table 5.2. The table contains results from both the raw OFMSW, the enzymatic hydrolysis as well as the fermentation processes.

Table 5.2: Summary of the most important results obtained in the time-studies conducted on OFMSW.

Food waste		
Dry matter	33.22 %	
Lipid content pr dry biomass	15.40 %	
Enzymatic hydrolysis		
	30 °C	50 °C
Maximum glucose concentration (product inhibition limit)	61.19 g/L	70.22 g/L
Time needed to reach maximum glucose concentration	64 h	16 h
Maximum biomass reduction	3.27 g	4.03 g
Fermentation (SHF vs. SSF)		
	SHF	SSF
Time for pre-hydrolysis at 50 °C	1 day	0 days
Optimal time for fermentation at 30 °C	4 days	7 days
Total time needed to reach maximum lipid production	5 days	7 days
Maximum lipid production by yeast	10.20 g/L	9.67 g/L
Lipids present in media before fermentation	24.33 g/L	25.53 g/L
Maximum total lipid production	34.53 g/L	35.20 g/L
Maximum total lipid content pr dry biomass after fermentation	31.03 %	30.57 %

5.1.5 Discussion on the sustainable industrial implementation of the process

Developing sustainable eco-efficient bioprocesses and producing renewable bio-resources is one of the present and future key challenges. Improved understanding of biodiversity, ecology, biology, and biotechnology is making it possible to sustainably increase productivity as well as to utilize biomass and waste organic materials in a highly efficient and sustainable manner. In general, a sustainable industrial development should increase eco-efficiency by decreasing pollution as well as the amount of energy, material and other inputs required to produce a given product.

Nevertheless, biotechnological processes often turn out to be uneconomical at an industrial scale. The cost competitiveness with fossil fuels is a barrier for large-scale production with the currently

developed technologies for production of biofuels, and in many cases, this is because oil and energy prices are far too low, which is why several improvements must be implemented to lower the financial expenses and thereby make the overall microbial lipid-producing fermentation process economically feasible.

The time-studies conducted in this master thesis aims to enlighten the optimal fermentation setup (SHF vs. SSF) to produce lipids using OFMSW as the feedstock while having an economic and sustainable point of view. Since the maximum lipid production from each of the two fermentation setups were found to be very similar, the selling price of the product after each batch will be equal. However, the time needed to reach the maximum lipid production is shorter for SHF compared to SSF, which means that the productivity is higher, and thereby also the yearly income based on the lipid production. Nevertheless, one of the major advantages of using SSF compared to SHF from an industrial point of view is the use of a single container for fermentation and hydrolysis, which reduces both residence times, the cost of capital of the process and the time and cost needed for sterilization after each batch. In addition, the entire SSF process is kept at 30 °C, whereas the SHF requires 24 hours at 50 °C for the pre-hydrolysis. The amount of energy needed for this extra heating increases the costs and decreases the sustainability of using the SHF process.

On the other hand, the extra container for pre-hydrolysis at 50 °C using SHF can be used for several batches in parallel since each batch only requires 24 hours of pre-hydrolysis, which lowers the extra cost of capital needed. And the shorter time needed for each batch using SHF compared to SSF may increase the income more than the extra container increases the expenses. These considerations mean that both process setups have advantages and disadvantages compared to one another and a process simulation is needed to make any conclusions on the optimal fermentation setup to use at an industrial scale.

In general, the development of a sustainable bioprocess involves the application of process modeling to ensure that the process is commercially successful in short and long term, that it is environmentally friendly, that it uses minimal and renewable resources, and overall, that the bioprocess contribute beneficially to the needs of society. The laboratory-scale results obtained in this master thesis provides several real-life inputs and outputs for the development of a process model, that can simulate an industrial scale of the lipid production using OFMSW as the feedstock. This simulation will be able to account for the economic feasibility of the process as well as providing information on the sustainability regarding waste streams, heat consumption, water usage, etc. The results obtained from the laboratory SHF and SSF fermentation processes can be implemented into the simulation model and the different outputs will contribute to the discussion on which fermentation setup to use for an industrial scale.

5.2 Genetic engineering of *Cutaneotrichosporon oleaginosus*

As described in the general laboratory workflow in Figure 4.3, this thesis aims to genetically engineer *C. oleaginosus* by inserting a codon optimized version of a *cbhl* gene responsible for the production of an exoglucanase into the genome of the yeast by ATMT. To fulfill this aim, several plasmids were constructed, *C. oleaginosus* was transformed and individual transformed mutants were validated and tested for their level of expression of the yellow fluorescence protein. The results from the genetic engineering of *C. oleaginosus* are presented in the following sections.

5.2.1 PCR products

To construct the plasmids needed for transformation of *C. oleaginosus*, it was necessary to obtain several PCR products. The purified PCR products obtained for the assembly of each plasmid are shown in the gels below in Figures 5.5, 5.6 and 5.7, respectively.

- pFLEXI-hyg-yfp

The purified PCR products needed for the assembly of the pFLEXI-hyg-yfp were loaded on a gel. A plasmid map of the assembled plasmid as well as an image of the gel with purified PCR products are illustrated in Figure 5.5. The expected lengths of the two DNA strands and several marker lengths are given in the figure.

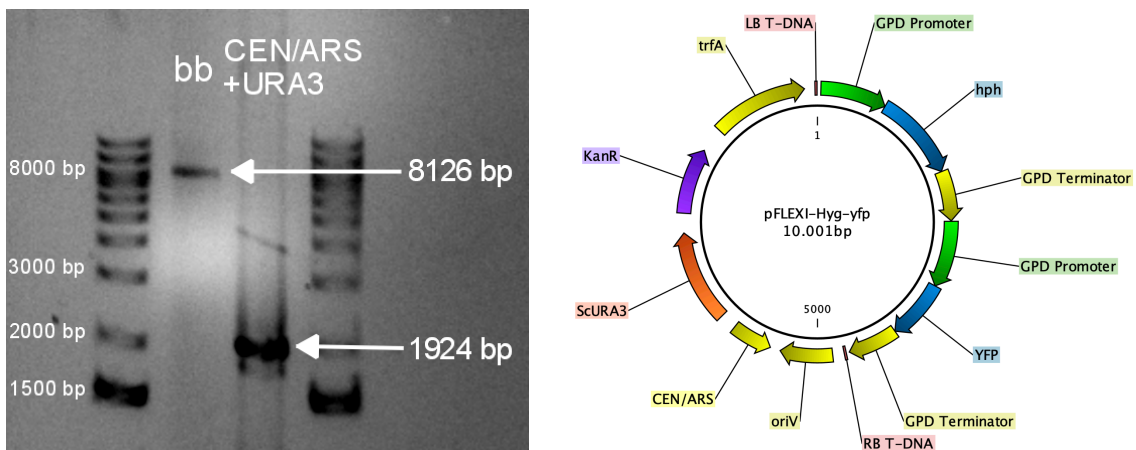


Figure 5.5: PCR products used for the plasmid assembly of pFLEXI-hyg-yfp is shown on a gel with the expected lengths of the products given in the figure (left) as well as the plasmid map of the expected assembled plasmid (right).

Since the expected lengths are present in both samples, it was safe to assume that the correct DNA fragments had been obtained. It also seems as if the samples were quite pure since there are no bands from the templates and no significant unspecific bands present in the lanes. However, the concentration of the CEN/ARS+URA3 insert (from the pSHUT3-32 plasmid) seems to be higher than the backbone obtained from the pRF-HU2-hyg-yfp plasmid. This can be explained by the difference in product size and in the method of purification since the CEN/ARS+URA3 insert was purified with PCR purification kit while the backbone was purified with the gel purification kit due to the presence of unspecific DNA fragments with different lengths. It was assumed that the concentrations obtained of each PCR products was sufficient for a successful plasmid assembly by yeast transformation.

- pFLEXI-hyg-cbhl

For the assembly of the pFLEXI-hyg-cbhl plasmid, the *yfp* gene of the pFLEXI-hyg-yfp plasmid should be exchanged with the codon optimized synthetic *cbhl* gene. To achieve this, three pieces from the pFLEXI-hyg-yfp plasmid were obtained; Hyg-P1, bb2-Hyg and T1-bb1, respectively. Furthermore, the *cbhl* gene was purified from the plasmid in which it was delivered by the manufacturer as described in the materials and methods. The expected plasmid map as well as the four purified DNA strands needed for the plasmid assembly of pFLEXI-hyg-cbhl is shown in Figure 5.6. The expected lengths of the four DNA strands and several marker lengths are given in the figure.

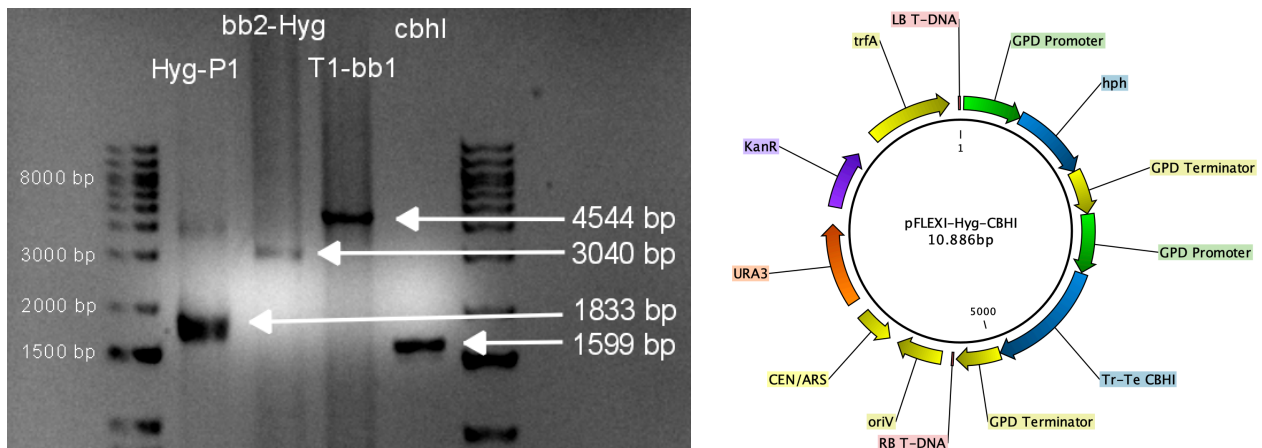


Figure 5.6: PCR products used for the plasmid assembly of pFLEXI-hyg-cbhl is shown on a gel with the expected lengths of the products given in the figure (left) as well as the plasmid map of the expected assembled plasmid (right).

The expected lengths were present in all purified DNA samples as it can be seen in the gel. However, for Hyg-P1, another unspecific band was present together with the desired DNA, but since the concentration of the desired DNA seems to be much larger in the sample, it was assumed that the chance for transformation success was high. Therefore, it was not attempted to further purify the sample by for example gel purification due to the chance of losing the desired DNA product. Furthermore, it is quite clear to see that the PCR products obtained from the miniprep of the pFLEXI-hyg-yfp plasmid are smeared compared to the *cbhl* product. This may be due to contamination of the miniprep from genomic DNA, but it was assumed that this contamination would not influence the rate of success for plasmid assembly.

- pFLEXI-hyg-(TEF1a)-cbhl

Due to the challenges experienced with the plasmid assembly of the pFLEXI-hyg-cbhl plasmid, it was attempted to construct another plasmid in which the entire (GPD)-yfp gene cassette was exchanged with a new codon optimized synthetic (TEF1a)-cbhl gene cassette. To achieve this, two backbone DNA pieces from the pFLEXI-hyg-yfp plasmid were obtained as described in the general laboratory workflow in Figure 4.3; bb1 and bb2, respectively. Furthermore, the synthetic (TEF1a)-cbhl gene cassette was purified from the plasmid in which it was delivered by the manufacturer as described in the materials and methods. The expected plasmid map as well as the three purified PCR products

needed for the plasmid assembly of pFLEXI-hyg-(TEF1a)-cbhl is shown in Figure 5.7. The expected lengths of the DNA products and several marker lengths are given in the figure.

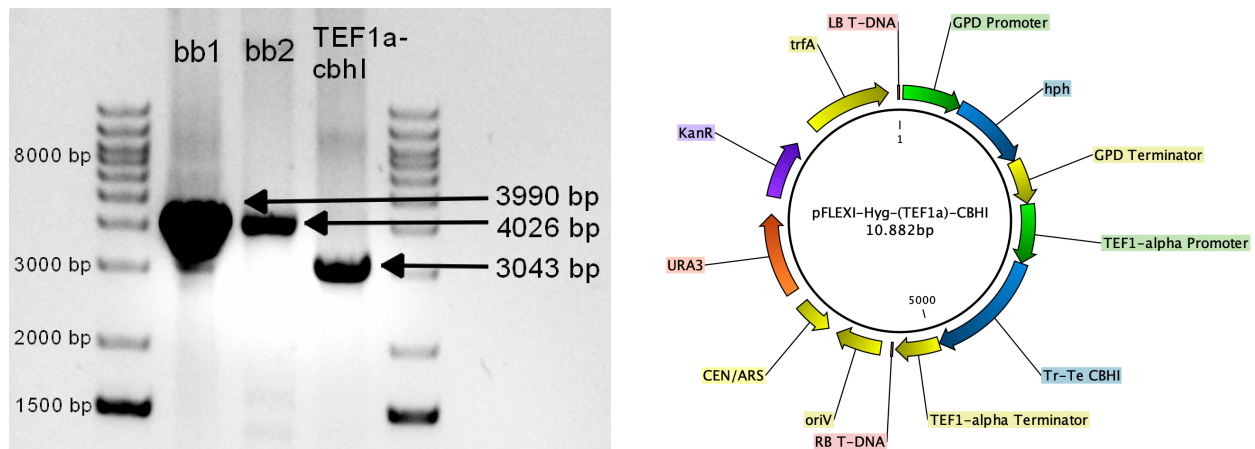


Figure 5.7: PCR products used for the plasmid assembly of pFLEXI-hyg-(TEF1a)-cbhl is shown on a gel with the expected lengths of the products given in the figure (left) as well as the plasmid map of the expected assembled plasmid (right).

Again, the expected lengths were present in the three purified DNA samples in very high concentration as it can be seen in the gel. Unfortunately, the sample containing the bb1 PCR product was overloaded on the gel which gives a smeared band. Furthermore, an unspecific DNA band was present with the desired DNA in the bb1 sample at 3000 bp, but since the concentration of the desired DNA products seems to be much larger in the sample, it was assumed that the chance for transformation success was high and if the sample had been diluted to avoid the overloading of the sample, the band would most likely not even be present on the gel. Therefore, it was not attempted to further purify the sample by gel purification. In addition, less smearing of the PCR products obtained using a new miniprep of the pFLEXI-hyg-yfp plasmid as the template were observed in the gel which can be used to argue that the smearing most likely was due to impurities in the template.

5.2.2 Plasmid validation

Because the plasmids will be used to instruct the yeast cells in how to code for, and ultimately express, new genetic material and proteins, it is very important to validate the construct before attempting to insert it into *C. oleagnosus*. By ensuring good quality control of the genetic starting material before transformation, complications related to sequence errors can be eliminated. In this master thesis, the plasmids were validated with colony PCR and restriction enzyme digests.

Colony PCR

The primers used for colony PCR were designed to be backbone-specific meaning that they anneal to sites that flank the insert site. This means that a positive clone will produce a larger size product than a negative clone without the insert. This type of primer pair can tell if the insert is the correct size and whether it has been inserted into the construct. This type of primer pair is great for

screening clones created with the same backbone but contain different inserts which is the case for all plasmids in this master thesis. When designing primers to anneal outside the cloning site, it does not matter what the sequence of the insert is, allowing to use the same primer pair to screen for the presence of many different inserts. The position of the primers used for colony PCR validation of the plasmids are shown as arrows in Figure 5.8 using a plasmid map of the pFLEXI-hyg-yfp plasmid as an example.

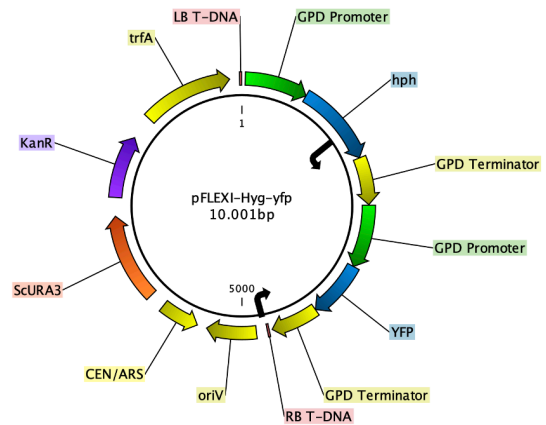


Figure 5.8: A plasmid map of the pFLEXI-hyg-yfp plasmid showing the position of the primers used for colony PCR validation.

- pFLEXI-hyg-yfp

The colony PCR product of the pFLEXI-hyg-yfp plasmid was expected to have a length of 3057 bp. As it can be seen in the gel in Figure 5.9, this band was observed for 6 out of 7 *S. cerevisiae* colonies which means that the plasmid most likely was assembled correctly in these yeast cells. On the other hand, no band was observed for colony number 7 and due to the primers chosen for colony PCR, this means that these yeast cells can not be carrying the pFLEXI-hyg-yfp plasmid. Furthermore, it is not possible for the cells to be carrying the pRF-HU2-hyg-yfp plasmid that was used as the template since this plasmid is missing the CEN/ARS and URA3 sequences that are necessary for survival in *S. cerevisiae*. However, the CEN/ARS+URA3 PCR product was obtained by using the pSHUT3-32 plasmid as the template, which means that yeast carrying this plasmid will be able to grow on the selection medium but will not show any band from colony PCR. Therefore, it was concluded that colony 7 was carrying the pSHUT3-32 template, while the colonies 1-6 was most likely carrying the pFLEXI-hyg-yfp plasmid of interest.



Figure 5.9: Results from colony PCR on *S. cerevisiae* expected to carry the pFLEXI-hyg-yfp plasmid after yeast transformation. The expected length of the PCR product for a correct assembled plasmid was 3057 bp.

- *pFLEXI-hyg-cbhl*

The colony PCR product of the *pFLEXI-hyg-cbhl* plasmid was expected to have a length of 4086 bp. As shown in the gels in Figure 5.10 and Figure 5.11 from plasmid assembly with yeast transformation and Gibson assembly, respectively, a band with this size was not observed for any of the colonies. Several rounds of attempts for plasmid assembly were carried out using both yeast transformation and Gibson assembly but, in all cases, a band of approximately 1000 bp or no bands at all were observed.

Since homologous regions of the plasmid will recombine with each other during cloning procedures, it is not optimal to reuse the same promoter and the same terminator twice in a plasmid. The colony PCR product with a size of 1000 bp could potentially correspond to the two GPD-terminators recombining with each other. In that case, the *yfp/cbhl* cassette will be looped out of the plasmid, leaving only the hygromycin cassette in the plasmid. The cases where no bands were observed from colony PCR, could be due to opposite situation in which the two GPD-promoters recombine with each other. In that case, the hygromycin cassette will be looped out of the plasmid, leaving only the *yfp/cbhl* cassette in the plasmid. And since one of the primers from colony PCR binds within the hygromycin cassette, no band will be observed in this case.



Figure 5.10: Results from colony PCR on *S. cerevisiae* expected to carry the *pFLEXI-hyg-cbhl* plasmid after yeast transformation. The expected length of the PCR product for a correct assembled plasmid was 4086 bp.

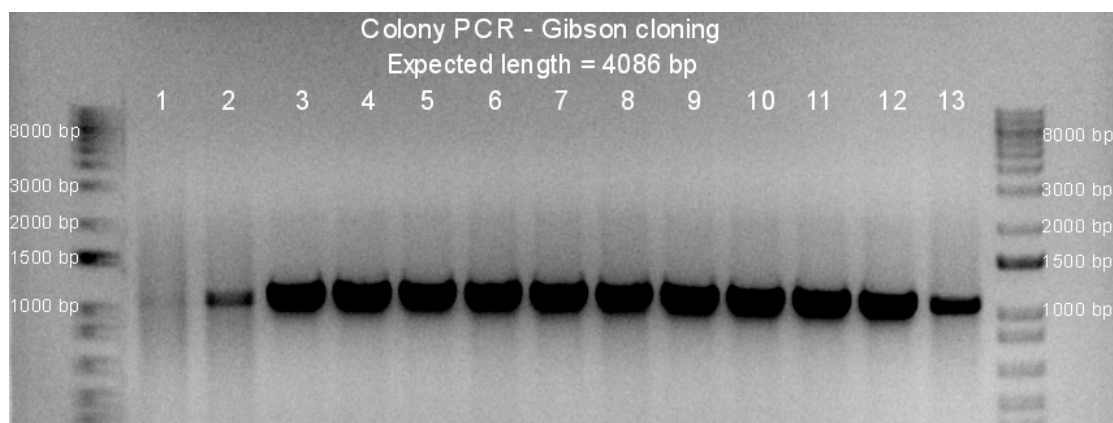


Figure 5.11: Results from colony PCR on *E. coli* expected to carry the *pFLEXI-hyg-cbhl* plasmid after transformation with the Gibson assembled plasmid. The expected length of the PCR product for a correct assembled plasmid was 4086 bp.

- pFLEXI-hyg-(TEF1a)-cbhl

Due to the several round of time-consuming unsuccessful attempts of plasmid assembly with pFLEXI-hyg-cbhl, it was decided to exchange the entire (GPD)-yfp gene cassette with a new (TEF1a)-cbhl gene cassette to increase the robustness of the transformation system. The colony PCR product of the pFLEXI-hyg-(TEF1a)-cbhl plasmid was also expected to have a length of 4086 bp. As shown in the gel in Figure 5.12, a band with the expected size was observed for colonies 2 and 3 after yeast transformation. Due to the backbone-specific design of the primers for colony PCR, this band at 4086 bp would not be present unless the yeast cells carry the plasmid of interest. However, as the gel shows, another band of approximately 1500 bp is also present in these lanes for colonies 2 and 3. This can be explained by one of two reasons; 1) the yeast is carrying more than one plasmid out of which one of them is the pFLEXI-hyg-(TEF1a)-cbhl plasmid or 2) one of the primers bind at an unspecific place in the plasmid. None of the other colonies showed a PCR product with the expected length and it was assumed that they did not carry the plasmid of interest.

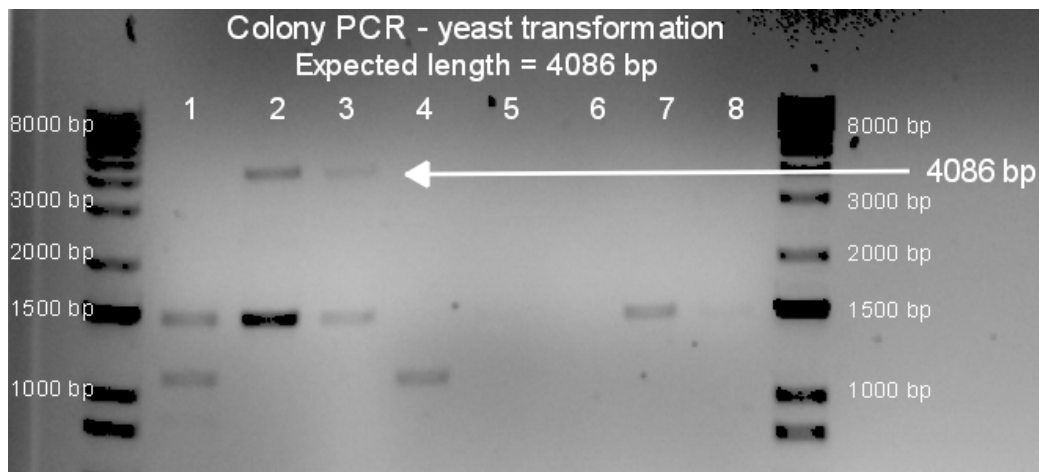


Figure 5.12: Results from colony PCR of *S. cerevisiae* transformants expected to carry the pFLEXI-hyg-(TEF1a)-cbhl plasmid from yeast transformation. The expected length of the PCR product for a correct assembled plasmid was 4086 bp.

Due to the time limit of the project, the DNA extract of *S. cerevisiae* colonies 2 and 3 was not electroporated into *E. coli*. However, if the colonies did carry more than one plasmid, it would be possible to extract both plasmids from *S. cerevisiae* but since each *E. coli* cell can only be transformed by one plasmid molecule, which is then propagated to make a clonal population of bacteria that contains only a single plasmid species, it would be possible to separate the two plasmids.

Restriction enzymes

Since it was concluded that colonies 1-6 from yeast transformation of pFLEXI-hyg-yfp was most likely carrying the plasmid of interest based on the colony PCR reactions, it was decided to further validate a plasmid extracted from a randomly chosen colony. Plasmid validation by restriction enzyme digest takes advantage of the fact that restriction enzymes cleave DNA at specific sequences called restriction sites. And if the size of the plasmid as well as the restriction sites are known, this technique can be quickly used to verify the plasmid.

The plasmids pRF-HU2-hyg-yfp and pFLEXI-hyg-yfp were validated by digestion with restriction enzymes PstI and SmaI and the results as well as the lengths of the expected bands are given in Figure 5.13.

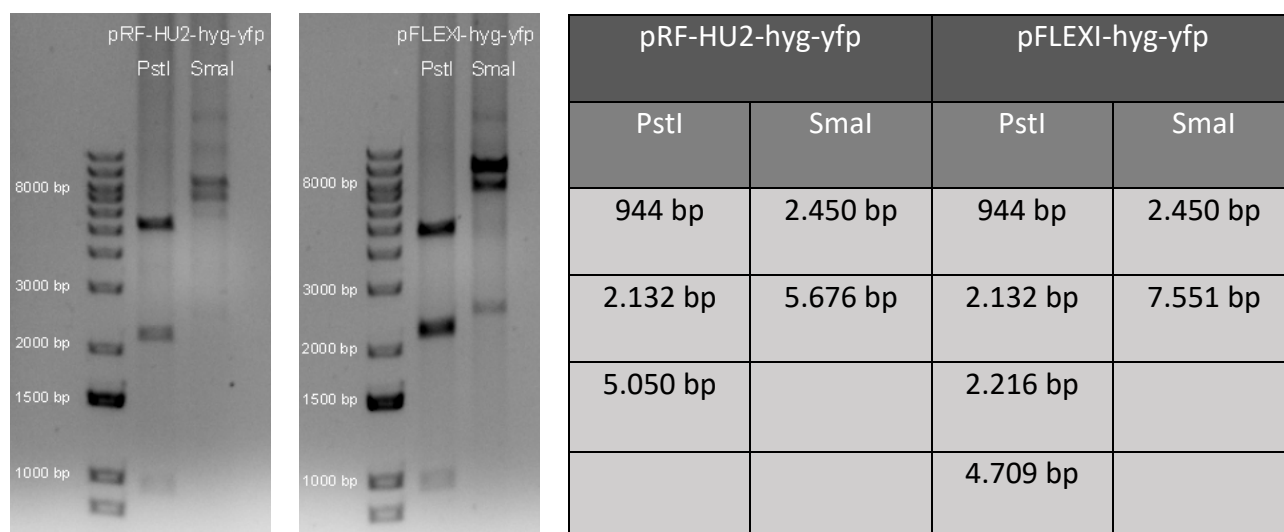


Figure 5.13: Results from restriction enzyme digest with PstI and SmaI of the pRF-HU2-hyg-yfp plasmid (left) and the pFLEXI-hyg-yfp plasmid (middle). The lengths of the expected bands are given in the figure table (right)

Since no template was observed in the gels after digestion with PstI, it was assumed that the digestion was complete. The expected products from digest with PstI are present for both plasmids, however, it can be difficult to see if there are two products present at 2132 bp and 2216 bp for the pFLEXI-hyg-yfp plasmid. Nevertheless, if we compare the concentration of the band above 2000 bp in the pRF-HU2-hyg-yfp plasmid with the same band in the pFLEXI-hyg-yfp plasmid, it seems as if the band in the pFLEXI-hyg-yfp plasmid is more concentrated which could indicate the presence of two DNA products.

On the other hand, some template can be observed in the gels after digestion with SmaI which could indicate an incomplete digestion. The expected bands after digestion with SmaI are present for both plasmids but in very low concentration. It was attempted to increase the incubation time, but the digestion was still insufficient which could mean that the activity of the enzyme was compromised. In addition, a band is observed at approximately 8000 bp for the pRF-HU2-hyg-yfp plasmid and at approximately 10000 bp for the pFLEXI-hyg-yfp plasmid which corresponds to the full length of the linear plasmids.

Based on the successful colony PCR and the digestion with PstI, it was concluded that the pRF-HU2-hyg-yfp and pFLEXI-hyg-yfp plasmids was validated and ready for transformation of *C. oleaginosus* with ATMT.

5.2.3 Transformation of *A. tumefaciens*

The two plasmids were electroporated into *A. tumefaciens* as described in the materials and methods to prepare for ATMT. The successfully transformed *A. tumefaciens* colonies were selected by plating the cell suspension on LB agar plates supplemented with 30 $\mu\text{g}/\text{mL}$ kanamycin and 20 $\mu\text{g}/\text{mL}$ rifampicin as shown in Figure 5.14.

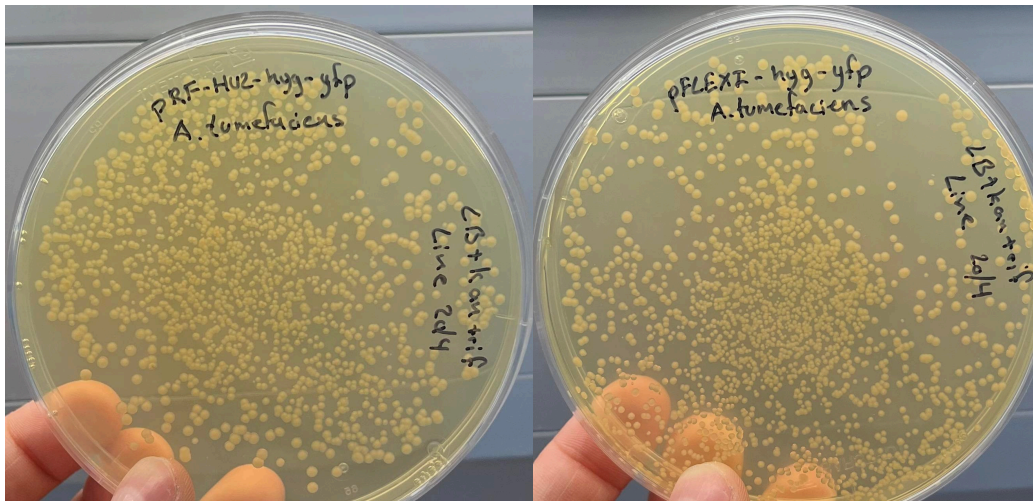


Figure 5.14: *A. tumefaciens* colonies transformed by electroporation with the pRF-HU2-hyg-yfp plasmid (left) and the pFLEXI-hyg-yfp plasmid (right) on LB agar plates supplemented with 30 $\mu\text{g}/\text{mL}$ kanamycin and 20 $\mu\text{g}/\text{mL}$ rifampicin.

5.2.4 Transformation of *C. oleaginosus*

A cell suspension mixture of the transformed *A. tumefaciens* and *C. oleaginosus* was plated on top of a black filter paper that was placed on S-IMAS agar plates. The plates were incubated at 24 $^{\circ}\text{C}$ for 48 hours, after which the filter was transferred to YPD agar plates supplemented with 200 $\mu\text{g}/\text{mL}$ hygromycin B and 300 $\mu\text{g}/\text{mL}$ cefotaxime. Incubation of the agar plates was carried out over 3 days at 28 $^{\circ}\text{C}$.



Figure 5.15: Results from ATMT with the pRF-HU2-hyg-yfp plasmid after 2 days of induction growth; black filter paper on S-IMAS plate.

There were no visible cells on any of the S-IMAS plates with black filter paper after two days of incubation as it can be seen in Figure 5.15. However, when the filter papers were transferred to the YPD selection plates, yeast cells appeared on the filters as shown in Figure 5.16. For the ATMT experiments, two control plates were included and no colonies appeared on either of the two plates. Since no colonies appeared on plate A containing the wild type *A. tumefaciens* and the wild type *C. oleaginosus*, neither of these two can grow without being transformed. And since no colonies were observed on plate B with *A. tumefaciens* that was transformed with pFLEXI-hyg-yfp, the colonies that can be seen on plates C, D, E and F can not just be from the transformed *A. tumefaciens* cells.

Plates C and E are transformation plates with wild type *C. oleaginosus* and *A. tumefaciens* transformed with pRF-HU2-hyg-yfp while plates D and F are transformation plates with wild type *C. oleaginosus* and *A. tumefaciens* transformed with pFLEXI-hyg-yfp. The colonies observed on these plates must be transformed *C. oleaginosus* cells due to the lack of colonies on the control plates. The difference between the plates C and D and plates E and F is found in the amount of cell suspension mixture plated on top of the black filter paper. 500 μ L of cell mixture was plated on plates C and D whereas 1000 μ L was plated on plates E and F. For further experiments, it would be optimal to plate only 500 μ L of cell mixture since it may be hard to separate individual colonies if the amount of cell mixture is too large.

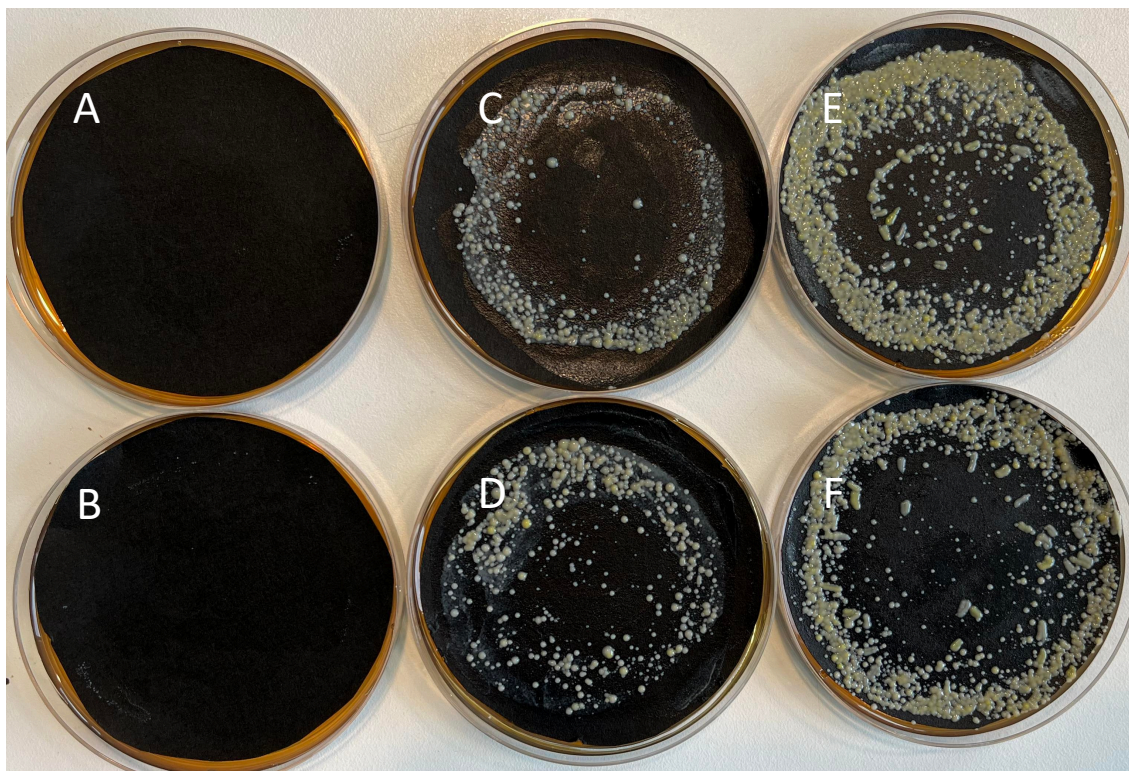


Figure 5.16: Results of ATMT after 4 days of selection growth; black filter paper on YPD plates supplemented with 200 μ g/mL hygromycin and 300 μ g/mL cefotaxime. Plate A) control plate with wild-type *A. tumefaciens* and wild-type *C. oleaginosus*; Plate B) control plate with *A. tumefaciens* transformed with pFLEXI-hyg-yfp; Plate C & E) transformation plate with *A. tumefaciens* carrying the pRF-HU2-hyg-yfp plasmid and wild-type *C. oleaginosus*; Plate D & F) transformation plate with *A. tumefaciens* carrying the pFLEXI-hyg-yfp plasmid and wild-type *C. oleaginosus*. The difference between plates C & E and plates D & F is the volume of cell mixture that was plated on top of the black filter paper (500 μ L and 1000 μ L).

Randomly chosen colonies that appeared on the black filter paper were isolated on new YPD agar plates supplemented with 200 $\mu\text{g}/\text{mL}$ hygromycin B. As shown in Figure 5.17, the appearance and growth of the individual colonies were very different. This observable difference can most likely be attributed to the random integration method used for transformation because random integration with ATMT do not allow a defined introduction of genes into the genome in terms of number or location and different levels of gene expression in independent transformants are common [122]. This variation in gene expression is attributed to several factors including chromosome location and copy number, as one or multiple gene copies can integrate at one or multiple loci. Furthermore, random integrations can lead to confounding effects on expression including gene silencing and the activation or disruption of genes [122]. Both factors cause unstable gene expression leading to unpredictable cell behavior and one of these or both two factors are most likely responsible for the difference in color appearance of the cells observed on the plate.

In the same way, the difference in growth may be attributed to the variation in gene expression since the wild type of *C. oleaginosus* is sensitive to hygromycin B. To circumvent the lethal effect of hygromycin B, a successfully transformed yeast must express the resistance gene *hph* that encodes the hygromycin B phosphotransferase and inactivates hygromycin B phosphorylation. Therefore, differences in the hygromycin B resistance, leading to reduced growth, are most likely caused by variable genomic copy numbers and loci.



Figure 5.17: Randomly selected individual colonies of *C. oleaginosus* mutants on YPD plates supplemented with 200 $\mu\text{g}/\text{mL}$ hygromycin. The colonies in this figure were picked from plate E) in Figure 5.14 in which the plasmid pRF-HU2-hyg-yfp was used for the ATMT.

5.2.5 Validation of the successful transformation of *C. oleaginosus*

To validate the *C. oleaginosus* mutants for successful integration of the DNA by ATMT, a colony PCR of the individual colonies was performed, and the primers were designed to yield a 579 bp PCR product within the hygromycin cassette. An example of the obtained results from colony PCR on *C.*

oleaginosus are shown in Figure 5.18 with the pRF-HU2-hyg-yfp plasmid as a control. A very clear band was observed for all colonies except for colony RF8, which did not show any band. This colony also showed very little growth on the YPD plates supplemented with hygromycin B which may indicate that the DNA of interest was not integrated successfully or that the genes are not expressed.

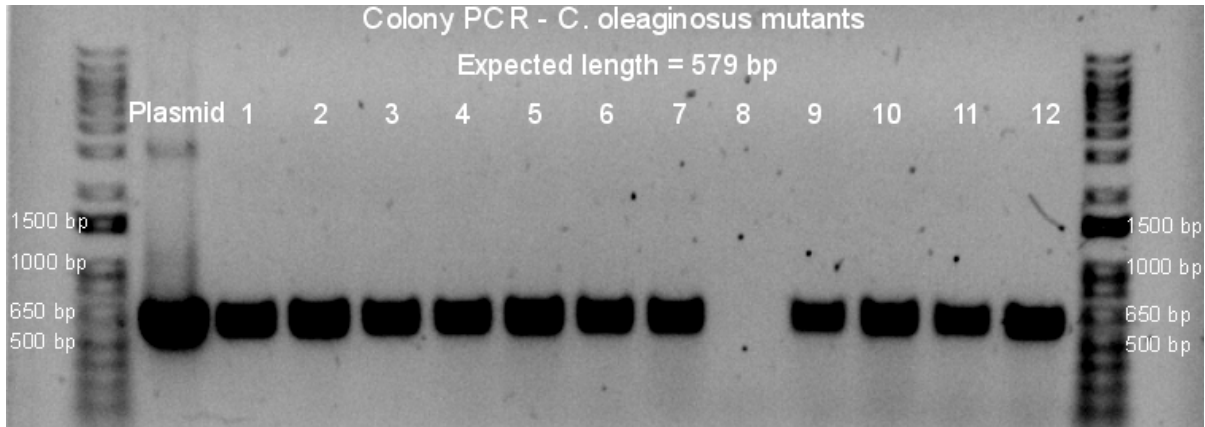


Figure 5.18: Example of results from colony PCR of *C. oleaginosus* mutants with primers binding within the hygromycin cassette. The expected length of the PCR product for a successfully transformed mutant was 579 bp. Purified pRF-HU2-hyg-yfp plasmid was used as positive control in the first lane.

5.2.6 Level of yellow fluorescence protein expression in *C. oleaginosus* mutants

To test the variation in gene expression due to random integration in the *C. oleaginosus* mutants, the level of yellow fluorescence protein expression was measured over time and the results are shown in Figure 5.19.

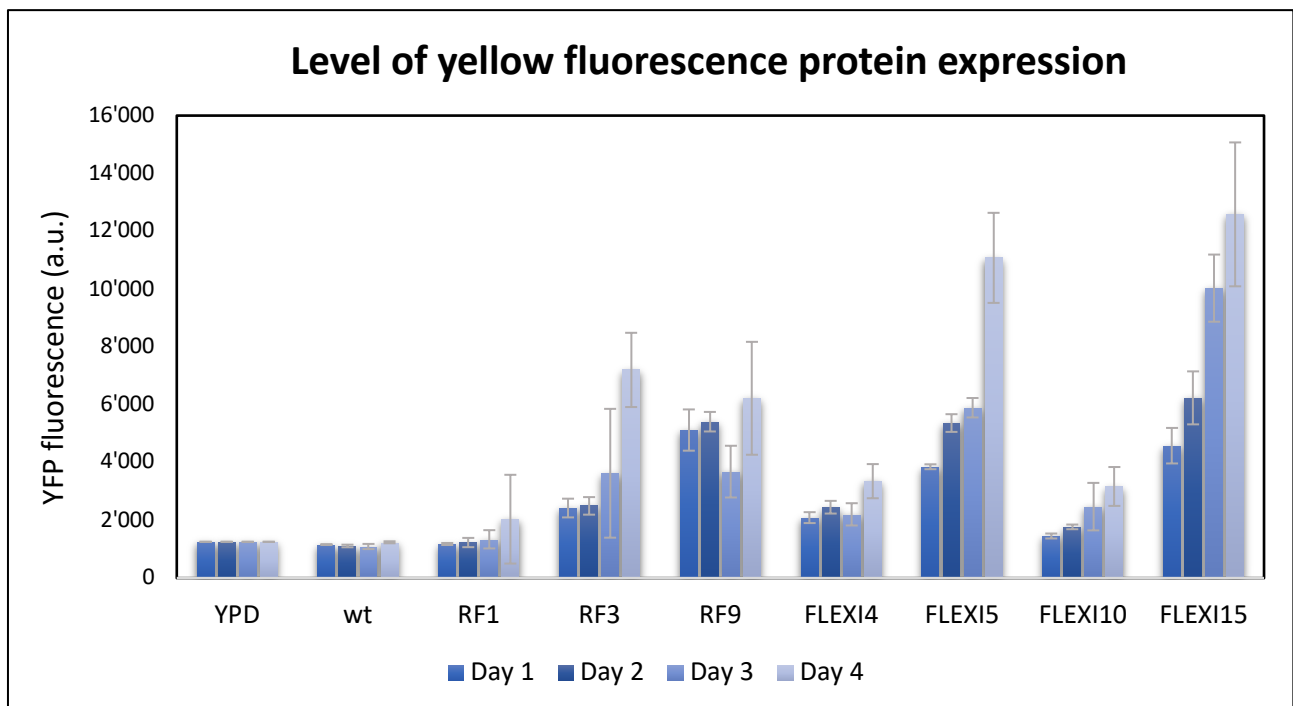


Figure 5.19: Level of yellow fluorescence protein expression over time in different *C. oleaginosus* mutants. The yfp fluorescence (a.u) was measured in liquid media, in a wild type *C. oleaginosus* culture as well as in 7 cultures with different mutants of *C. oleaginosus*. The standard deviation of three samples is illustrated with the grey error bar.

The wild type of *C. oleaginosus* did not show any expression of yellow fluorescence protein during the 4 days of measurements since the fluorescence that was measured for the wild type corresponds to the background fluorescence from the YPD media as it is illustrated in Figure 5.19. For the 7 mutants that were randomly chosen, they all show a development in the level of yfp expression over time but the speed in which the fluorescence developed, and the initial fluorescence varies significantly. This must naturally be attributed to the random integration of yfp. To make sure that the difference in level of yfp expression was not due to a difference in growth, the OD₆₀₀ was measured simultaneously, and the results are shown in Figure 5.20. It is obvious that the growth of the different cultures was similar and that the difference in yfp expression can not be attributed to this factor.

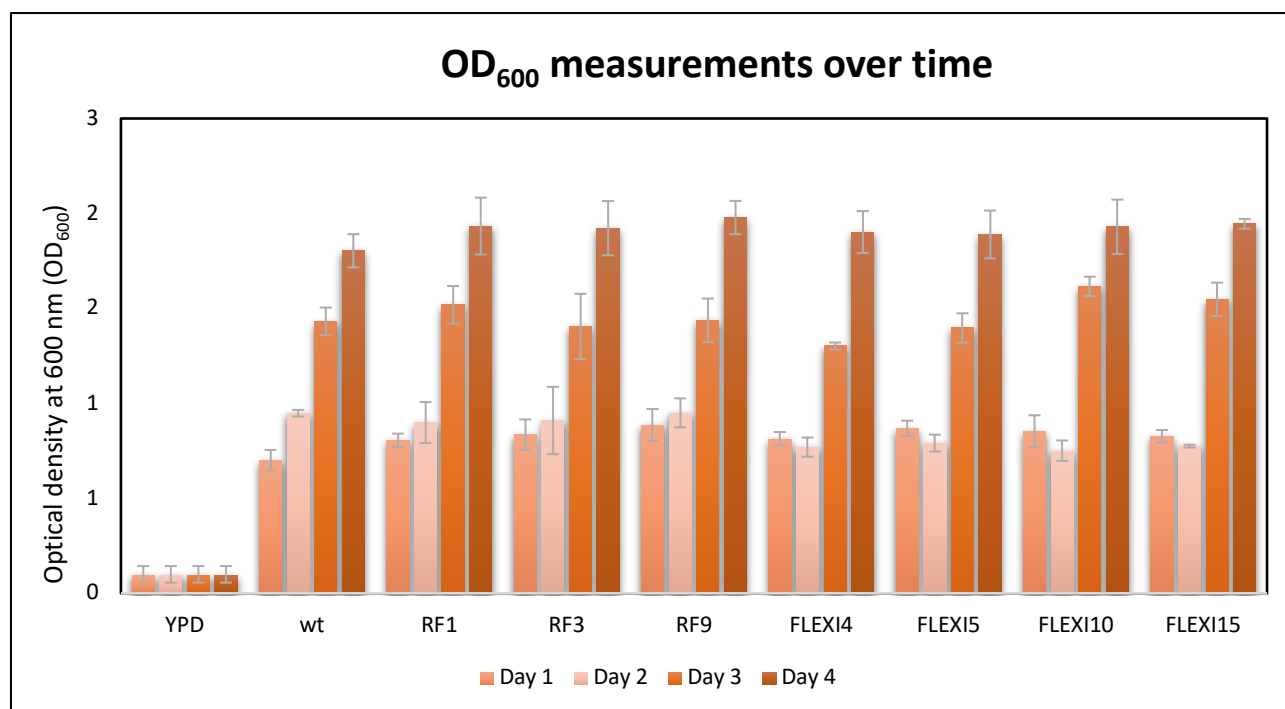


Figure 5.20: OD₆₀₀ measurements over time in different *C. oleaginosus* mutants. The optical density at 600 nm (OD₆₀₀) was measured in liquid media, in a wild type *C. oleaginosus* culture as well as in 7 cultures with different mutants of *C. oleaginosus*. The standard deviation of three samples is illustrated with the grey error bar.

A summary of the molecular laboratory work that was successfully achieved during this master thesis is given in Table 5.3.

Table 5.3: Summary table of the genetic engineering of *C. oleaginosus* conducted in this laboratory work.

Plasmid	Validated	Successfully transformed into <i>A. tumefaciens</i>	Successfully transformed into <i>C. oleaginosus</i>
pRF-HU2-hyg-yfp	Yes	Yes	Yes
pFLEXI-hyg-yfp	Yes	Yes	Yes
pFLEXI-hyg-cbhl	No	No	No
pFLEXI-hyg-(TEF1α)-cbhl	Partially	No	No

6 Conclusions

The overall objective of this master thesis was to examine the lipid production during fermentation with the yeast *Cutaneotrichosporon oleaginosus* using the organic fraction of municipal solid waste (OFMSW) as the feedstock and thereby determine the optimal time of fermentation as well as the optimal setup for the fermentation process. Based on the results from the time studies presented in this thesis, it can be concluded that the optimal time of fermentation was successfully determined for both a separate hydrolysis and fermentation (SHF) process and for a simultaneous saccharification and fermentation (SSF) process, while a process simulation with a techno economical evaluation is needed to make any conclusions on the optimal fermentation setup to use at an industrial scale. This is due to the fact that several internal and external factors must be taking into consideration and both process setups have advantages and disadvantages compared to one another. Nevertheless, the laboratory-scale results obtained in this master thesis provides several real-life inputs and outputs for the development of a process model, that can simulate an industrial scale of the lipid production using OFMSW as the feedstock.

Another objective of this master thesis was to genetically engineer *C. oleaginosus* by inserting a codon optimized version of a *cbh1* gene responsible for the production of an exoglucanase into the genome of the yeast by *Agrobacterium tumefaciens* mediated transformation (ATMT). Unfortunately, it must be concluded that the time frame of the project and the challenges experienced in the laboratory regarding vector cloning procedures limited the genetic engineering results. Nevertheless, a new vector system, pFLEXI-hyg-yfp, was developed and it was shown that this plasmid could be successfully transformed into *C. oleaginosus* by random integration with ATMT. Furthermore, it was shown that random gene integration leads to observable differences in appearance and growth of the individual colonies, and it can be concluded that the level of gene expression in randomly selected colonies was found to be very different.

7 Perspectives

The cost competitiveness of biofuels with fossil fuels is one of the great barriers for large-scale production of biofuels with the currently developed technologies. Therefore, it is interesting to further work with this study to obtain optimized results that is advantageous when speaking of industrial commercialization.

In this thesis, it was concluded that a process simulation was needed to make any conclusions on the optimal fermentation setup to use at an industrial scale, which is why it is suggested to develop such a process model as the next step in this area of research. This simulation will be able to account for the economic feasibility of the process as well as providing information on the sustainability regarding waste streams, heat consumption, water usage, etc. The results obtained from the laboratory SHF and SSF fermentation processes can be implemented into the simulation model and the different outputs will contribute to the discussion on which fermentation setup to use for an industrial scale.

Furthermore, it would be optimal to further improve the overall sugar to lipid fermentation process regarding lipid yield, process sustainability, economic perspectives, etc. This could for example be investigating how different ratios of enzyme mixtures can influence the lipid production to uncover the optimal conditions for lipid production in accordance with the technology highlighted in this project. The proposed enzyme mixture composition included in this project is solely based on published data and suggestions by the manufacturer, therefore it is intriguing to experiment with different ratios as well as different enzymes to minimize the costs of this factor. It is also interesting to track, how the addition of nutrients and other components facilitate the fermentation process and thereby the lipid accumulation in the yeast. The purpose of such intervention will be to map out the most optimized version of organic municipal solid waste media, which still retains a good foundation for industrial setup. Another part of the process in which improvements could be implemented is within the recovery and extraction of lipids. This could for example include an investigation of the possibilities of using critical CO₂ extraction or it could include a screening of different extraction solvents.

It was also concluded that a new vector system, pFLEXI-hyg-yfp, was developed and that this plasmid could be successfully transformed into *C. oleaginosus* by random integration with ATMT. Further projects could involve a genome sequencing of the different mutants of *C. oleaginosus* to find loci that lead to a high level of gene expression without compromising the growth of the yeast. In addition, it would be optimal to develop of transformation system that allows for multiple gene insertions and deletions and develop a faster and easier transformation method for *C. oleaginosus*. Lastly, it is suggested to continue the work started in this master thesis regarding genetic engineering of *C. oleaginosus* with the aim of producing enzymes with cellulolytic activity and testing the activity of these enzymes. Potentially, a fermentation without the addition of commercial enzymes could be investigated as well to completely remove this cost from the process.

8 Bibliography

- [1] Zhu, L.D., Li, Z.H. and Hiltunen, E. (2016) *Strategies for Lipid Production Improvement in Microalgae as a Biodiesel Feedstock*. BioMed Research International, vol. **2016**. <https://doi.org/10.1155/2016/8792548>
- [2] Alishah Aratboni, H., Rafiei, N., Garcia-Granados, R., Alemzadeh, A. and Morones-Ramírez, J.R. (2019) *Biomass and lipid induction strategies in microalgae for biofuel production and other applications*. Microbial Cell Factories, vol. **18**. <https://doi.org/10.1186/s12934-019-1228-4>
- [3] Vasconcelos, B., Teixeira, J.C., Dragone, G. and Teixeira, J.A. (2019) *Oleaginous yeasts for sustainable lipid production—from biodiesel to surf boards, a wide range of “green” applications*. Applied Microbiology and Biotechnology, vol. **103**. <https://doi.org/10.1007/s00253-019-09742-x>
- [4] Petrovič, U. (2015) *Next-generation biofuels: a new challenge for yeast*. Yeast, vol. **32**. <https://doi.org/10.1002/yea.3082>
- [5] Popp, J., Lakner, Z., Harangi-Rákos, M. and Fári, M. (2014) *The effect of bioenergy expansion: Food, energy, and environment*. Renewable and Sustainable Energy Reviews, vol. **32**. <https://doi.org/10.1016/j.rser.2014.01.056>
- [6] Khan, M.A.H., Bonifacio, S., Clowes, J., Foulds, A., Holland, R., Matthews, J.C. et al. (2021) *Investigation of Biofuel as a Potential Renewable Energy Source*. Atmosphere, vol. **12**. <https://doi.org/10.3390/atmos12101289>
- [7] Ghanavati, H., Nahvi, I. and Karimi, K. (2015) *Organic fraction of municipal solid waste as a suitable feedstock for the production of lipid by oleaginous yeast *Cryptococcus aerius**. Waste Management, vol. **38**. <https://doi.org/10.1016/j.wasman.2014.12.007>
- [8] Gong, Z., Shen, H., Wang, Q., Yang, X., Xie, H. and Zhao, Z.K. (2013) *Efficient conversion of biomass into lipids by using the simultaneous saccharification and enhanced lipid production process*. Biotechnology for Biofuels, vol. **6**. <https://doi.org/10.1186/1754-6834-6-36>
- [9] Jeswani, H.K., Chilvers, A. and Azapagic, A. (2020) *Environmental sustainability of biofuels: a review*. Proceedings of the Royal Society A: Mathematical, Physical and Engineering Sciences, vol. **476**. <https://doi.org/10.1098/rspa.2020.0351>
- [10] Bombo, K., Lekgoba, T., Azeez, O. and MUZENDA, E. (2021) *The Sustainability of Biodiesel Synthesis from Different Feedstocks: A Review*. Petroleum and Coal, vol. **63**, pp. 284–91.
- [11] Hu, C., Zhao, X., Zhao, J., Wu, S. and Zhao, Z.K. (2009) *Effects of biomass hydrolysis by-products on oleaginous yeast *Rhodospiridium toruloides**. Bioresource Technology, vol. **100**. <https://doi.org/10.1016/j.biortech.2009.04.041>
- [12] Phukan, M.M., Bora, P., Gogoi, K. and Konwar, B.K. (2019) *Biodiesel from *Saccharomyces cerevisiae*: fuel property analysis and comparative economics*. SN Applied Sciences, vol. **1**. <https://doi.org/10.1007/s42452-019-0159-3>
- [13] Olofsson, K., Bertilsson, M. and Lidén, G. (2008) *A short review on SSF – an interesting process option for ethanol production from lignocellulosic feedstocks*. Biotechnology for Biofuels, vol. **1**. <https://doi.org/10.1186/1754-6834-1-7>
- [14] Damayanti, D., Supriyadi, D., Amelia, D., Saputri, D.R., Devi, Y.L.L., Auriyani, W.A. et al. (2021) *Conversion of Lignocellulose for Bioethanol Production, Applied in Bio-Polyethylene Terephthalate*. Polymers, vol. **13**. <https://doi.org/10.3390/polym13172886>
- [15] Tsai, C.-S., Kwak, S., Turner, T.L. and Jin, Y.-S. (2014) *Yeast synthetic biology toolbox and*

- applications for biofuel production*. FEMS Yeast Research, . <https://doi.org/10.1111/1567-1364.12206>
- [16] Shi, S. and Zhao, H. (2017) *Metabolic Engineering of Oleaginous Yeasts for Production of Fuels and Chemicals*. *Frontiers in Microbiology*, vol. **8**. <https://doi.org/10.3389/fmicb.2017.02185>
- [17] Görner, C., Redai, V., Bracharz, F., Schrepfer, P., Garbe, D. and Brück, T. (2016) *Genetic engineering and production of modified fatty acids by the non-conventional oleaginous yeast Trichosporon oleaginosus ATCC 20509*. *Green Chem*, The Royal Society of Chemistry. vol. **18**, pp. 2037–46. <https://doi.org/10.1039/C5GC01767J>
- [18] Wang, Y., Chen, H. and Yu, O. (2014) *A plant malonyl-CoA synthetase enhances lipid content and polyketide yield in yeast cells*. *Applied Microbiology and Biotechnology*, vol. **98**. <https://doi.org/10.1007/s00253-014-5612-z>
- [19] Koivuranta, K., Castillo, S., Jouhten, P., Ruohonen, L., Penttilä, M. and Wiebe, M.G. (2018) *Enhanced Triacylglycerol Production With Genetically Modified Trichosporon oleaginosus*. *Frontiers in Microbiology*, vol. **9**. <https://doi.org/10.3389/fmicb.2018.01337>
- [20] Kricka, W., Fitzpatrick, J. and Bond, U. (2014) *Metabolic engineering of yeasts by heterologous enzyme production for degradation of cellulose and hemicellulose from biomass: a perspective*. *Frontiers in Microbiology*, vol. **5**. <https://doi.org/10.3389/fmicb.2014.00174>
- [21] Fitzpatrick, J., Kricka, W., James, T.C. and Bond, U. (2014) *Expression of three Trichoderma reesei cellulase genes in Saccharomyces pastorianus for the development of a two-step process of hydrolysis and fermentation of cellulose*. *Journal of Applied Microbiology*, vol. **117**. <https://doi.org/10.1111/jam.12494>
- [22] Moodley, P. (2021) *Sustainable biofuels: opportunities and challenges*. *Sustainable Biofuels*, Elsevier. p. 1–20. <https://doi.org/10.1016/B978-0-12-820297-5.00003-7>
- [23] Alalwan, H.A., Alminshid, A.H. and Aljaafari, H.A.S. (2019) *Promising evolution of biofuel generations. Subject review*. *Renewable Energy Focus*, vol. **28**, pp. 127–39. <https://doi.org/10.1016/j.ref.2018.12.006>
- [24] Chintagunta, A.D., Zuccaro, G., Kumar, M., Kumar, S.P.J., Garlapati, V.K., Postemsky, P.D. et al. (2021) *Biodiesel Production From Lignocellulosic Biomass Using Oleaginous Microbes: Prospects for Integrated Biofuel Production*. *Frontiers in Microbiology*, vol. **12**. <https://doi.org/10.3389/fmicb.2021.658284>
- [25] Subramaniam, R., Dufreche, S., Zappi, M. and Bajpai, R. (2010) *Microbial lipids from renewable resources: production and characterization*. *Journal of Industrial Microbiology & Biotechnology*, vol. **37**, pp. 1271–87. <https://doi.org/10.1007/s10295-010-0884-5>
- [26] Wahlen, B.D., Morgan, M.R., McCurdy, A.T., Willis, R.M., Morgan, M.D., Dye, D.J. et al. (2013) *Biodiesel from Microalgae, Yeast, and Bacteria: Engine Performance and Exhaust Emissions*. *Energy & Fuels*, vol. **27**, pp. 220–8. <https://doi.org/10.1021/ef3012382>
- [27] Görner, C. (2015) *Genetic Engineering of the Oleaginous Yeast Trichosporon oleaginosus and the Bacteria Escherichia Coli Aimed at the Production of High Value Lipids and Bioactive Diterpenes* [Internet]. München.
- [28] Lamers, D., van Biezen, N., Martens, D., Peters, L., van de Zilver, E., Jacobs-van Dreumel, N. et al. (2016) *Selection of oleaginous yeasts for fatty acid production*. *BMC Biotechnology*, vol. **16**. <https://doi.org/10.1186/s12896-016-0276-7>
- [29] Pham, N., Reijnders, M., Suarez-Diez, M., Nijssen, B., Springer, J., Eggink, G. et al. (2021) *Genome-scale metabolic modeling underscores the potential of Cutaneotrichosporon oleaginosus ATCC 20509 as a cell factory for biofuel production*. *Biotechnology for Biofuels*,

- vol. **14**, pp. 2. <https://doi.org/10.1186/s13068-020-01838-1>
- [30] Fuchs, T., Melcher, F., Rerop, Z.S., Lorenzen, J., Shaigani, P., Awad, D. et al. (2021) *Identifying carbohydrate-active enzymes of Cutaneotrichosporon oleaginosus using systems biology*. Microbial Cell Factories, vol. **20**, pp. 205. <https://doi.org/10.1186/s12934-021-01692-2>
- [31] Awad, D., Bohnen, F., Mehlmer, N. and Brueck, T. (2019) *Multi-Factorial-Guided Media Optimization for Enhanced Biomass and Lipid Formation by the Oleaginous Yeast Cutaneotrichosporon oleaginosus*. Frontiers in Bioengineering and Biotechnology, vol. **7**. <https://doi.org/10.3389/fbioe.2019.00054>
- [32] Di Fidio, N., Minonne, F., Antonetti, C. and Raspolli Galletti, A.M. (2021) *Cutaneotrichosporon oleaginosus: A Versatile Whole-Cell Biocatalyst for the Production of Single-Cell Oil from Agro-Industrial Wastes*. Catalysts, vol. **11**, pp. 1291. <https://doi.org/10.3390/catal11111291>
- [33] Šantek, M.I., Lisičar, J., Mušak, L., Špoljarić, I.V., Beluhan, S. and Šantek, B. (2018) *Lipid Production by Yeast Trichosporon oleaginosus on the Enzymatic Hydrolysate of Alkaline Pretreated Corn Cobs for Biodiesel Production*. Energy & Fuels, vol. **32**. <https://doi.org/10.1021/acs.energyfuels.8b02231>
- [34] Younes, S., Bracharz, F., Awad, D., Qoura, F., Mehlmer, N. and Brueck, T. (2020) *Microbial lipid production by oleaginous yeasts grown on Scenedesmus obtusiusculus microalgae biomass hydrolysate*. Bioprocess and Biosystems Engineering, vol. **43**, pp. 1629–38. <https://doi.org/10.1007/s00449-020-02354-0>
- [35] Yaguchi, A., Robinson, A., Mihealsick, E. and Blenner, M. (2017) *Metabolism of aromatics by Trichosporon oleaginosus while remaining oleaginous*. Microbial Cell Factories, vol. **16**, pp. 206. <https://doi.org/10.1186/s12934-017-0820-8>
- [36] Yaguchi, A., Franaszek, N., O'Neill, K., Lee, S., Sitepu, I., Boundy-Mills, K. et al. (2020) *Identification of oleaginous yeasts that metabolize aromatic compounds*. Journal of Industrial Microbiology and Biotechnology, vol. **47**, pp. 801–13. <https://doi.org/10.1007/s10295-020-02269-5>
- [37] Yu, X., Zheng, Y., Dorgan, K.M. and Chen, S. (2011) *Oil production by oleaginous yeasts using the hydrolysate from pretreatment of wheat straw with dilute sulfuric acid*. Bioresource Technology, vol. **102**, pp. 6134–40. <https://doi.org/10.1016/j.biortech.2011.02.081>
- [38] Bracharz, F., Beukhout, T., Mehlmer, N. and Brück, T. (2017) *Opportunities and challenges in the development of Cutaneotrichosporon oleaginosus ATCC 20509 as a new cell factory for custom tailored microbial oils*. Microbial Cell Factories, vol. **16**, pp. 178. <https://doi.org/10.1186/s12934-017-0791-9>
- [39] Caporusso, A., Capece, A. and De Bari, I. (2021) *Oleaginous Yeasts as Cell Factories for the Sustainable Production of Microbial Lipids by the Valorization of Agri-Food Wastes*. Fermentation, vol. **7**, pp. 50. <https://doi.org/10.3390/fermentation7020050>
- [40] Chen, L., Lee, J. and Ning Chen, W. (2016) *The use of metabolic engineering to produce fatty acid-derived biofuel and chemicals in Saccharomyces cerevisiae: a review*. AIMS Bioengineering, vol. **3**, pp. 468–92. <https://doi.org/10.3934/bioeng.2016.4.468>
- [41] Ahern, K. and Rajagopal, I. *Fatty Acid Synthesis* [Internet]. Oregon State University.
- [42] Park, G.W., Kim, N.-J. and Chang, H.N. (2018) *Microbial Lipid Production from Volatile Fatty Acids by Oleaginous Yeast*. Emerging Areas in Bioengineering, Wiley-VCH Verlag GmbH & Co. KGaA, Weinheim, Germany. p. 203–13. <https://doi.org/10.1002/9783527803293.ch12>
- [43] Campuzano, R. and González-Martínez, S. (2016) *Characteristics of the organic fraction of municipal solid waste and methane production: A review*. Waste Management, vol. **54**.

- <https://doi.org/10.1016/j.wasman.2016.05.016>
- [44] Paritosh, K., Yadav, M., Mathur, S., Balan, V., Liao, W., Pareek, N. et al. (2018) *Organic Fraction of Municipal Solid Waste: Overview of Treatment Methodologies to Enhance Anaerobic Biodegradability*. *Frontiers in Energy Research*, vol. **6**. <https://doi.org/10.3389/fenrg.2018.00075>
- [45] Alibardi, L. and Cossu, R. (2015) *Composition variability of the organic fraction of municipal solid waste and effects on hydrogen and methane production potentials*. *Waste Management*, vol. **36**, pp. 147–55. <https://doi.org/10.1016/j.wasman.2014.11.019>
- [46] Albanna, M. (2013) *Anaerobic Digestion of the Organic Fraction of Municipal Solid Waste*. *Management of Microbial Resources in the Environment*, Springer Netherlands, Dordrecht. p. 313–40. https://doi.org/10.1007/978-94-007-5931-2_12
- [47] Pecorini, I., Rossi, E. and Iannelli, R. (2020) *Bromatological, Proximate and Ultimate Analysis of OFMSW for Different Seasons and Collection Systems*. *Sustainability*, vol. **12**, pp. 2639. <https://doi.org/10.3390/su12072639>
- [48] Mussatto, S. and Teixeira, J. (2010) *Lignocellulose as raw material in fermentation processes*. *Current Research, Technology and Education Topics in Applied Microbiology and Microbial Biotechnology*, p. 897–907.
- [49] López-Gómez, J.P., Latorre-Sánchez, M., Unger, P., Schneider, R., Coll Lozano, C. and Venus, J. (2019) *Assessing the organic fraction of municipal solid wastes for the production of lactic acid*. *Biochemical Engineering Journal*, vol. **150**, pp. 107251. <https://doi.org/10.1016/j.bej.2019.107251>
- [50] Lange, L. (2017) *Fungal Enzymes and Yeasts for Conversion of Plant Biomass to Bioenergy and High-Value Products*. *Microbiology Spectrum*, vol. **5**. <https://doi.org/10.1128/microbiolspec.FUNK-0007-2016>
- [51] Mithra, M.G., Sajeev, M.S. and Padmaja, G. (2019) *Comparison of SHF and SSF Processes under Fed Batch Mode on Ethanol Production from Pretreated Vegetable Processing Residues*. *European Journal of Sustainable Development Research*, vol. **3**. <https://doi.org/10.20897/ejosdr/3950>
- [52] Kumar, A.K. and Sharma, S. (2017) *Recent updates on different methods of pretreatment of lignocellulosic feedstocks: a review*. *Bioresources and Bioprocessing*, vol. **4**, pp. 7. <https://doi.org/10.1186/s40643-017-0137-9>
- [53] Galbe, M. and Wallberg, O. (2019) *Pretreatment for biorefineries: a review of common methods for efficient utilisation of lignocellulosic materials*. *Biotechnology for Biofuels*, vol. **12**, pp. 294. <https://doi.org/10.1186/s13068-019-1634-1>
- [54] Mankar, A.R., Pandey, A., Modak, A. and Pant, K.K. (2021) *Pretreatment of lignocellulosic biomass: A review on recent advances*. *Bioresource Technology*, vol. **334**, pp. 125235. <https://doi.org/10.1016/j.biortech.2021.125235>
- [55] Amin, F.R., Khalid, H., Zhang, H., Rahman, S. u, Zhang, R., Liu, G. et al. (2017) *Pretreatment methods of lignocellulosic biomass for anaerobic digestion*. *AMB Express*, vol. **7**, pp. 72. <https://doi.org/10.1186/s13568-017-0375-4>
- [56] Baruah, J., Nath, B.K., Sharma, R., Kumar, S., Deka, R.C., Baruah, D.C. et al. (2018) *Recent Trends in the Pretreatment of Lignocellulosic Biomass for Value-Added Products*. *Frontiers in Energy Research*, vol. **6**. <https://doi.org/10.3389/fenrg.2018.00141>
- [57] Teixeira, R.S., Silva, A.S., Moutta, R.O., Ferreira-Leitão, V.S., Barros, R.R., Ferrara, M.A. et al. (2014) *Biomass pretreatment: a critical choice for biomass utilization via biotechnological*

- routes. BMC Proceedings, vol. **8**, pp. O34. <https://doi.org/10.1186/1753-6561-8-S4-O34>
- [58] Blue, D., Fortela, D., Holmes, W., LaCour, D., LeBoeuf, S., Stelly, C. et al. (2019) *Valorization of Industrial Vegetable Waste Using Dilute HCl Pretreatment*. Processes, vol. **7**, pp. 853. <https://doi.org/10.3390/pr7110853>
- [59] Brodeur, G., Yau, E., Badal, K., Collier, J., Ramachandran, K.B. and Ramakrishnan, S. (2011) *Chemical and Physicochemical Pretreatment of Lignocellulosic Biomass: A Review*. Enzyme Research, vol. **2011**, pp. 1–17. <https://doi.org/10.4061/2011/787532>
- [60] Fan, Z. (2014) *Consolidated Bioprocessing for Ethanol Production*. Biorefineries, Elsevier. p. 141–60. <https://doi.org/10.1016/B978-0-444-59498-3.00007-5>
- [61] Speight, J.G. (2020) *Production of fuels from nonfossil fuel feedstocks*. The Refinery of the Future, Elsevier. p. 391–426. <https://doi.org/10.1016/B978-0-12-816994-0.00011-7>
- [62] Razzaq, M. (2018) *Feedback inhibition of cellulolytic enzymes during saccharification of cellulosic biomass in order to enhance the productivity*. Pure and Applied Biology, vol. **7**. <https://doi.org/10.19045/bspab.2018.700124>
- [63] Broeker, J., Mechelke, M., Baudrexl, M., Mennerich, D., Hornburg, D., Mann, M. et al. (2018) *The hemicellulose-degrading enzyme system of the thermophilic bacterium Clostridium stercorarium: comparative characterisation and addition of new hemicellulolytic glycoside hydrolases*. Biotechnology for Biofuels, vol. **11**, pp. 229. <https://doi.org/10.1186/s13068-018-1228-3>
- [64] Madadi, M., Penga, C. and Abbas, A. (2017) *Advances in Genetic Manipulation of Lignocellulose to Reduce Biomass Recalcitrance and Enhance Biofuel Production in Bioenergy Crops*. Journal of Plant Biochemistry & Physiology, vol. **05**. <https://doi.org/10.4172/2329-9029.1000182>
- [65] Chaturvedi, T., Torres, A.I., Stephanopoulos, G., Thomsen, M.H. and Schmidt, J.E. (2020) *Developing Process Designs for Biorefineries—Definitions, Categories, and Unit Operations*. Energies, vol. **13**, pp. 1493. <https://doi.org/10.3390/en13061493>
- [66] Pollegioni, L., Tonin, F. and Rosini, E. (2015) *Lignin-degrading enzymes*. FEBS Journal, vol. **282**, pp. 1190–213. <https://doi.org/10.1111/febs.13224>
- [67] Galbe, M., Wallberg, O. and Zacchi, G. (2011) *Techno-Economic Aspects of Ethanol Production from Lignocellulosic Agricultural Crops and Residues*. Comprehensive Biotechnology, Elsevier. p. 615–28. <https://doi.org/10.1016/B978-0-08-088504-9.00298-1>
- [68] Rana, V., Eckard, A.D. and Ahring, B.K. (2014) *Comparison of SHF and SSF of wet exploded corn stover and loblolly pine using in-house enzymes produced from T. reesei RUT C30 and A. saccharolyticus*. SpringerPlus, vol. **3**, pp. 516. <https://doi.org/10.1186/2193-1801-3-516>
- [69] Chen, H. and Wang, L. (2017) *Microbial Fermentation Strategies for Biomass Conversion*. Technologies for Biochemical Conversion of Biomass, Elsevier. p. 165–96. <https://doi.org/10.1016/B978-0-12-802417-1.00007-7>
- [70] Marulanda, V.A., Gutierrez, C.D.B. and Alzate, C.A.C. (2019) *Thermochemical, Biological, Biochemical, and Hybrid Conversion Methods of Bio-derived Molecules into Renewable Fuels*. Advanced Bioprocessing for Alternative Fuels, Biobased Chemicals, and Bioproducts, Elsevier. p. 59–81. <https://doi.org/10.1016/B978-0-12-817941-3.00004-8>
- [71] Tsoutsos, T. (2010) *Modelling hydrolysis and fermentation processes in lignocelluloses-to-bioalcohol production*. Bioalcohol Production, Elsevier. p. 340–62. <https://doi.org/10.1533/9781845699611.4.340>
- [72] García-Torreiro, M., López-Abelairas, M., Lu-Chau, T.A. and Lema, J.M. (2016) *Production of*

- poly(3-hydroxybutyrate) by simultaneous saccharification and fermentation of cereal mash using Halomonas boliviensis*. Biochemical Engineering Journal, vol. **114**, pp. 140–6. <https://doi.org/10.1016/j.bej.2016.07.002>
- [73] Qiao, K., Imam Abidi, S.H., Liu, H., Zhang, H., Chakraborty, S., Watson, N. et al. (2015) *Engineering lipid overproduction in the oleaginous yeast Yarrowia lipolytica*. Metabolic Engineering, vol. **29**, pp. 56–65. <https://doi.org/10.1016/j.ymben.2015.02.005>
- [74] Spagnuolo, M., Yaguchi, A. and Blenner, M. (2019) *Oleaginous yeast for biofuel and oleochemical production*. Current Opinion in Biotechnology, vol. **57**, pp. 73–81. <https://doi.org/10.1016/j.copbio.2019.02.011>
- [75] Dulermo, T. and Nicaud, J.-M. (2011) *Involvement of the G3P shuttle and β -oxidation pathway in the control of TAG synthesis and lipid accumulation in Yarrowia lipolytica*. Metabolic Engineering, vol. **13**, pp. 482–91. <https://doi.org/10.1016/j.ymben.2011.05.002>
- [76] Tai, M. and Stephanopoulos, G. (2013) *Engineering the push and pull of lipid biosynthesis in oleaginous yeast Yarrowia lipolytica for biofuel production*. Metabolic Engineering, vol. **15**, pp. 1–9. <https://doi.org/10.1016/j.ymben.2012.08.007>
- [77] Dulermo, T., Tréton, B., Beopoulos, A., Kabran Gnankon, A.P., Haddouche, R. and Nicaud, J.-M. (2013) *Characterization of the two intracellular lipases of Y. lipolytica encoded by TGL3 and TGL4 genes: New insights into the role of intracellular lipases and lipid body organisation*. Biochimica et Biophysica Acta (BBA) - Molecular and Cell Biology of Lipids, vol. **1831**, pp. 1486–95. <https://doi.org/10.1016/j.bbalip.2013.07.001>
- [78] Blazeck, J., Hill, A., Liu, L., Knight, R., Miller, J., Pan, A. et al. (2014) *Harnessing Yarrowia lipolytica lipogenesis to create a platform for lipid and biofuel production*. Nature Communications, vol. **5**, pp. 3131. <https://doi.org/10.1038/ncomms4131>
- [79] Niehus, X., Crutz-Le Coq, A.-M., Sandoval, G., Nicaud, J.-M. and Ledesma-Amaro, R. (2018) *Engineering Yarrowia lipolytica to enhance lipid production from lignocellulosic materials*. Biotechnology for Biofuels, vol. **11**, pp. 11. <https://doi.org/10.1186/s13068-018-1010-6>
- [80] Ledesma-Amaro, R., Lazar, Z., Rakicka, M., Guo, Z., Fouchard, F., Coq, A.-M.C.-L. et al. (2016) *Metabolic engineering of Yarrowia lipolytica to produce chemicals and fuels from xylose*. Metabolic Engineering, vol. **38**, pp. 115–24. <https://doi.org/10.1016/j.ymben.2016.07.001>
- [81] Anwar, Z., Gulfranz, M. and Irshad, M. (2014) *Agro-industrial lignocellulosic biomass a key to unlock the future bio-energy: A brief review*. Journal of Radiation Research and Applied Sciences, vol. **7**, pp. 163–73. <https://doi.org/10.1016/j.jrras.2014.02.003>
- [82] Ledesma-Amaro, R., Dulermo, R., Niehus, X. and Nicaud, J.-M. (2016) *Combining metabolic engineering and process optimization to improve production and secretion of fatty acids*. Metabolic Engineering, vol. **38**, pp. 38–46. <https://doi.org/10.1016/j.ymben.2016.06.004>
- [83] Liu, Z., Gao, Y., Chen, J., Imanaka, T., Bao, J. and Hua, Q. (2013) *Analysis of metabolic fluxes for better understanding of mechanisms related to lipid accumulation in oleaginous yeast Trichosporon cutaneum*. Bioresource Technology, vol. **130**, pp. 144–51. <https://doi.org/10.1016/j.biortech.2012.12.072>
- [84] Tsai, Y.-Y., Ohashi, T., Kanazawa, T., Polburee, P., Misaki, R., Limtong, S. et al. (2017) *Erratum to: Development of a sufficient and effective procedure for transformation of an oleaginous yeast, Rhodosporidium toruloides DMKU3-TK16*. Current Genetics, vol. **63**, pp. 373–373. <https://doi.org/10.1007/s00294-017-0678-7>
- [85] Kourist, R., Bracharz, F., Lorenzen, J., Kracht, O.N., Chovatia, M., Daum, C. et al. (2015) *Genomics and Transcriptomics Analyses of the Oil-Accumulating Basidiomycete Yeast*

- Trichosporon oleaginosus* : *Insights into Substrate Utilization and Alternative Evolutionary Trajectories of Fungal Mating Systems*. MBio, vol. **6**. <https://doi.org/10.1128/mBio.00918-15>
- [86] Yaguchi, A., Spagnuolo, M. and Blenner, M. (2018) *Engineering yeast for utilization of alternative feedstocks*. Current Opinion in Biotechnology, vol. **53**, pp. 122–9. <https://doi.org/10.1016/j.copbio.2017.12.003>
- [87] Amit, K., Nakachew, M., Yilkal, B. and Mukesh, Y. (2018) *A Review of Factors affecting Enzymatic Hydrolysis of Pretreated Lignocellulosic Biomass*. Res. J. Chem. Environ.
- [88] Weiss, N., Börjesson, J., Pedersen, L.S. and Meyer, A.S. (2013) *Enzymatic lignocellulose hydrolysis: Improved cellulase productivity by insoluble solids recycling*. Biotechnology for Biofuels, vol. **6**, pp. 5. <https://doi.org/10.1186/1754-6834-6-5>
- [89] Rosgaard, L., Andric, P., Dam-Johansen, K., Pedersen, S. and Meyer, A.S. (2007) *Effects of Substrate Loading on Enzymatic Hydrolysis and Viscosity of Pretreated Barley Straw*. Applied Biochemistry and Biotechnology, vol. **143**, pp. 27–40. <https://doi.org/10.1007/s12010-007-0028-1>
- [90] Rodrigues, A.C., Leitão, A.F., Moreira, S., Felby, C. and Gama, M. (2012) *Recycling of cellulases in lignocellulosic hydrolysates using alkaline elution*. Bioresource Technology, vol. **110**, pp. 526–33. <https://doi.org/10.1016/j.biortech.2012.01.140>
- [91] Narra, M., Balasubramanian, V. and James, J.P. (2016) *Enhanced enzymatic hydrolysis of mild alkali pre-treated rice straw at high-solid loadings using in-house cellulases in a bench scale system*. Bioprocess and Biosystems Engineering, vol. **39**, pp. 993–1003. <https://doi.org/10.1007/s00449-016-1578-9>
- [92] Vega, K., Villena, G.K., Sarmiento, V.H., Ludeña, Y., Vera, N. and Gutiérrez-Correa, M. (2012) *Production of Alkaline Cellulase by Fungi Isolated from an Undisturbed Rain Forest of Peru*. Biotechnology Research International, vol. **2012**, pp. 1–7. <https://doi.org/10.1155/2012/934325>
- [93] Ilmén, M., den Haan, R., Brevnova, E., McBride, J., Wiswall, E., Froehlich, A. et al. (2011) *High level secretion of cellobiohydrolases by Saccharomyces cerevisiae*. Biotechnology for Biofuels, vol. **4**, pp. 30. <https://doi.org/10.1186/1754-6834-4-30>
- [94] Shoemaker, S., Watt, K., Tsitovsky, G. and Cox, R. (1983) *Characterization and properties of cellulases purified from Trichoderma reesei strain L27*. Biotechnology (NY), vol. **1**, pp. 687–90.
- [95] Den Haan, R., McBride, J.E., Grange, D.C. La, Lynd, L.R. and Van Zyl, W.H. (2007) *Functional expression of cellobiohydrolases in Saccharomyces cerevisiae towards one-step conversion of cellulose to ethanol*. Enzyme and Microbial Technology, vol. **40**, pp. 1291–9. <https://doi.org/10.1016/j.enzmictec.2006.09.022>
- [96] Penttilä, M.E., André, L., Lehtovaara, P., Bailey, M., Teeri, T.T. and Knowles, J.K.C. (1988) *Efficient secretion of two fungal cellobiohydrolases by Saccharomyces cerevisiae*. Gene, vol. **63**, pp. 103–12. [https://doi.org/10.1016/0378-1119\(88\)90549-5](https://doi.org/10.1016/0378-1119(88)90549-5)
- [97] Godbole, S., Decker, S.R., Nieves, R.A., Adney, W.S., Vinzant, T.B., Baker, J.O. et al. (1999) *Cloning and Expression of Trichoderma reesei Cellobiohydrolase I in Pichia pastoris*. Biotechnology Progress, vol. **15**, pp. 828–33. <https://doi.org/10.1021/bp9901116>
- [98] Wei, H., Wang, W., Alahuhta, M., Vander Wall, T., Baker, J.O., Taylor, L.E. et al. (2014) *Engineering towards a complete heterologous cellulase secretome in Yarrowia lipolytica reveals its potential for consolidated bioprocessing*. Biotechnology for Biofuels, vol. **7**, pp. 148. <https://doi.org/10.1186/s13068-014-0148-0>
- [99] Meesters, P.A.E.P., Springer, J. and Eggink, G. (1997) *Cloning and expression of the D9 fatty*

acid desaturase gene from Cryptococcus curvatus ATCC 20509 containing histidine boxes and a cytochrome b 5 domain. Appl Microbiol Biotechnol, pp. 663–7.

- [100] Shi, T.-Q., Liu, G.-N., Ji, R.-Y., Shi, K., Song, P., Ren, L.-J. et al. (2017) *CRISPR/Cas9-based genome editing of the filamentous fungi: the state of the art.* Applied Microbiology and Biotechnology, vol. **101**, pp. 7435–43. <https://doi.org/10.1007/s00253-017-8497-9>
- [101] Frandsen, R. (2010) *ATMT* [Internet].
- [102] Lee, L.-Y. and Gelvin, S.B. (2008) *T-DNA Binary Vectors and Systems.* Plant Physiology, vol. **146**, pp. 325–32. <https://doi.org/10.1104/pp.107.113001>
- [103] Das, A., Thakur, S., Shukla, A., Singh, P., Ansari, J. and Singh, N.P. (2020) *Genetic transformation.* Chickpea: Crop Wild Relatives for Enhancing Genetic Gains, Elsevier. p. 205–24. <https://doi.org/10.1016/B978-0-12-818299-4.00008-7>
- [104] Nora, L.C., Westmann, C.A., Martins-Santana, L., Alves, L. de F., Monteiro, L.M.O., Guazzaroni, M.-E. et al. (2019) *The art of vector engineering: towards the construction of next-generation genetic tools.* Microbial Biotechnology, vol. **12**, pp. 125–47. <https://doi.org/10.1111/1751-7915.13318>
- [105] Kuijpers, N.G., Solis-Escalante, D., Bosman, L., van den Broek, M., Pronk, J.T., Daran, J.-M. et al. (2013) *A versatile, efficient strategy for assembly of multi-fragment expression vectors in Saccharomyces cerevisiae using 60 bp synthetic recombination sequences.* Microbial Cell Factories, vol. **12**, pp. 47. <https://doi.org/10.1186/1475-2859-12-47>
- [106] Joska, T.M., Mashruwala, A., Boyd, J.M. and Belden, W.J. (2014) *A universal cloning method based on yeast homologous recombination that is simple, efficient, and versatile.* Journal of Microbiological Methods, vol. **100**, pp. 46–51. <https://doi.org/10.1016/j.mimet.2013.11.013>
- [107] Lund, A.M., Kildegaard, H.F., Petersen, M.B.K., Rank, J., Hansen, B.G., Andersen, M.R. et al. (2014) *A Versatile System for USER Cloning-Based Assembly of Expression Vectors for Mammalian Cell Engineering.* PLoS ONE, vol. **9**, pp. e96693. <https://doi.org/10.1371/journal.pone.0096693>
- [108] van Leeuwen, J., Andrews, B., Boone, C. and Tan, G. (2015) *Construction of Multifragment Plasmids by Homologous Recombination in Yeast.* Cold Spring Harbor Protocols, vol. **2015**, pp. pdb.top084111. <https://doi.org/10.1101/pdb.top084111>
- [109] van Leeuwen, J., Andrews, B., Boone, C. and Tan, G. (2015) *Rapid and Efficient Plasmid Construction by Homologous Recombination in Yeast.* Cold Spring Harbor Protocols, vol. **2015**, pp. pdb.prot085100. <https://doi.org/10.1101/pdb.prot085100>
- [110] Gietz, R.D. and Schiestl, R.H. (2007) *Frozen competent yeast cells that can be transformed with high efficiency using the LiAc/SS carrier DNA/PEG method.* Nature Protocols, vol. **2**, pp. 1–4. <https://doi.org/10.1038/nprot.2007.17>
- [111] Finnigan, G. and Thorner, J. (2015) *Complex in vivo Ligation Using Homologous Recombination and High-efficiency Plasmid Rescue from Saccharomyces cerevisiae.* BIO-PROTOCOL, vol. **5**. <https://doi.org/10.21769/BioProtoc.1521>
- [112] Bitoun, R. and Zamir, A. (1986) *Spontaneous amplification of yeast CEN ARS plasmids.* Molecular and General Genetics MGG, vol. **204**, pp. 98–102. <https://doi.org/10.1007/BF00330194>
- [113] IMADEARTIKA. (2009) *The Use of HIS6 Gene as a Selectable Marker for Yeast Vector.* HAYATI Journal of Biosciences, vol. **16**, pp. 40–2. <https://doi.org/10.4308/hjb.16.1.40>
- [114] Müllleder, M., Campbell, K., Matsarskaia, O., Eckerstorfer, F. and Ralser, M. (2016) *Saccharomyces cerevisiae single-copy plasmids for auxotrophy compensation, multiple*

- marker selection, and for designing metabolically cooperating communities. *F1000Research*, vol. **5**, pp. 2351. <https://doi.org/10.12688/f1000research.9606.1>
- [115] Edjabou, M.E., Petersen, C., Scheutz, C. and Astrup, T.F. (2016) *Food waste from Danish households: Generation and composition*. *Waste Management*, Elsevier Ltd. vol. **52**, pp. 256–68. <https://doi.org/10.1016/j.wasman.2016.03.032>
- [116] Yan, S., Yao, J., Yao, L., Zhi, Z., Chen, X. and Wu, J. (2012) *Fed batch enzymatic saccharification of food waste improves the sugar concentration in the hydrolysates and eventually the ethanol fermentation by *Saccharomyces cerevisiae* H058*. *Brazilian Archives of Biology and Technology*, vol. **55**. <https://doi.org/10.1590/S1516-89132012000200002>
- [117] Nielsen, M.R., Wollenberg, R.D., Westphal, K.R., Sondergaard, T.E., Wimmer, R., Gardiner, D.M. et al. (2019) *Heterologous expression of intact biosynthetic gene clusters in *Fusarium graminearum**. *Fungal Genetics and Biology*, vol. **132**, pp. 103248. <https://doi.org/10.1016/j.fgb.2019.103248>
- [118] Onu, P. and Mbohwa, C. (2021) *Methodological approaches in agrowaste preparation and processes*. *Agricultural Waste Diversity and Sustainability Issues*, Elsevier. p. 37–54. <https://doi.org/10.1016/B978-0-323-85402-3.00009-7>
- [119] Beopoulos, A., Mrozova, Z., Thevenieau, F., Le Dall, M.-T., Hapala, I., Papanikolaou, S. et al. (2008) *Control of Lipid Accumulation in the Yeast *Yarrowia lipolytica**. *Applied and Environmental Microbiology*, vol. **74**, pp. 7779–89. <https://doi.org/10.1128/AEM.01412-08>
- [120] Thanapimmetha, A., Peawsuphon, N., Chisti, Y., Saisriyoot, M. and Srinophakun, P. (2021) *Lipid production by the yeast *Lipomyces starkeyi* grown on sugars and oil palm empty fruit bunch hydrolysate*. *Biomass Conversion and Biorefinery*, vol. **11**, pp. 1197–210. <https://doi.org/10.1007/s13399-019-00532-z>
- [121] Ma, X., Gao, Z., Gao, M., Ma, Y., Ma, H., Zhang, M. et al. (2018) *Microbial lipid production from food waste saccharified liquid and the effects of compositions*. *Energy Conversion and Management*, vol. **172**, pp. 306–15. <https://doi.org/10.1016/j.enconman.2018.07.005>
- [122] Kirchhoff, J., Schiermeyer, A., Schneider, K., Fischer, R., Ainley, W.M., Webb, S.R. et al. (2020) *Gene expression variability between randomly and targeted transgene integration events in tobacco suspension cell lines*. *Plant Biotechnology Reports*, vol. **14**, pp. 451–8. <https://doi.org/10.1007/s11816-020-00624-7>

9 Appendices

9.1 Appendix A – Protein sequence of the Tr-Te chimeric CBH1 (Tr-TeCBH1)

MLLLAALALTSARAQLTQQACSLTAENHPSLTWKRCTSGGSCSTVNGAVTIDANWRWHTVSGSTNCYTGNQ
WDTSLCTDGKSCAQTCCEVDGADYSSTYGITTSGDLSLNLKFVTKHQYGTNVGSRVYLMENDTKYQMFELLGNEF
TFDVDVSNLGCGLNGALYFVSMADADGGMSKYSGNKAGAKYGTGYCDAQCPDLKFINGEANVGNWTPSTND
ANAGFGRYGSCCEMDVWEANNMATAFTPHPCCTTVGQSRCEADTCGGTYSSDRYAGVCDPDGCDNFAYRQ
GDKTFYGGKGMTVDTNKKMTVVVTFHKNSAGVLSEIKRFYVQDGKIIANAESKIPGNPGNSITQEYCDAQKVAFS
NTDDFNKGGMAQMSKALAGPMVLVMSVWDDHYANMLWLDSTYPIDQAGAPGAERGACPTTSGVPAEIE
AQVPNSNVIFSNIRFGPIGSTVPLDGSNPGNPPTTVVPPASTSTSRPTSSTSSPVSTPTGQPGGCTTQKWGQCG
GIGYTGCTNCVAGTTCTQLNPWYSQCL

___ Signal peptide from an endoglucanase from *C. oleaginosus* (NCBI Reference Sequence: XP_018277748.1)

9.2 Appendix B – Codon optimized gene sequence of *Tr-Te cbh1*

ATGCTGCTGCTGGCGGCGCTGGCGCTGACCAGCGCGCTGCGCAGCTGACCCAGCAGGCCTGCTCGCTCACCGCCGA
GAACCACCCCTCGCTCACCTGGAAGCGTTGCACCTCGGGCGGCTCGTGCTCGACCGTCAACGGCGCCGTCACCATCGA
CGCCAAGTGGCGTTGGACCCACACCGTCTCGGGCTCGACCAACTGCTACACCGGCAACCAAGTGGGACACCTCGCTCTG
CACCGACGGCAAGTCGTGCGCCAGACCTGCTGCGTGCACGGCGCCGACTACTCGTGCACCTACGGCATCACCACTC
GGGCGACTCGCTCAACCTCAAGTTCGTACCAAGCACCAGTACGGCACCAACGTCGGCTCGCGTGTCTACCTCATGGA
GAACGACACCAAGTACCAGATGTTTCGAGCTCCTCGGCAACGAGTTCACCTTCGACGTCGACGTCTCGAACCTCGGCTG
CGGCCTCAACGGCGCCCTCTACTTCGTCTCGATGGACGCCGACGGCGGCATGTCGAAGTACTCGGGCAACAAGGCCG
GCGCCAAGTACGGCACCGGCTACTGCGACGCCAGTGCCCCCGGACCTCAAGTTCATCAACGGCGAGGCCAACGTC
GGCAACTGGACCCCTCGACCAACGACGCCAACGCCGCTTCGGCCGTTACGGCTCGTGCTCGGAGATGGACGT
CTGGGAGGCCAACACATGGCCACCGCCTTACCCCCACCCCTGCACCACCGTCGGCCAGTCGCGTTGCGAGGCCGA
CACCTGCGGCGGCACCTACTCGTCGGACCGTTACGCCGGCGTCTGCGACCCCGACGGCTGCGACTTCAACGCCTACCG
CCAGGGCGACAAGACCTTCTACGGCAAGGGCATGACCGTCGACACCAACAAGAAGATGACCGTCGTCACCCAGTTCC
ACAAGAACTCGGCCGGCGTCTCTCGGAGATCAAGCGTTTCTACGTCCAGGACGGCAAGATCATCGCCAACGCCGAG
TCGAAGATCCCCGGCAACCCCGGCAACTCGATCACCCAGGAGTACTGCGACGCCAGAAGGTCGCCTTCTCGAACACC
GACGACTTCAACCGCAAGGGCGGCATGGCCAGATGTCGAAGGCCCTCGCCGGCCCCATGGTCTCGTCATGTCGGT
CTGGGACGACCACTACGCCAACATGCTCTGGCTCGACTCGACCTACCCCATCGACCAGGCCGGCGCCCCGGCGCCGA
GCGTGGCGCCTGCCCCACCACCTCGGGCGTCCCCGCCGAGATCGAGGCCAGGTCCCCAACTCGAACGTCATCTTCTC
GAACATCCGTTTTCGGCCCATCGGCTCGACCGTCCCCGGCCTCGACGGCTCGAACCCCGGCAACCCACCACCACCGT
CGTCCCCCGCCTCGACCTCGACCTCGCGTCCCACCTCGTCGACCTCGTCGCCGTCTCGACCCCAACGGCCAGCCC
GGCGGCTGCACCACCCAGAAGTGGGGCCAGTGGCGCGGCATCGGCTACACCGGCTGCACCAACTGCGTCGCCGGCA
CCACTGCACCCAGCTCAACCCCTGGTACTCGAGTGCCTC

The gene was codon optimized for expression in C. oleaginosus and synthesized by GenScript.

9.3 Appendix C – Cassette sequence of the TEF1- α + *Tr-Te cbhl*

```
CTCCTTCCTTCCTTCTTCCCTCCTGCCCTCCTGGCATCAAATTAACGTGAGGGGATCGGATAAACATTGCGCCA
AATCACCCCGTACGGTGAGCAAGCCGACGTCAGGCTGCCACACAAGGGCCCTCTAGCGGCTTATAGACCCCGCCAC
ACGTCATAACACCATAACGCCGTGACTGGGCTTTGAGTAGACAAAGGCAATTCAGGGTCTGTTGGAGGGGCGAGCTC
CAGTGCCAGCGCACTGTAAAATCCGCGTGCATCCGCTTCTCTCTCACTCCCACCCTCTCTCTCTCCTCAAAAAACA
GTGAGTAGCACCAACGACAACCATGGCAATGGTGGTCGCCAAAGAGGCAAAGACAGCGAGCGCACTGCGACCGACA
ACGACCTGCCCGTCATCGACTCGAACAACCTGCAGCACCATCGCTCTCGTCATCGCCGCGGCCACTTGCCCTGACTC
TTCCCCCACCCTCATCCATCCATCCTTCTCTCGACCATGCAAGGCCACTGCCTCGAGTGCATGCGCTCTTGGC
GATGCTCGCGCATTGGTATCGTGGTCGTCTGCATCGTCGTCAAACAGACGGAGCACGACGACCGTGACGAATTGGAT
GGCACAAGGGTCCATGTCAAATTTGACCTCCGCTTCCACCTTCAACCTTCTCCATCCAACATCCTCCGCCTTGACT
CGCAATGCGCATGCTGCTTTGTCTCCCACTCCACCATTGACTGCCACTCTCAGAGAATGTCGACTAACATTGCAGA
CAAAACCTATTCAAAGCTTATGCTGCTGCTGGCGGCGCTGGCGCTGACCAGCGCGCGTGCAGCTGACCCAGCA
GGCCTGCTCGCTCACCGCCGAGAACCACCCTCGCTCACCTGGAAGCGTTGACCTCGGGCGGCTCGTGTCTGACCGT
CAACGGCGCCGTACCATCGACGCCAAGTGGCGTTGGACCCACACCGTCTCGGGCTCGACCAACTGCTACACCGGCAA
CCAGTGGGACACCTCGCTCTGCACCGACGGCAAGTCGTGCGCCAGACCTGCTGCGTGCAGCGCGCCGACTACTCGT
CGACCTACGGCATACCACCTCGGGCGACTCGCTCAACCTCAAGTTCGTACCAAGCACCAGTACGGCACCAACGTCG
GCTCGCGTGTCTACCTCATGGAGAACGACACCAAGTACCAGATGTTGAGCTCCTCGGCAACGAGTTCACCTTCGACG
TCGACGTCTCGAACCTCGGCTGCGGCCTCAACGGCGCCCTCTACTTCGTCTCGATGGACGCCGACGGCGGCATGTCGA
AGTACTCGGGCAACAAGGCCGGCGCAAGTACGGCACCGGCTACTGCGACGCCAGTGCCCCGCGACCTCAAGTTC
ATCAACGGCGAGGCCAACGTGGCAACTGGACCCCTCGACCAACGACGCCAACGCCGGCTTCGGCCGTTACGGCTC
GTGCTGCTCGGAGATGGACGTCTGGGAGGCCAACAAACATGGCCACCGCCTTACCCCCACCCTGCACCACCGTCCG
CCAGTCGCGTTGCGAGGCCGACACCTGCGGCGGCACCTACTCGTCGGACCGTTACGCCGGCGTCTGCGACCCCGACG
GCTGCGACTTCAACGCCTACCGCCAGGGCGACAAGACCTTCTACGGCAAGGGCATGACCGTGCACCAACAAGAAG
ATGACCGTCGTACCCAGTTCACAAGAAGTCCGCGCGGCTCTCTCGGAGATCAAGCGTTTCTACGTCCAGGACGGC
AAGATCATCGCCAACGCCGAGTGAAGATCCCCGGCAACCCGGCAACTCGATCACCCAGGAGTACTGCGACGCCCA
GAAGGTGCGCTTCTCGAACACCGACGACTTCAACCGCAAGGGCGGCATGGCCCAGATGTCGAAGGCCCTCGCCGGCC
CCATGGTCTCGTCATGTCGGTCTGGGACGACCACTACGCCAACATGCTCTGGCTCGACTCGACCTACCCCATCGACCA
GGCCGGCGCCCCGGCGCCGAGCGTGGCGCCTGCCCCACCACCTCGGGCGTCCCCGCCGAGATCGAGGCCAGGTCC
CCAACCTCGAACGTCATCTTCTCGAACATCCGTTTCGGCCCCATCGGCTCGACCGTCCCCGGCCTCGACGGCTCGAACCC
CGGCAACCCACCACCACCGTGTCCCCCGCCTCGACCTCGACCTCGCGTCCCACCTCGTCGACCTGTGCGCCGTC
TCGACCCACCACCGCCAGCCGCGGCTGCACCACCCAGAAGTGGGGCCAGTGCGGCGGCATCGGCTACACCGGCT
GCACCAACTGCGTCGCCGGCACCACCTGCACCCAGCTCAACCCCTGGTACTCGAGTGCCTCTGAGGATCCTTGTGCTT
CGAGCGTGCTTATTTGTATGTCTTTCATCCTTAGTTCCTCAGATAGGCCTCTCGGCGATGCACCGTTGAAGGCTAC
CATTCTAAAGTTTCGTTGCGGGTGTGAGTGTGAGATAGCGTTGCTTACCTGTAGAATACGAGGCAGCACCAACGCC
GATAACATCCAAGTCAGGCTTAGCACTGGTCTGCTTGGTTGCTGATGAGGCGCGGGTTCGACGAGCCGATCTCGTT
GAAGCCGTGTATCGTATCAGCTTTCGAGTCTACTGTAGGCTTTGTTGTGGTGTACGCCCTTTCAGTGCCTACTGCAGA
TCGTAGATGTCGCATGCATGTTGCGTGCAGTACCCAAACGTCTGATATCTGATGTTTACGTACATCGGGGGTCAATTT
CTCTGTGCTTCGATGATGCCACGCCGCTGATCTGCTGAAGGTAGAGAGAGAGTACGAGAGATCCCACTAGCAGTCTT
GGCCATGCATTGTCGTGTTGCCAGCAGTCGAGTCTCTGGTGGCGTTTCAAACGATGGATCGTGAGCTTGCATGCTT
GGTTGAATCAGCCCAATAGCTGGCAGTCAAATACATTCTGACTCC
```

- 800 bp upstream of the TEF1- α gene in *C. oleaginosus* – used as the TEF1- α promotor
- Codon optimized gene sequence of *Tr-Te cbhl* – see appendix B
- 600 bp downstream of the TEF1- α gene in *C. oleaginosus* – used as the TEF1- α terminator

Restriction sites has been inserted on each side of the gene

The cassette was synthesized by GenScript

9.4 Appendix D – Primer sequences and PCR settings

Bold: stop codon

Lowercase letters: tail

Primer	Sequence	PCR settings	Function
CA-Ura3-Fw	tcagtaagttggcagcatcacccat CTTTCGCTCCTTGAACCTGG	TD-PCR. Melting-temp. starting at 63 °C with -0.1°C per cycle for 35 cycles. Elongation was performed for 1:30 min at 72 °C.	Amplify the CEN4/ARSH6 and URA3 genes from the pSHUT3-32 plasmid (in-house shuttle vector) and insert to pRF-HU2-hyg-yfp to allow for plasmid assembly in <i>S. cerevisiae</i>
CA-Ura3-Rv	GGAGCCGATTTTGAAACCAC		
T1-bb1-Fw	ggtactcgcagtgctcgat TGACTTTCTAGGTTGTAGCATGG	Normal PCR with melting-temp. set to 58.5 °C, and elongation was 3:30 min at 72 °C.	Cut out the yfp gene from pFLEXI-hyg-yfp plasmid by creating three overlapping PCR pieces. The two tails match the synthetic <i>Tr-Te cbhl</i> gene and include a stop codon for the synthetic gene. The three PCR pieces together with the synthetic <i>Tr-Te cbhl</i> gene will yield the pFLEXI-hyg-cbhl plasmid.
T1-bb1-Rv	ATCTTGCCCTGCACGAATAC		
bb2-Hyg-Fw	GGCAAGTATTTGGGCAAGG	TD-PCR. Melting-temp. starting at 62 °C with -0.1°C per cycle for 35 cycles. Elongation was performed for 2:30 min at 72 °C.	
bb2-Hyg-Rv	GCGACCTCGTATTGGGAAT		
Hyg-P1-Fw	ACTGGAGCGAGGCGATGT	TD-PCR. Melting-temp. starting at 65 °C with -0.1°C per cycle for 35 cycles. Elongation was performed for 2:00 min at 72 °C.	
Hyg-P1-Rv	gccccagcagcagcatgat CTTGCCCATTTGTTGATCAAGTT		
TEF1a-Fw	tcagcggatactagagggga CTCCTTCCTCCTTCTTTCCTT		Amplify the synthetic TEF1a <i>Tr-Te cbhl</i> gene cassette from GeneScript.
TEF1a-Rv	actgaaggcgggaaaggtac CAGAATGTATTTGACTGCCAGCTA		

bb1-Fw	tggcagtcaaatacattctg GTACCTTCCCGCCTTCAGT	TD-PCR. Melting-temp. starting at 65 °C with -0.1°C per cycle for 35 cycles. Elongation was performed for 2:30 min at 72 °C.	Cut out the yfp cassette from the pFLEXI-hyg-yfp plasmid by creating two overlapping PCR pieces. The two tails match the synthetic TEF1a <i>Tr-Te cbhl</i> gene cassette. The two PCR pieces together with the synthetic TEF1a <i>Tr-Te cbhl</i> cassette will yield the pFLEXI-hyg-(TEF1a)-cbhl plasmid.
bb1-Rv	ATCTTGCCCTGCACGAATAC		
bb2-Fw	GGCAAGTATTTGGGCAAGG	TD-PCR. Melting-temp. starting at 65 °C with -0.1°C per cycle for 35 cycles. Elongation was performed for 2:30 min at 72 °C.	Validation of the plasmids. The primers bind outside of the yfp gene cassette and can be used to check for the correct insert
bb2-Rv	ggaaagaaggaaggaaggag TCCCCTCTAGTATCCGCTGAC		
cPCR-Fw	ACTGGAGCGAGGCGATGT	TD-PCR. Melting-temp. starting at 63 °C with -0.1°C per cycle for 35 cycles. Elongation was performed for 3:00 min at 72 °C.	Validation of integration of DNA by ATMT into <i>C. oleagnosus</i> mutants. The primers bind within the hygromycin cassette.
cPCR-Rv	CTCTTAGGTTTACCCGCCAATAT		
Co-cPCR-Fw	GATGTAGGAGGGCGTGGATA	TD-PCR. Melting-temp. starting at 62 °C with -0.1°C per cycle for 35 cycles. Elongation was performed for 1:00 min at 72 °C.	
Co-cPCR-Rv	GATGTTGGCGACCTCGTATT		

9.5 Appendix E – Protocol for ATMT of *C. oleagnosus*

Introduction:

Agrobacterium tumefaciens mediated transformation is a far more complicated procedure compared to classical transformation techniques. The procedure consists of two phases. In the first phase, *C. oleagnosus* and *A. tumefaciens* containing the plasmid are mixed and co-cultivated on a filter membrane, which is placed on top of induction medium agar plates (IMAS plates). IMAS plates contain a low pH (between 5-6), a shortage of nutrition, and are supplemented with the plant pheromone acetosyringone to trigger the virulence of the *Agrobacterium*. After several days, the second phase starts. The membrane is transferred to selection agar plates, which consist of YPD media supplemented with antibiotic cefotaxime to kill the *Agrobacterium* cells as well as hygromycin B to select for transformed yeast cells. The second phase takes up to one week.

Strains:

- AGL1 *A. tumefaciens*
- ATCC 20509 *C. oleagnosus*

Media used for the ATMT of *C. oleagnosus*:

- LB agar plates with 30 µg/mL kanamycin
- LB liquid medium with 30 µg/mL kanamycin
- YPD liquid medium
- Liquid induction medium with acetosyringone (L-IMAS): (2.05 g/L K₂HPO₄, 1.45 g/L KH₂PO₄, 0.15 g/L NaCl, 0.5 g/L MgSO₄ · 7H₂O, 67.0 mg/L CaCl₂·2H₂O, 7.8 g/L 2-4-Morpholineethanesulfonic acid monohydrate (MES), 1.8 g/L glucose, 39.24 mg/L acetosyringone, 2.5 mg/L FeSO₄ · 7H₂O, 0.5 g/L (NH₄)₂SO₄, 5 % (v/v) glycerol, 5 % (v/v) trace elements solution (100 mg Na₂MoO₄, MnSO₄ · H₂O, ZnSO₄ · 7H₂O, CuSO₄ · 5H₂O, H₃BO₃ in 1L H₂O), pH adjusted to 5.6
- Solid induction medium with acetosyringone (S-IMAS): equivalent to L-IMAS, without glucose and supplemented with 18 g/L agar.
- YPD agar plates with 200 µg/mL hygromycin B and 300 µg/mL cefotaxime
- YPD medium with 300 µg/mL cefotaxime

Procedure:

Day 1:

- Introduce the plasmids to *Agrobacterium tumefaciens* using electroporation using the method described in the Bio-Rad Micro-Pulser user protocol (section 7)
- Plate the cell suspension on LB agar plates supplemented with 50 $\mu\text{g}/\text{mL}$ kanamycin and 20 $\mu\text{g}/\text{mL}$ rifampicin and incubate for 72 h at 30 °C

Day 4:

- Prepare a culture of transformed *A. tumefaciens* by inoculating one colony from the selection plate to 30 mL of LB medium supplemented with 30 $\mu\text{g}/\text{mL}$ kanamycin at 30 °C until OD₆₀₀ reaches 1 (should take about 18 h)
- Prepare a culture of *C. oleaginosus* by inoculating one colony in 30 mL YPD medium at 30 °C until OD₆₀₀ reaches 2-3 (should take about 24 h)

Day 5:

- Centrifuge the overnight culture of *A. tumefaciens* and inoculate the cell pellet in a shake flask with 10 mL L-IMAS medium and cultivate at 30 °C for approximately 6 hours
- Centrifuge the overnight culture of *C. oleaginosus* and resuspend in an appropriate volume of L-IMAS medium to dilute the cell concentration to an OD₆₀₀ of 0.5
- Mix 500 μL of the *C. oleaginosus* in L-IMAS medium (OD₆₀₀ = 0.5) with 500 μL of today's culture of *A. tumefaciens* in L-IMAS medium
- Plate 500 μL of the *A. tumefaciens* and *C. oleaginosus* cell suspension mix on top of a filter membrane that is placed on S-IMAS agar plates and incubate the plates at 25 °C for 48 h

Day 7:

- Transfer the membrane to YPD agar plates supplemented with 200 $\mu\text{g}/\text{mL}$ hygromycin B and 300 $\mu\text{g}/\text{mL}$ cefotaxime and incubate for 3-5 days at 30 °C. Check the size of colonies daily and isolate before they can not be separated.

Day 12:

- Pick the yeast colonies that appeared on the filter membrane and streak them onto new YPD plates supplemented with 200 $\mu\text{g}/\text{mL}$ hygromycin B and 300 $\mu\text{g}/\text{mL}$ cefotaxime and incubate for 2-3 days at 30 °C

Day 14:

- To prepare a pre-culture for subsequent inoculation in liquid media, transfer one transformed yeast colony to 10 mL YPD medium overnight

Day 16:

- Centrifuge the cells and wash with MQ-water
- Transfer the cell pellet to liquid media for fermentation